

INFORMATION TO USERS

This manuscript has been reproduced from the microfilm master. UMI films the text directly from the original or copy submitted. Thus, some thesis and dissertation copies are in typewriter face, while others may be from any type of computer printer.

The quality of this reproduction is dependent upon the quality of the copy submitted. Broken or indistinct print, colored or poor quality illustrations and photographs, print bleedthrough, substandard margins, and improper alignment can adversely affect reproduction.

In the unlikely event that the author did not send UMI a complete manuscript and there are missing pages, these will be noted. Also, if unauthorized copyright material had to be removed, a note will indicate the deletion.

Oversize materials (e.g., maps, drawings, charts) are reproduced by sectioning the original, beginning at the upper left-hand corner and continuing from left to right in equal sections with small overlaps.

Photographs included in the original manuscript have been reproduced xerographically in this copy. Higher quality 6" x 9" black and white photographic prints are available for any photographs or illustrations appearing in this copy for an additional charge. Contact UMI directly to order.

Bell & Howell Information and Learning
300 North Zeeb Road, Ann Arbor, MI 48106-1346 USA
800-521-0600

UMI[®]



Université d'Ottawa • University of Ottawa

Removal of Phenol from Water by Adsorption

by

© Nadia Roostaei

A thesis submitted to the School of Graduate Studies and Research

in partial fulfillment of the requirements for the

degree of

MASTER OF APPLIED SCIENCE IN

CHEMICAL ENGINEERING

July 1999

Department of Chemical Engineering

University of Ottawa

Ottawa, Canada



National Library
of Canada

Acquisitions and
Bibliographic Services

395 Wellington Street
Ottawa ON K1A 0N4
Canada

Bibliothèque nationale
du Canada

Acquisitions et
services bibliographiques

395, rue Wellington
Ottawa ON K1A 0N4
Canada

Your file *Votre référence*

Our file *Notre référence*

The author has granted a non-exclusive licence allowing the National Library of Canada to reproduce, loan, distribute or sell copies of this thesis in microform, paper or electronic formats.

The author retains ownership of the copyright in this thesis. Neither the thesis nor substantial extracts from it may be printed or otherwise reproduced without the author's permission.

L'auteur a accordé une licence non exclusive permettant à la Bibliothèque nationale du Canada de reproduire, prêter, distribuer ou vendre des copies de cette thèse sous la forme de microfiche/film, de reproduction sur papier ou sur format électronique.

L'auteur conserve la propriété du droit d'auteur qui protège cette thèse. Ni la thèse ni des extraits substantiels de celle-ci ne doivent être imprimés ou autrement reproduits sans son autorisation.

0-612-46605-1

Canada

Erratum

In this thesis, wherever the adsorbent HiSiv 1000 is mentioned, it should be substituted for adsorbent HiSiv 3000 and vice versa.

Abstract

Phenol and its derivatives are compounds that are found in many industrial wastewaters such as in paint, paper, plastics, oil and gasoline, steel, textile, and wood industries. They are considered as toxic to humans and aquatic life. A minute concentration of phenol (2.5 ppm) causes objectionable taste in potable water.

In this study, liquid phase adsorption of phenol from water has been investigated. Kinetic and equilibrium experiments have been performed for several adsorbents. The influence of particle size, temperature, and thermal regeneration on adsorption were also evaluated.

Results of kinetic experiments indicate that HiSiv 3000 has the highest rate of adsorption by reaching equilibrium in less than 3 hours while filtrisorb-400 and activated carbon did not reach complete equilibrium even after 1 month. Results of equilibrium experiments showed that the capacity of activated carbon and filtrisorb-400 were 14 and 9 times higher than HiSiv 3000, respectively (when the phenol concentration in the liquid phase was 150 mg/l). From particle size experiments it appears that the adsorption capacity of HiSiv 3000 does not change by changing the particle size, but the rate of adsorption decreases considerably by increasing the particle size.

The effect of temperature on adsorption was studied by determining equilibrium

isotherms for HiSiv 3000 (Particle size=50×70 mesh) at 25, 40, and 55°C. The results show that the capacity of adsorption decreases with increasing temperature.

Thermal regeneration was performed for HiSiv 3000 at 360°C, and the results were compared with the regeneration efficiency of activated carbon obtained from literature. The adsorption capacity of HiSiv 3000 did not change during 14 regeneration cycles. The loss of adsorbent particles during regeneration of HiSiv 3000 was determined and compared to that of activated carbon.

Two kinetic models were studied and applied to kinetic data for activated carbon, F-400, and HiSiv 3000 (four different particle sizes). Rates of adsorption and diffusion coefficients were determined by applying these models to the initial rapid stage of adsorption.

Three equilibrium isotherm models were also examined for the above-mentioned adsorbents. Among them 3-parameter isotherm model was the best to represent the isotherm data.

In conclusion, although the adsorption equilibrium capacity for HiSiv 3000 is lower than activated carbon and F-400, HiSiv 3000 reaches equilibrium faster than other adsorbents, and can be used in several adsorption cycles without losing its adsorption capacity. The loss of adsorbent particles during adsorption and regeneration is much lower for HiSiv 3000 compared to the relative loss of activated carbon particles. In addition, HiSiv 3000 can be regenerated at 360°C while regeneration of activated carbon is performed at 800°C.

Résumé

Le phénol et ses dérivées sont des substances qui sont présentes dans les eaux lourdes industrielles provenant de la fabrication de la peinture, du papier, des plastiques, de l'huile et de l'essence, de l'acier, du textile et de la transformation du bois. Ces eaux lourdes sont considérés comme étant toxiques pour l'humain et pour la faune aquatique. Une concentration de phénol d'environ 2.5 ppm peut causer un goût désagréable à l'eau de consommation.

Dans ce rapport, l'adsorption ont phase liquide du phénol à partir de l'eau a été étudiée. Des expériences visant la cinétique et l'équilibre ont été exécutés pour plusieurs adsorbants. Des expériences ont aussi été exécutés pour déterminer l'influence de la taille des particules, de la température et de la régénération thermique sur l'adsorption.

Les expériences sur la cinétique a démontré que le HiSiv 3000 a le meilleur taux d'adsorption et atteint l'équilibre en moins de 3 heures, à comparaison du filtrasorb et du carbone activé qui n'atteint pas l'équilibre complet, même après 1 mois. Les expériences d'équilibre démontrent que la capacité du carbone activé et du filtrasorb-400 sont de 14 et 9 fois plus haut que celui du HiSiv 3000 respectivement (lorsque la concentration du phénol

dans le liquide était de 150 mg/l). À partir des expériences sur la taille des particules, il semble que la capacité de l'adsorption du HiSiv 3000 ne change pas avec la taille des particules, mais le taux d'adsorption diminue considérablement avec l'augmentation de la taille des particules.

L'effet de la température sur l'adsorption a été étudié en déterminant les isothermes à l'équilibre pour le HiSiv 3000 (Taille des particules = 50 x 70 mesh) à 25°C, 40°C et 55°C. Les résultats démontrent que la capacité d'adsorption diminue avec l'augmentation de la température.

La régénération thermique a été réalisée pour le HiSiv 3000 à 360°C, et les résultats ont été comparés avec l'efficacité de régénération du carbone activé obtenu dans la littérature. La capacité d'adsorption du HiSiv 3000 ne change pas suite à 14 cycles de régénération. La perte de particules d'adsorbant pendant la régénération du HiSiv 3000 a été déterminée et a été comparée à celle du carbone activé.

Les deux modèles cinétiques ont été étudiés et appliqués aux données du carbone activé, F-400 et HiSiv 3000 (pour quatre différentes tailles de particules). Aussi, trois modèles d'équilibres ont été examinés pour les adsorbants ci-haut mentionnés. Il a été montré que le modèle à trois paramètres de Langmuir-Freundlich décrit l'équilibre de façon plus précise que les deux autres modèles.

En conclusion, même si la capacité de l'adsorption à l'équilibre pour le HiSiv 3000 est inférieure à celle des carbone activé, F-400. HiSiv 3000 atteint l'équilibre plus rapidement et, même avec plusieurs cycles d'adsorption, sa capacité d'adsorption ne diminue presque pas. Aussi, la perte de particules d'adsorbant pendant les cycles d'adsorption et de régénération est inférieure pour le HiSiv 3000 relativement au carbone activé.

Acknowledgments

I would like to express my sincere appreciation to my supervisor Dr. F. Handan Tezel for her guidance, encouragement, patience and support.

I am thankful to NSERC, for partially funding this work. I am also thankful to Dr. V. Hornof, former chairman of Chemical Engineering Department, for the departmental financial support.

I am grateful to technical staff of the Department of Chemical Engineering, particularly Mr. L. Tremblay who assisted to expand the liquid adsorption laboratory. I would further like to thank my fellow colleagues for their comments and cooperation.

I am greatly thankful to my husband, and my children who without their support and encouragement this work could not have been produced. My deepest appreciation goes to my parents Mr. Roostaei and Mrs. Bahari-Javan for their sacrifices which helped me to improve my life.

Table of Contents

Abstract	i
Résumé	iii
Acknowledgments	vi
Table of Contents	vii
List of Figures	xii
List of Tables	xvii
Nomenclature	xviii
Chapter One: Introduction	1
Chapter Two: Literature Survey	5
2.1 Different Adsorbents Used for Phenol Adsorption	5
2.1.1 Activated Carbon	5
2.1.2 Fiber Activated Carbon	6
2.1.3 Peat, Fly Ash, and Bentonite	6
2.1.4 Fly Ash and Impregnated Fly Ash	7
2.1.5 Conclusion of section 2.1:	7
2.2 Effect of Temperature	7
2.3 Effect of pH	9
2.4 Effect of Dissolved Oxygen	13

2.5 Regeneration Procedures	14
2.5.1 Thermal Regeneration	15
2.5.2 Chemical Regeneration	16
2.5.3 Biological Regeneration	16
2.5.4 Electrochemical Regeneration	17
2.5.5 Conclusion of Section 2.5	17
2.6 Modelling	18
2.6.1 Kinetic Modelling	18
2.6.1.1 First Order Reversible Model	22
2.6.1.2 Isothermal Diffusion Model	26
2.6.2 Equilibrium Modelling	27
2.6.2.1 Linear Isotherm (Henry's Law)	32
2.6.2.2 Langmuir Model	33
2.6.2.3 Freundlich Model	34
2.6.2.4 Three-parameter Isotherm	35
Chapter Three: Materials and Methods	36
3.1 Materials	36
3.2 Experimental Methods	38
3.2.1 Kinetic Experiments	38
3.2.2 Equilibrium Experiments	38
3.2.3 Methods of Analysis	39
3.2.4 Regeneration Method	44

Chapter Four: Experimental Results	46
4.1 Silica Gel	46
4.1.1 Kinetic Data	47
4.2 Activated Alumina	49
4.2.1 Kinetic data	49
4.3 Activated Carbon	52
4.3.1 Kinetic data	52
4.3.2 Adsorption Equilibrium Isotherm	55
4.4 Filtrasorb 400	59
4.4.1 Kinetic Experiments:	59
4.4.2 Adsorption Equilibrium Isotherm	59
4.5 HiSiv 1000	63
4.5.1 Kinetic Results	64
4.5.2 Adsorption Equilibrium Isotherm	64
4.6 HiSiv 3000	66
4.6.1 Kinetic Results	66
4.6.2 Adsorption Equilibrium Isotherm	67
4.6.3 Comparison between HiSiv 3000 and HiSiv 1000	68
4.6.4 Problem Associated Working With HiSiv 3000 Powder:	70
4.6.5 Effect of Particle Size on Adsorption Equilibrium Capacity	70
4.6.6 Effect of Particle Size on Rate of Adsorption	72
4.7 HiSiv 3000 (50×70 mesh)	74

4.7.1 Kinetic Experiments	75
4.7.2 Adsorption Equilibrium Isotherm	77
4.7.3 Effect of Temperature	80
4.7.4 Regeneration	82
4.8 Modeling	84
4.8.1 Kinetic Modeling	84
4.8.1.1 First Order Reversible Model	84
4.8.1.2 Isothermal Diffusion Model	90
4.8.2 Equilibrium Modelling	95
Chapter Five: Conclusions	100
Chapter Six: Recommendations	101
6.1 Continuous Systems	101
6.2 Multi-component Adsorption	102
6.3 Enhancing the Adsorption Capacity	102
6.4 Regeneration Time	102
References	104
Appendices	113
A1. Phenol Structure and Size	113
A2. Adsorption Isotherm Curve	115
B. Raw Data from Adsorption Experiments	116
B.1 Kinetic Experiments	116

B.2 Equilibrium Experiments:	126
C. Raw Data from Regeneration Experiments	135
C.1 Result of adsorption cycles performed after each regeneration cycle	135
C.2 Loss of adsorbent particles during filtration.	149
C.3 Total Loss of adsorbent particles during each adsorption and regeneration cycle.	150
D. Kinetic Models	151
D.1 First Order Reversible model Applied to Kinetic Data	151
D.2 Isothermal Diffusion Model	154
E. Equilibrium Models	157

List of Figures

Figure 1: Influence of temperature on the adsorption of phenol on granular activated carbon	9
Figure 2: Isotherms for phenol at different pH on coconut-shell based	11
Figure 3: Adsorption isotherms for phenol by granular activated carbon	13
Figure 4: Mass transfer in adsorption process.	20
Figure 5: Schematic diagram of composite adsorbent pellet.	22
Figure 6: Classification of solute in solution	31
Figure 7: Results of phenol adsorption on activated carbon, using spectrophotometer and TOC analyser	43
Figure 8: Pore size distribution for	47
Figure 9: Kinetic data for adsorption of phenol on silica gel at 25°C.	48
Figure 10: Kinetic data for adsorption of phenol on activated alumina (basic)	50
Figure 11: Kinetic data for adsorption of phenol on activated alumina	51
Figure 12: Kinetic data for adsorption of phenol on activated carbon.	53
Figure 13: Adsorption isotherm comparison of phenol on activated carbon with literature	57
Figure 14: Kinetic data for adsorption of phenol on F-400 at 25°C.	60

Figure 15: Literature comparison for adsorption isotherms of phenol on F-400 at 26.5°C	61
Figure 16: Kinetic data for adsorption of phenol onto HiSiv 1000 at 25°C.	65
Figure 17: Equilibrium isotherm for adsorption of phenol onto HiSiv 1000 at 25°C. ...	66
Figure 18: Kinetic data for adsorption of phenol on HiSiv 3000 powder at 25°C.	67
Figure 19: Equilibrium isotherm for HiSiv 3000 powder at 25°C.	68
Figure 20: Effect of particle size on adsorption capacity of HiSiv 3000 for phenol at 25°C.	71
Figure 21: Effect of particle size on rate of adsorption of phenol on HiSiv 3000	73
Figure 22: Effect of particle size on rate of adsorption of phenol on HiSiv 3000	74
Figure 23: Kinetic data for adsorption of phenol on HiSiv 3000 (50x70) at 25°C.	75
Figure 24: Kinetic rate comparison for adsorption of phenol on HiSiv 3000 (50x70mesh), F-400 and activated carbon at 25°C.	76
Figure 25: Kinetic rate comparison for adsorption of phenol on HiSiv 3000 (50x70mesh), F-400 and activated carbon at 25°C	77
Figure 26: Adsorption isotherm of phenol on HiSiv 3000 (50x70 mesh).	78
Figure 27: Equilibrium isotherm comparison for adsorption of phenol on activated carbon, F-400, and HiSiv 3000 (50x70 mesh), at room temperature	79
Figure 28: Adsorption isotherms for phenol onto HiSiv 3000 (50x70 mesh), at different temperatures.	80
Figure 29: Adsorption isotherms for phenol on filtrisorb 400 at different temperatures.	81

Figure 30: Effect of regeneration on adsorption of phenol on HiSiv 3000 (50x70 mesh)	83
Figure 31: First order reversible kinetic fit of phenol adsorption data on activated carbon .	87
Figure 32: First order reversible kinetic fit of phenol adsorption data on F400	88
Figure 33: First order reversible kinetic fit of phenol adsorption data on HiSiv 3000 (50 × 70 mesh size)	89
Figure 34: Plot of q against $t^{1/2}$ for adsorption of phenol on activated carbon at 25°C.	92
Figure 35: Plot of q against $t^{1/2}$ for adsorption of phenol on F-400 at 25°C.	93
Figure 36: Plot of q against $t^{1/2}$ for adsorption of phenol on HiSiv 3000 (particle size =50×70 mesh) at 25°C.	94
Figure 37: Isotherm models applied to phenol adsorption data with activated carbon at 25°C	97
Figure 38: Isotherm models applied to phenol adsorption data with F-400, at 25°C.	98
Figure 39: Isotherm models applied to phenol adsorption data with HiSiv 3000 (50×70 mesh), at 25°C. In this figure Freundlich model coincides with 3- parameter model.	99
Figure 40: Phenol structure	113
Figure 41: An example for plotting adsorption isotherm curve.	115

Figure 42: First order reversible kinetic fit of phenol adsorption data on HiSiv 3000 (powder particles), at T=25°C.	151
Figure 43: First order reversible kinetic fit of phenol adsorption data on HiSiv 3000 (20 × 50 mesh size), at T=25°C.	152
Figure 44: First order reversible kinetic fit of phenol adsorption data on HiSiv 3000 (extrude, particle size =1.5 mm), at T=25°C.	153
Figure 45: Plot of q against $t^{1/2}$ for adsorption of phenol on HiSiv 3000 (powder particle size) at 25°C.	154
Figure 46: plot of q against $t^{1/2}$ for adsorption of phenol on HiSiv 3000 (particle size =20×50 mesh) at 25°C.	155
Figure 47: plot of q against $t^{1/2}$ for adsorption of phenol on HiSiv 3000 (particle size =1.5 mm, extrude) at 25°C.	156
Figure 48: Equilibrium isotherm models applied to HiSiv 3000 (50×70) data at 40 °C.	157
Figure 49: Isotherm models applied to HiSiv 3000 (50×70) adsorption data at 55 °C.	158
Figure 50: Isotherm models applied to HiSiv 3000 adsorption data at 25 °C, particle size = powder.	159
Figure 51: Isotherm models applied to HiSiv 3000 adsorption data at 25 °C, particle size = 50×70 mesh.	160
Figure 52: Isotherm models applied to HiSiv 3000 adsorption data at 25 °C, particle size = 20×50 mesh..	161

Figure 53: Isotherm models applied to HiSiv 3000 adsorption data at 25 °C, particle size = extrude (1.5 mm).

..... 162

List of Tables

Table 1: Phenol Properties.	2
Table 2: Sorption isotherm parameters of phenol by fly ash at different pH.	12
Table 3: Freundlich parameters for phenol adsorption by GAC at 23 °C for oxic and anoxic experiments.	14
Table 4: List of adsorbents.	37
Table 5: Legends for Figure 13	58
Table 6: Legends for Figure 15.	62
Table 7: The values of rate constants and diffusion coefficients for different adsorbents	86
Table 8: Rate parameters obtained from isothermal diffusion model for phenol adsorption at 25 °C	91
Table 9: Equilibrium model's parameters.	96

Nomenclature

Symbols

C	the adsorbate concentration in the solution, mg/L
$1/n$	Freundlich constant, dimensionless
b, k_1	Langmuir constants, L/mg
b'	pre-exponential factor of b , L/mg
C, C_{Ae}	concentration of phenol in solution at equilibrium, mg/L
C_0, C_{A0}	initial concentration of phenol in solution, mg/L
C_A	concentration of phenol in solution at any time, mg/L
C_A/C_0	normalized concentration, dimensionless
C_{B0}	initial concentration of phenol in adsorbent, mg/L
C_{Be}	concentration of phenol in adsorbent at equilibrium, mg/L
C_B, \bar{C}	concentration of phenol in adsorbent at any time, mg/L
D	intracrystalline diffusivity, cm^2/s
D_f	the film diffusion coefficient, cm^2/s
\bar{D}	the pore diffusion coefficient, cm^2/s
K_c	equilibrium constant, dimensionless
K_f	Freundlich constant, $(\text{mg/g})(\text{L/mg})^{1/n}$
K_h	Henry's constant, L/g

k	rate parameter in isotherm diffusion model, $\text{mg/g}\cdot\text{min}^{1/2}$
k'	overall rate constant, $1/\text{h}$
k_1 and k_2	first order rate constants for adsorption and desorption, respectively, $1/\text{h}$
m	amount of adsorbent used in each bottle, g.
m_n	mass of adsorbent particles used in n^{th} adsorption cycle, g
m_{n+1}	mass of adsorbent particles used in $(n+1)^{\text{th}}$ adsorption cycle, g
q	concentration of phenol in adsorbed phase after reaching equilibrium, mg/g .
q_m	maximum value of q , mg/g
q_0	initial concentration of phenol in adsorbed phase, mg/g .
Q, Q_0	maximum adsorption due to monolayer coverage, mg/g
r_0	radius of the adsorbent particle, cm
t	contact time, min (or h)
$t_{1/2}$	time required to reach 50% of equilibrium capacity, h
T	temperature, $^{\circ}\text{C}$
TOC	total organic carbon mg/L
$U(t)$	fractional uptake, dimensionless
V	volume of solution in each bottle, L
$W_{\text{+ads.}}$	weight of filter paper containing adsorbent particles, g
W_0	weight of filter paper before it was used, g
W_{end}	weight of filter paper after removing the adsorbent particles, g
X_A	fraction of adsorption of phenol at equilibrium, dimensionless

Greek Symbols

δ	film thickness, cm.
α	parameter used in 3-parameter equilibrium isotherm model, L/mg
β	parameter used in 3-parameter equilibrium isotherm model, (L/mg) ^r
γ	parameter used in 3-parameter equilibrium isotherm model, dimensionless
ΔG	free energy change, kcal/mol
ΔH	apparent enthalpy change, kcal/mol
ΔS	entropy of adsorption, kcal/mol
σ_0	free energy of the surface covered with pure solvent, kcal/mol
σ_1	free energy of the surface covered with a monolayer of solute, kcal/mol

Chapter One

Introduction

Phenol is utilized in manufacturing or produced as a side product in the following industries: coking, domestic gas, insulation, paint, paper, plastics, pharmaceuticals, oil and gasoline, steel, textiles, and wood. Appreciable portions of phenolic material leave the manufacturing facility as phenol-laden aqueous wastes. These phenolic wastes are largely resistant to biological degradation in municipal wastewater treatment plants.

Phenols and related compounds are potentially toxic to humans and aquatic life, create an oxygen demand in receiving waters, and impart a taste and odour to drinking water with even minute concentrations of their chlorinated derivatives. Water treatment plants normally disinfect water by chlorination, consequently forming the undesirable chlorophenols when phenols are present (Bharat et al., 1996).

Minute concentration of phenol cause objectionable tastes in potable water and also may taint the flesh of fish. Larger concentrations not only kill fish, but also completely destroy all life in the stream (Abdo et al., 1997).

Phenol is highly toxic by inhalation, ingestion and dermal absorption. The central nervous system may initially be stimulated followed by severe profound depression progressing to the coma. The heart rate may increase then become slow and irregular. The blood pressure may increase slightly and then fall markedly with dyspnea and fall in body temperature. Death may occur from respiratory, circulatory or cardiac failure (Crute, 1992).

US Environmental Protection Agency (EPA) established a standard for phenols in drinking water of one ppb or less, due to their potential toxicity (EPA, 1976). Phenol properties are illustrated in Table 1. Additional information about structure of phenol and determining the size of phenol molecule is discussed in Appendix A1.

Table 1: Phenol Properties (CRC Handbook of Chemistry and physics, 1985).

Molecular Weight	94.11
Water Solubility @19°C	50-100 mg/ml
pK _a @ 25°C	9.92
Boiling Point:	182°C
Vapor Pressure @ 25°C	0.350 mm Hg
Melting Point:	40.90°C

It has been demonstrated that conventional water treatment processes are ineffective in removing organic micropollutants (Robeck et al., 1965). The effective and economic removal of organic micropollutants from water is an urgent task in drinking water treatment.

Numerous unit operations have been evaluated for advanced waste treatment of water and waste water such as, chemical clarification, adsorption, oxidation, foam separation, distillation, electrodialysis, freezing ion exchange, reverse osmosis, and filtration. Among these, adsorption has emerged as the most efficient and economical process of removing undesirable organic materials from solution (Zogorski, 1975).

Different kinds of activated carbon are used for removal of organic compounds from water and wastewater. However, high capital and regeneration cost of activated carbon encouraged researchers to look for low-cost adsorbents.

The objective of this research project was to screen various adsorbents for potential application in the removal of phenol from water and compare their adsorption characteristics with commercial adsorbents such as activated carbon. Adsorbents which were used in this research are activated alumina (basic and acidic), activated carbon, filtrisorb 400, silica gel, HiSiv 1000, and HiSiv 3000. Kinetic experiments were performed for these adsorbents at room temperature. It was discovered that HiSiv 3000 had the highest rate of adsorption. Equilibrium experiments were performed for HiSiv 3000 and two commercial adsorbents (activated carbon and filtrisorb 400). Effect of particle size on rate and capacity of adsorption for HiSiv 3000 was investigated by using four different particle sizes (powder, extrude, 50×70 mesh, and 20×50 mesh). Effect of temperature on rate and capacity of adsorption of HiSiv 3000 was studied at 25, 40, and 55°C. Regeneration of HiSiv 3000 was also investigated at 360 °C and the results were compared with activated carbon regeneration obtained from literature.

Having determined the adsorption equilibrium experimentally, various models were applied to the adsorption isotherms for systems in question. Different kinetic models were also evaluated by using the kinetic data obtained for different adsorbents.

Chapter Two

Literature Survey

By increasing the quantity of industrial waste waters, demand for the removal of organic compounds including phenol, has been increased. Adsorption of phenol onto different adsorbents has been investigated to find the relation between adsorption capacity and adsorbent characteristics (such as surface area, pore size distribution, and polarity). Researchers have also studied the effect of other parameters on adsorption capacity such as: temperature, pH of solution, and dissolved oxygen. The results of their studies are discussed in this chapter.

2.1 Different Adsorbents Used for Phenol Adsorption

2.1.1 Activated Carbon

Peel and Benedek (1980), examined the adsorption of phenol from aqueous solution by activated carbon (F-400). Adsorption took up to three weeks to reach equilibrium. Up to

80% of adsorptive equilibrium was reached in the first few hours, but the remaining capacity was utilized very slowly. This study indicated that variations in isotherm behaviour previously reported in literature was not only due to variation in carbon properties and environmental conditions (such as temperature, pH, and buffer strength) but also due to problems in determining attainment of the real equilibrium. Equilibrium results showed that when concentration of phenol in solution was 250 mg/L, capacity of phenol on activated carbon was 258 mg/g.

2.1.2 Fiber Activated Carbon

Juang et al. (1996) studied the adsorption of phenol and its derivatives on fiber activated carbon at 30°C. The adsorption capacity of phenol on fiber activated carbon was %50 lower than related capacity on activated carbon used by Peel and Benedek.

2.1.3 Peat, Fly Ash, and Bentonite

Viraraghavan and Alfaro (1992) investigated the adsorption of phenol by peat, fly ash, and bentonite. The capacities of these adsorbents were much lower than that of activated carbon. Batch kinetic studies showed that an equilibrium time of 16, 15, and 16 hours was needed for the adsorption of phenol by peat, fly ash, and bentonite, respectively. Isotherm experiments showed that phenol removal by peat, fly ash, and bentonite were 46.1%, 41.6%, and 42.5% respectively from initial concentration of approximately 1000 µg/l.

2.1.4 Fly Ash and Impregnated Fly Ash

Singh and Rawat (1994) studied the sorption of phenol by fly ash and impregnated fly ash. They investigated the influence of various factors such as particle size, impregnation of the fly ash, pH, and temperature on the sorption capacity. It was observed that 90% of the sorption capacity of fly ash was achieved within two hours. The capacity of phenol adsorption on fly ash was only %3 of related capacity on activated carbon used by peel and Benedek. Impregnating fly ash by Fe^{3+} , and Al^{3+} ions could only increase the capacity of adsorption by small amount (5 mg/g).

2.1.5 Conclusion of section 2.1:

It was concluded from literature search that activated carbon has a high affinity to remove phenol from water. Therefore activated carbon was chosen as a base of comparison for other adsorbents studied in the present work.

2.2 Effect of Temperature

It has been observed that increasing the temperature enhanced the adsorption capacity of some adsorbents while the opposite phenomenon occurred for other adsorbents. Parfitt and Rochester (1983), reported that the level of adsorption at any particular concentration usually decreases with increasing temperature (in exothermic processes).

This phenomenon might be explained by the effect of temperature on solubility of solute. Generally speaking, solubility will increase by increasing the temperature, as a result the affinity of solute for adsorption will be decreased. However Parfitt and Rochester believed that solubility is not the only factor in reduction of adsorption when the temperature increases. They mentioned that if the increased solubility was the only factor, isotherms obtained at different temperatures could be superimposed when plotted against the relative concentration (x/x_0) where x_0 is the mole fraction at the solubility limit. However, there is not much evidence of this applying. Zogorski and Faust (1978) reported that adsorptive capacity of phenol on granular activated carbon was increased with decreasing temperature (Figure 1). The same phenomenon was observed by Vidic and Suidan (1991) as they investigated the effect of dissolved oxygen on capacity of phenol adsorption on granular activated carbon at 21 and 35°C. Singh and Rawat (1994) studied the sorption of phenol by fly ash and impregnated fly ash. They found that sorption of phenol by fly ash increased as the temperature increased in the range of 30-50°C. Ma et al. (1996), investigated the influence of temperature on the adsorption of phenol by GH-82 powder activated carbon. They observed that with increasing temperature the Freundlich isotherm moves progressively downward, with the gradient of the isotherms ($1/n$) remaining generally constant, but the intercept (K_f) decreasing with increasing temperature.

The effect of temperature on the rate of adsorption always showed that kinetic rate increased with increasing temperature. As a diffusion-limited process, the rate of adsorption of the organics from solution increases as the temperature of the system is increased.

Zogorski et al. (1976) showed that raising the temperature from 10 to 30°C increases the removal rate of phenol by 21%.

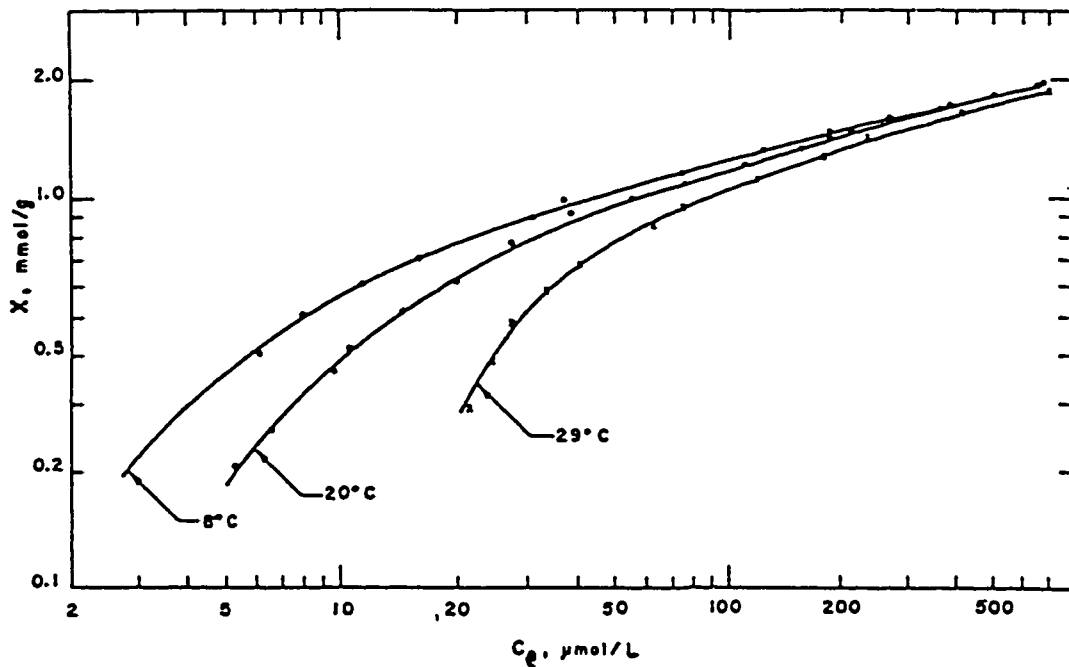


Figure 1: Influence of temperature on the adsorption of phenol on granular activated carbon at pH 6.3 (Zogorski and Faust, 1978).

2.3 Effect of pH

In adsorption of organic solutes from aqueous solutions, the pH value of solution may significantly influence the extent of adsorption if the solute (adsorbate) is dissociated. The

total adsorption includes both the ionized as well as the nonionized species of the adsorbate, and the electrostatic field between the solution and the charged adsorbent surfaces may also play a role in determining the adsorption equilibrium. When solute is dissociated to its components ($\text{pH} \geq \text{pK}_a$) the adsorption process involves more than one species of the adsorbate, so the problem can be seen as a special case of multi-component adsorption (Tien, 1994).

Snoeyink et al. (1969) conducted phenol adsorption isotherms for a coconut-shell based carbon at pH values of 2, 5.6, 7.5, and 10.6 (Figure 2). Results showed that the highest adsorptive capacity was obtained at pH 7.5. In Figure 2 reduction of capacity in the acidic range of pH may be described as competition between acid (used for pH adjustment) and phenol for adsorption sites of adsorbent. As a result the capacity of phenol adsorption was decreased.

Viraraghavan and Alfaro (1992) have studied the effect of pH on adsorption capacity of phenol by peat, fly ash, and bentonite. They found that maximum adsorption capacity was obtained in acidic range of pH.

Singh and Rawat (1994), found the same result for adsorption of phenols by fly ash at different pH values (Table 2). A decrease in pH probably results in a reduction of the negative charges at the surface of fly ash, thus enhancing the sorption of the negatively charged phenolic ions. From Table 2, it is clear that a lower pH value is favourable for higher sorption of phenols (Singh and Rawat, 1994). In general, the adsorption rate of industrial organic pollutants from waste water increases with decreasing pH. An explanation that appears more reasonable is that the increase in sorption observed at decreasing pH values

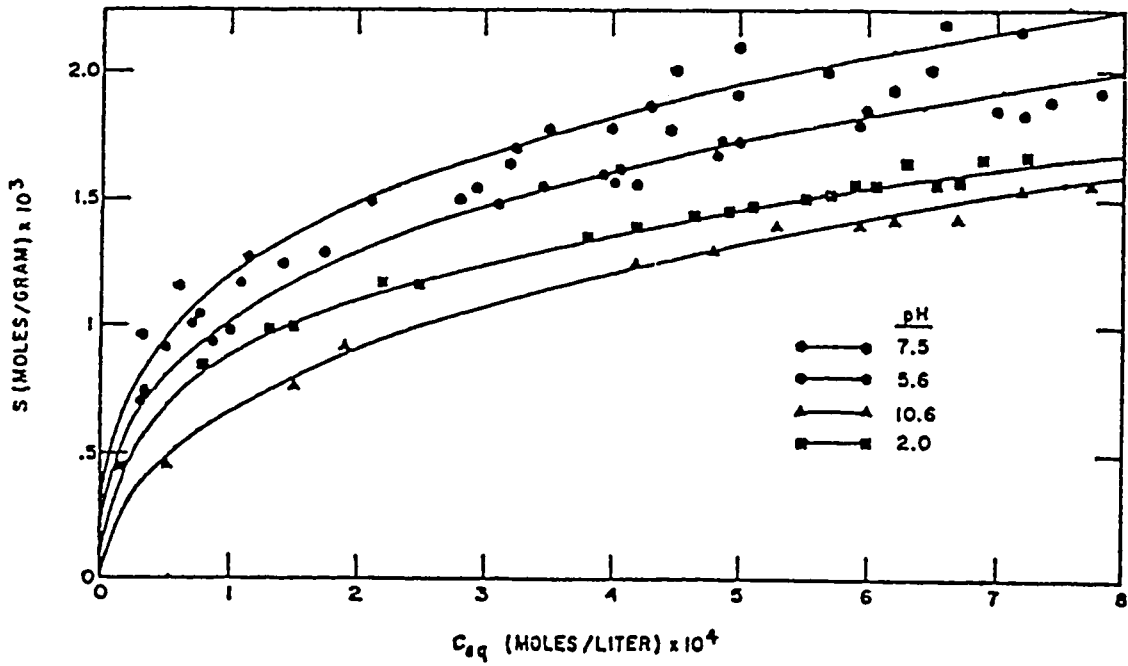


Figure 2: Isotherms for phenol at different pH on coconut-shell based GAC (Snoeyink et al., 1969).

may be caused by alterations in the sorbent surface, particularly its electrokinetic character, with changing hydrogen ion concentration.

Table 2: Sorption isotherm parameters of phenol by fly ash at different pH. Conditions: size 150 μm ; temperature 30 $^{\circ}\text{C}$ (Singh and Rawat 1994).

pH	Freundlich parameters		Langmuir parameter	
	K (mg/g)	1/n	Q_0 (mg/g ⁻¹)	K(mg dm ³)
2	2.483	0.268	4.648	46.48
4	2.317	0.264	4.39	46.1
6.5	2.29	0.212	3.852	38.52
8	2.239	0.181	3.504	36.79
10	1.758	0.247	3.231	35.54

In the present work, adsorption of phenol was studied as a single-component adsorption. Therefore no buffer solution was added to prevent buffer molecules from interfering with phenol molecules for occupying the sites of adsorption.

2.4 Effect of Dissolved Oxygen

Vidic and Suidan (1991), studied the role of dissolved oxygen on capacity of activated carbon. The experiments were conducted at 21 and 35°C. Experimental results proved that the presence of molecular oxygen (oxic procedures) significantly increased the adsorptive capacity of granular activated carbon for phenol (Figure 3). Anoxic procedure requires exclusion of oxygen from isotherm bottles, while oxic procedure provides no control over the amount of oxygen that influence the adsorption process.

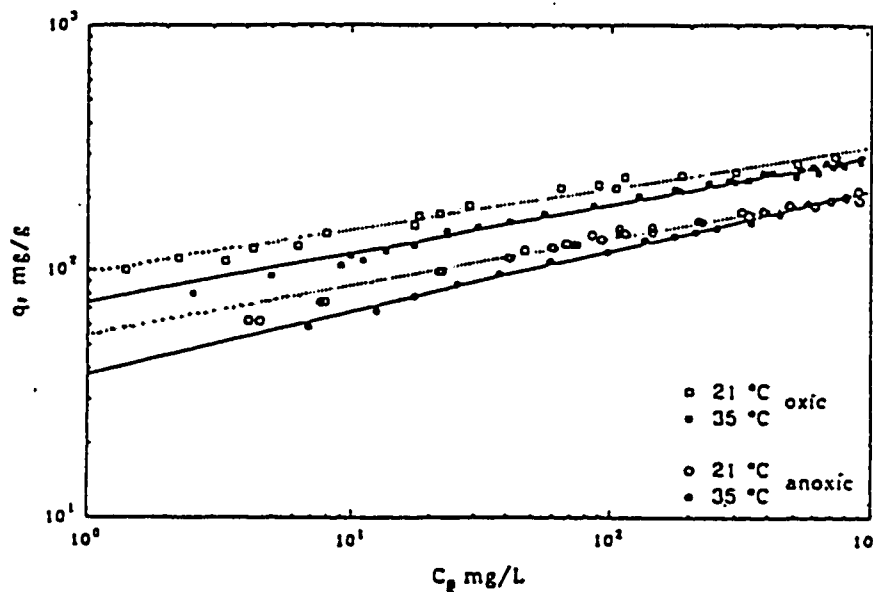


Figure 3: Adsorption isotherms for phenol by granular activated carbon at 21 and 35 °C (Vidic and Suidan, 1991).

Abuzeid, et al. (1995) obtained similar results in their investigation for oxic and anoxic adsorption of phenol by activated carbon. They found that the existence of oxygen in the test environment has tremendously enhanced the adsorptive capacity of GAC for phenol. The values of Freundlich constants for oxic adsorption are higher than the related values for anoxic adsorption (Table 3).

Table 3: Freundlich parameters for phenol adsorption by GAC at 23 °C for oxic and anoxic experiments (Abuzeid et al., 1995).

Isotherm type	k_f (mg/g)(L/mg) ^{1/n}	n	R ²
Oxic	83.5	0.18	0.97
Anoxic	31.7	0.24	0.99

2.5 Regeneration Procedures

In adsorption process when the adsorbent is saturated with pollutant molecules it should be either replaced with a fresh (virgin) adsorbent, or regenerated and reused in another adsorption cycle. Different methods of regeneration have been developed for commercial adsorbents. Regeneration efficiency is affected by the degree of irreversibility of the adsorption. Irreversible solute adsorption on a sorbent surface can be the combined result of the formation of permanent bonds between the solute and the surface (chemisorption) and the irreversible transformation of the adsorbed solute into other species through chemical reactions catalysed by the adsorbent surface (Chatzopoulos and Varma, 1993).

There are different regeneration methods such as: thermal regeneration, chemical regeneration, biological regeneration, and electrochemical regeneration.

2.5.1 Thermal Regeneration

During thermal regeneration of granular activated carbon, physically adsorbed phenol reacts with oxygenated groups of the carbon, and is converted into chemically adsorbed phenol. Between 600 and 900 K (327 and 627°C), the chemically adsorbed phenol decomposes and is released in the form of light gases. Above 900 K (627°C), the chemically adsorbed phenol is degraded into condensation products and graphite (Cook and Lables, 1994). Studies of thermal regeneration have focussed on the optimum condition to restore the maximum adsorbent capacity and to retain, as much as possible, the original pore structure.

Waer et al. (1992) have investigated fluidized-bed regeneration to determine the effects of regeneration temperature and time on volume losses and recovery of adsorptive capacity. The results indicated that for coal-based fiber activated carbon loaded with naturally occurring organic material and methylene blue, the capacity of adsorption was returned to that of virgin carbon at a temperature of 850°C in 15 minutes. Shorter time and lower temperature for regeneration resulted in a loss of adsorptive capacity.

In their investigation, Van Vliet and Venter (1984) found that the optimum regeneration condition for spent granular activated carbon (came from GAC contactor treating secondary effluent) was 8-minute oxidation at 800 °C in an infrared furnace. Although, they were able to restore only 70% of the virgin micropore volume (on a unit bed volume basis) after the fourth regeneration cycle.

The main disadvantages of the thermal regeneration of the activated carbon are: a) the loss of carbon (5-10% per cycle) due to oxidation and attrition and b) the energy cost of heating the GAC to approximately 800 °C (Cen, 1994).

2.5.2 Chemical Regeneration

The basis of chemical regeneration is that adsorbate can be partially desorbed from the adsorbent. Adsorbed phenol reacts with the caustic soda to form sodium phenate which is readily desorbed from the carbon bed. Goto et al. (1986) found that the total amount of sodium phenate desorbed from GAC was only 70% of adsorbed phenol and adsorptive capacity of GAC gradually decreased during the repetition process.

Cooney et al. (1983) chose methanol as the best solvent among nineteen other solvents for phenol adsorption-regeneration. Methanol restored 88% of the fixed-bed adsorptive capacity for phenol after one regeneration, and 81% of the capacity after five cycles. The most disadvantage associated with chemical regeneration is the low regeneration efficiency. Most of the regeneration systems have achieved efficiencies below 70% (Cen, 1994).

2.5.3 Biological Regeneration

Many studies on biological regeneration have been carried out. Sigurdson and Robinson (1978) have investigated the *in situ* biological regeneration of activated carbon loaded with phenol by a pure-culture of *Pseudomonas putida*. The regenerated carbon was found to have only 47% of the adsorptive capacity of the fresh carbon. Wallis and Bolton (1982) found a similar reduction in adsorptive capacity for GAC loaded with phenol and regenerated using *P. putida*. Up to 87% of the activated carbon's original adsorptive capacity was recovered. Hutchinson and Robinson (1990 a and b) have described microbial regeneration of activated carbon loaded with a single-solute (phenol) and a bisolute system containing phenol and *p*-cresol, by a pure culture of *Pseudomonas putida*. Up to 56% of

virgin carbon adsorptive capacity was achieved for the first regeneration cycle, and decreased further with subsequent regenerations.

2.5.4 Electrochemical Regeneration

Sveshinikova, et al. (1987) investigated electrochemical regeneration of activated carbon loaded with phenol in a plexiglass cell. Graphite rods were used as the current conductors, and the electrolyte was a NaCl solution. After five adsorption-regeneration cycles, the adsorptive capacity decreased to 40% of the virgin capacity and it remained unchanged for subsequent cycles.

2.5.5 Conclusion of Section 2.5

In the present study thermal regeneration was chosen because of higher regeneration efficiency.

2.6 Modelling

Two models were applied to kinetic data obtained for activated carbon, F-400, and HiSiv 3000. Also three different models were applied to equilibrium isotherm data obtained for the above mentioned adsorbents.

2.6.1 Kinetic Modelling

The uptake of the adsorbate from a solution by the adsorbent pellet involves several steps causing the adsorbate to go from the bulk fluid phase to the specific sites within the interior of the pellet. The following mass-transfer mechanisms may be present:

1- *Interpellet mass transfer*, which is also referred to as diffusion and mixing of adsorbates in bulk fluid occupying the spaces between the pellets, such as in the case of fixed bed, moving bed, or fluidized-bed operations. In a well-agitated batch system, interpellet mass transfer is so rapid that it is not considered as the rate controlling step.

2- *Interphase mass transfer*, which is also called “film diffusion”, refers to the transfer of the adsorbate across the fluid pellet interface.

3- *Intrapellet mass transfer* which refers to the diffusion of adsorbates (either dissolved or adsorbed) within the pellet. There are two mechanisms for diffusion of adsorbate within the adsorbent particle:

- ▶ Pore diffusion
- ▶ Surface diffusion

For intrapellet diffusion, since the intracrystalline pores (micropores) are small, the diffusing molecules are always within the force field of the adsorbing surface, and their

transport takes place in the form of “molecule hopping” between adsorption sites. Thus, the process is more similar to surface diffusion than to ordinary pore (or macropore) diffusion, except that the domain through which diffusing molecules migrate is not a two-dimensional surface but rather a three-dimensional space (Tien, 1994). A schematic diagram showing various mass transfer mechanisms is shown in Figure 4. The numbers shown in this figure are related to different mass transfer mechanisms as follows:

- 1: Interphase mass transfer
- 2: Intrapellet mass transfer
 - 2a: Pore diffusion
 - 2b: Surface diffusion
- 3: Adsorption

A common feature of adsorbent materials is their large specific surface area. Structurally, adsorbent pellets are inevitably microporous and adsorption takes place almost exclusively in the pellets' internal void surface. Consequently, uptake of adsorbates requires their molecules to diffuse into the interior of the pellets. Since pellets are microporous and their void (pore space) is occupied by the fluid to be treated by adsorption, adsorbate may diffuse within the fluid because of the presence of the radial concentration gradient (pore diffusion). The presence of concentration gradient implies the existence of a similar concentration gradient in the adsorbed phase, which in turn, causes the diffusion of adsorbed molecules (surface diffusion, Figure 4-2b). Both types of diffusion may be operative simultaneously or individually.

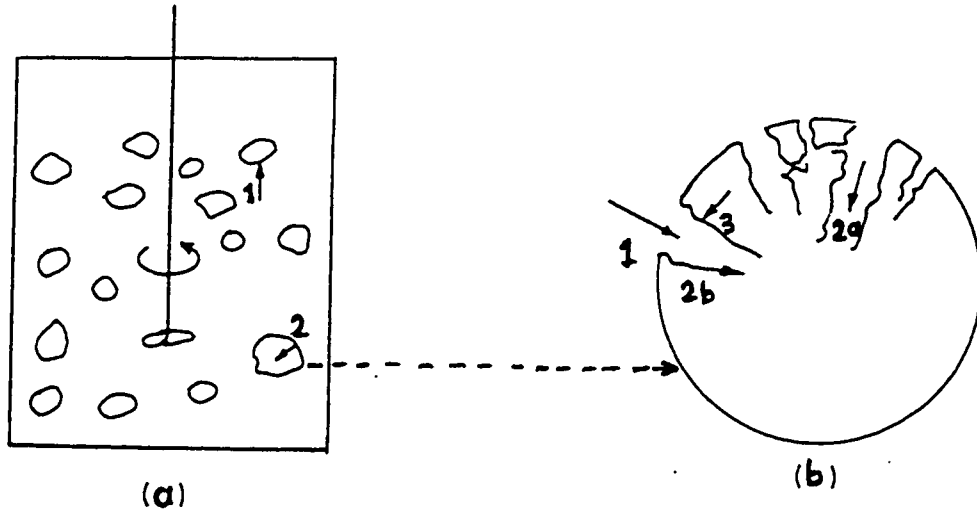


Figure 4: Mass transfer in adsorption process. (a) batch system, (b) intrapellet mass transfer (Tien, 1994).

Pore diffusion (Figure 4-2a) operates if the intrapellet mass transfer is due only to the diffusion of adsorbate molecules through the pore fluid. Generally speaking, diffusion in the fluid phase results from collisions between molecules and with surfaces. Molecular diffusion, would be dominant if the pores were sufficiently large. On the other hand, if pore size is small, collisions between the fluid molecules and the pore surface become significant, and must be considered in the intrapellet diffusion process. In the limiting case, in which the pores are small (to the extent that the pore radius is less than the mean free path of fluid molecules), collisions of fluid molecules with the pore surface dominate, resulting in an entirely different type of diffusion known as Knudsen diffusion. (Tien, 1994).

Pore diffusion may occur by several different mechanisms depending on the pore size, the sorbate concentration, and other conditions. In fine micropores such as the intracrystalline pores of zeolites, the diffusing molecule never escapes from the force field of the adsorbent surface and transport occurs by an activated process involving jumps between adsorption “sites”. Such a process is often called “surface diffusion” (Figure 4-2b), but the implication of a two-dimensional surface is unnecessarily restrictive since the micropore structure in a zeolite crystal is often three-dimensional. Diffusion in larger pores such that the diffusing molecule escapes from the surface field is referred to as macropore diffusion. This distinction between micropore and macropore diffusion is useful since, in a zeolitic adsorbent, the diameter of the intracrystalline micropores is generally much smaller than that of the smallest intercrystalline macropores. Generally the size of micropores is less than 2 nm, and the size of macropores is larger than 50 nm (Ruthven, 1984).

Many commercial adsorbents consist of small microporous crystals formed into a macroporous pellet. Such adsorbents offer two distinct diffusional resistances to mass transfer: the micropore resistance of the adsorbent crystals and the macropore diffusional resistance of the pellet. When adsorption occurs from a binary fluid mixture, there may be an additional resistance to mass transfer associated with transport through the laminar fluid boundary layer surrounding the particle (Ruthven, 1984). These principal resistances are sketched in Figure 5. The pellet has a radius of R_p and is composed of many spherical microporous crystals of radius r_c , with $r_c \ll R_p$.

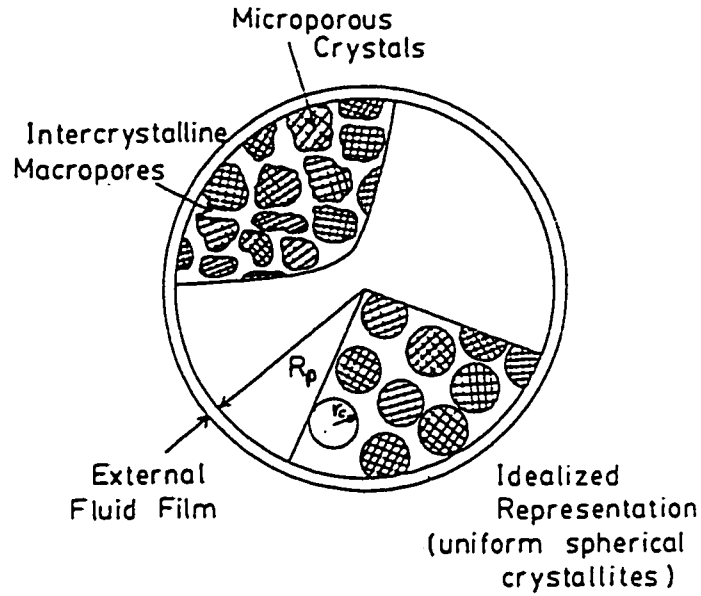


Figure 5: Schematic diagram of composite adsorbent pellet showing the three principal resistances to mass transfer (Ruthven, 1984).

2.6.1.1 First Order Reversible Model

An adsorption model similar to first order reversible kinetic reaction model (Bhattacharya and Venkobachar, 1984) was used to establish the rates of adsorption which can be expressed as:



where A and B represent the liquid phase and adsorbed phase, respectively. k_1 and k_2 are first order rate constants for adsorption and desorption, respectively (1/h).

If the first order reversible kinetic model holds true, the rate equation for the adsorption is expressed as:

$$\frac{dC_B}{dt} = -\frac{dC_A}{dt} = C_{A0} \frac{dX_A}{dt} = k_1 C_A - k_2 C_B = k_1 (C_{A0} - C_{A0} X_A) - k_2 (C_{B0} + C_{A0} X_A) \quad (2)$$

where:

C_B = Concentration of phenol in adsorbent at any time (mg/L)

C_A = Concentration of phenol in solution at any time (mg/L)

C_{B0} = Initial Concentration of phenol in adsorbent (mg/L)

C_{A0} = Initial Concentration of phenol in solution (mg/L)

X_A = Fractional adsorption of phenol

At equilibrium conditions, Equation 2 can be written as:

$$\frac{dC_B}{dt} = -\frac{dC_A}{dt} = 0 \quad (3)$$

and

$$X_{A_e} = \frac{K_c \cdot C_{B0}}{K_c + 1} \quad (4)$$

where K_c is the equilibrium constant and its value is given as:

$$K_c = \frac{C_{B_e}}{C_{A_e}} = \frac{C_{B_0} + C_{A_0} X_{A_e}}{C_{A_0} - C_{A_0} X_{A_e}} = \frac{k_1}{k_2} \quad (5)$$

and X_{A_e} = Fraction of adsorption of phenol at equilibrium

C_{B_e} = Concentration of phenol in adsorbent at equilibrium (mg/L)

C_{A_e} = Concentration of phenol in solution at equilibrium (mg/L)

The rate equation in terms of equilibrium adsorption can be obtained from Equation 2, 4, and 5 as follows:

$$\frac{dX_{A_e}}{dt} = (k_1 + k_2)(X_{A_e} - X_A) \quad (6)$$

Integration of Equation 6 and substituting for k_2 from Equation 5 gives:

$$-\ln\left(1 - \frac{X_A}{X_{A_e}}\right) = k_1\left(1 + \frac{1}{K_c}\right)t \quad (7)$$

Equation 7 can be rewritten as:

$$\ln[1 - U(t)] = -k't \quad (8)$$

in which k' is the overall rate constant. Further

$$k' = k_1\left(1 + \frac{1}{K_c}\right) = k_1 + k_2 \quad (9)$$

and

$$U(t) = \frac{C_{A0} - C_A}{C_{A0} - C_{Ae}} = \frac{X_A}{X_{Ae}} \quad (10)$$

where, $U(t)$ is called the fractional uptake. By plotting the value of $\ln[1 - U(t)]$ vs. time, the overall rate constant k' can be determined from the initial slope of this curve (see Eq. 8). After finding k' the value of $t_{1/2}$ (time required to reach half of the equilibrium capacity) can be calculated from Eq. 8 by substituting $U(t) = 1/2$.

If pore diffusion is rate controlling, the value of $t_{1/2}$ can be correlated to the pore diffusion coefficient as described in Eq. 11:

$$t_{1/2} = 0.030 \frac{r_0^2}{\bar{D}} \quad (11)$$

r_0 = the radius of the adsorbent particle (cm)

\bar{D} = the pore diffusion coefficient (cm²/s)

If film diffusion is dominant, diffusion coefficient D_f can be defined by Eq. 12, assuming spherical geometry for the adsorbent particles (Helfferich, 1962).

$$t_{1/2} = 0.23 \frac{r_0 \delta \bar{C}}{D_f C} \quad (12)$$

where:

δ = The film thickness generally in the order of 10^{-3} to 10^{-2} cm, depending on agitation. In well-stirred solution $\delta = 10^{-3}$ cm.

D_f = the film diffusion coefficient (cm^2/s)

\bar{C} = the adsorbate concentration in the adsorbent particle (mg/L)

C = the adsorbate concentration in the solution (mg/L)

2.6.1.2 Isothermal Diffusion Model

Rates of adsorption and desorption in porous adsorbents are generally controlled by transport within the pore network, rather than by the intrinsic kinetics of sorption at the surface. Since there is generally little, if any, bulk flow through the pores, it is convenient to consider intraparticle transport as a diffusive process and to correlate kinetic data in terms of a diffusivity defined in accordance with Fick's first equation (Ruthven, 1984):

$$J = -D \frac{\partial c}{\partial X} \quad (13)$$

where D is the intracrystalline diffusivity.

The simplest case to consider is a single microporous adsorbent particle, such as a zeolite crystal, exposed to a step change in sorbate concentration at the external surface of the particle at time zero. For most particle shapes, representation as an equivalent sphere is an acceptable approximation and transport may therefore be described by a diffusion equation, written in spherical coordinates:

$$\frac{\partial q}{\partial t} = \frac{1}{r^2} \frac{\partial}{\partial r} \left(r^2 D \frac{\partial q}{\partial r} \right) \quad (14)$$

where q is the adsorbed phase concentration. By solving this equation with appropriate initial and boundary conditions, for fractional uptake less than 30% the solution of Eq. 14 can be simplified as shown in the following expression:

$$U(t) \approx \frac{2A}{V} \left(\frac{Dt}{\pi} \right)^{1/2} \quad (15)$$

which shows a linear relationship between the fractional uptake $U(t)$, and the square root of time (Ruthven, 1984). $\frac{A}{V}$ is the ratio of external area to partial volume (for spherical particles, $\frac{A}{V} = 3/\text{radius of adsorbent particle}$). Since the diffusivity (D) and adsorbent particle size (r) were assumed constant the adsorbate uptake was linearly dependent on the square root of time. Consequently, a rate parameter (k) was defined, as the initial slope of the graph of: the amount of adsorbate per gram of adsorbent, versus $t^{1/2}$ (McKay, 1983).

2.6.2 Equilibrium Modelling

Van der Waals or cohesive forces act between the molecules of all substances irrespective of their state of aggregation. In the bulk of a phase, intermolecular cohesive forces are balanced. But in solids, liquids or gases the atoms, ions or molecules in the interface (surface layer) are exposed to the action of unbalanced forces due to both phases, these resultant forces act normal to the phase boundary. The unbalanced forces at the phase boundary cause changes in the number of molecules (atoms, ions) existing on the boundary surface as compared to the corresponding numbers within the bulk phases (Ościak, 1982).

This change in concentration at the surface is referred to adsorption, which may be a physical process (physisorption) taking place due to Van der Waals forces, hydrogen bonding, etc., or it may be due to chemical processes and to the formation of chemical compounds (chemisorption). An adsorption isotherm is an expression of the equilibrium distribution between the concentration of a species on the adsorbent surface and the concentration in solution at constant temperature.

Adsorption processes are classified as purification processes if the components which are adsorbed are present only at low concentration, and have little or non economic value, and are frequently not recovered. Another application of adsorption is separation of mixtures into two or more streams, each enriched in a valuable component which is to be recovered (Ruthven, 1984).

The interaction between the surface and adsorbed species may be either chemical or physical. Several types of bonding can be identified as follows:

- 1) Chemical adsorption (chemisorption),
- 2) Hydrogen binding,
- 3) Hydrophobic bonding, and
- 4) Van der Waals forces.

The net interaction of an adsorbate molecule with a surface might involve more than one type of interaction, depending on the chemical structure of both the adsorbent and the adsorbate.

The most favoured approach to an investigation of the adsorption mechanism is a study of the isotherm. The important aspects are: (a) the rate of adsorption; (b) the shape of the isotherm; (c) the significance of the plateau found in many isotherms; (d) the extent of solvent adsorption; (e) whether the adsorption is monomolecular or extends over several

layers; (f) the orientation of the adsorbed molecules; (g) the effect of temperature; (h) the nature of the interaction between adsorbate and adsorbent (Parfitt and Rochester, 1983).

A variety of isotherm shapes have been reported for adsorption from dilute solutions, and a theoretical basis was given to the classification adopted. The various isotherm shapes considered are shown in Figure 6. Four characteristic classes are identical, based on the form of the initial part of the isotherm; the subgroups relate to the behaviour at higher concentrations. The L (Langmuir) class is the most common and is characterized by an initial region which is concave to the concentration axis. The L2 isotherm reaches a plateau, further adsorption above this value gives the L3 isotherm, and if that reaches a second plateau it is designated L4. The fifth L type shows a maximum and reflects a special set of circumstances—they are found with solutes that associate in solution (certain dyes) and contain highly surface-active impurities (a maximum is not thermodynamically possible in a pure system). A similar set of isotherms are associated with the other classes, although not all have been observed. For the S class the initial slope is convex to the concentration axis, and this is frequently followed by a point of inflection leading to an S-shaped isotherm. The H (high affinity) class results from extremely strong adsorption at very low concentrations giving an apparent intercept on the ordinate; the C class has an initial linear portion which indicates constant partition of the solute between solution and adsorbent, and occurs with micro-porous adsorbents. The H (high affinity) class results from extremely strong adsorption at very low concentrations giving an apparent intercept on the ordinate; the C class has an initial linear portion which indicates constant partition of the solute between solution and adsorbent, and occurs with micro-porous adsorbents. If the interaction between adsorbed molecules is negligible, the activation energy will be independent of coverage, and this leads to an L or

H isotherm. When the force of interaction between adsorbed molecules is significant relative to that between solute and adsorbent, the activation energy will be higher, and cooperative adsorption occurs corresponding to the S isotherm. In this case the solute molecules tend to be packed in rows or clusters on the surface and this situation is encouraged when the solvent is strongly adsorbed and the solute is mono-functional, e.g. the adsorption of a mono-hydric phenol on a polar surface (alumina) from a polar solvent (water). The adsorption isotherm for *p*-nitrophenol on silica from dry benzene is L shape; saturation of the benzene with water leads to the S shape, since the water strongly competes with the solvent for the surface. Parallel orientation of solute gives L type isotherms. Some dyes form aggregates in solution, and these are adsorbed giving the S shape (e.g. certain cyanine dyes on silver halides). The H curves are associated with chemisorption or other strong interactions e.g. stearic acid from benzene on metal powders. The C curve is found with micro-porous adsorbents, and is consistent with conditions in which the number of adsorption sites remains constant throughout the concentration range.

As sites are covered new sites appear, and the surface available expands proportionally with the amount of solute adsorbed. The inflections in subgroup 3 and the second plateau in subgroup 4 may reflect a change in orientation of the adsorbed solute, e.g. sodium dodecyl sulfate on carbon from aqueous solution, or the formation of a second layer, e.g. long-chain ammonium salts on polystyrene latexes (Parfitt and Rochester, 1983).

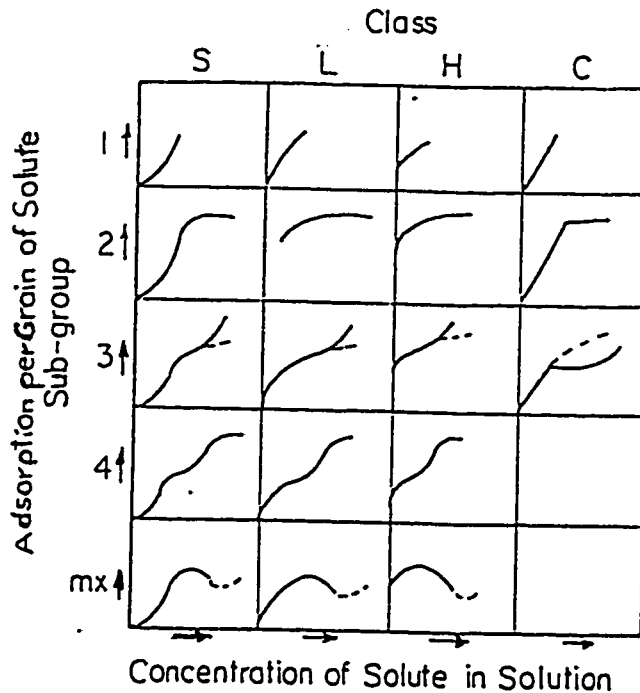


Figure 6: Classification of solute in solution (Tien, 1994)

Mechanism of adsorption is affected by different possible variables. It will be convenient to identify certain critical features of these variables.

(i) The properties of the adsorbent, such as the surface area, pore size and distribution, surface functional groups, and other surface characteristics. Surface contamination from exposure to the environment might be sufficient to cause significant variations. Preparative methods vary, and removal of surface impurities is usually not always treated with the attention it deserves.

(ii) The nature of the adsorbate: several features of solute structure are obviously relevant, e.g. chain length, ring structure, nature of polar groups, and physical state in

solution. Solubility is also important, a factor naturally related to the others. Deviations from ideality in solution might also be expected to affect the adsorption behaviour.

(iii) The properties of the solution, such as pH, temperature, pressure, adsorbate concentration, ionic strength, presence of background and competitive solutes (Parfitt and Rochester, 1983).

For liquid systems, the term *single-component adsorption* refers to the adsorption of a single adsorbate from liquid solutions in which the activity of the solvent is constant, or, in other words, the presence of the solvent may be ignored. Single-solute equilibrium data can generally be described adequately by one or more isotherm equations. The most widely used equilibrium models describing single solute adsorption are summarized below.

2.6.2.1 Linear Isotherm (Henry's Law)

The linear isotherm is valid only at very low concentration ranges. The relation between capacity and concentration is described by following equation:

$$q = K_h \cdot C \quad (16)$$

where q , C , and K_h are solid concentration of the adsorbate (mg of adsorbate/g of adsorbent), solution concentration of the adsorbate (mg/L), and Henry's constant respectively. This equation is inadequate in characterizing the adsorption of organics from aqueous solution over large concentration ranges. Therefore this equation was not applied in present study.

2.6.2.2 Langmuir Model

The simplest and by far the most widely used expression for physical adsorption (or even chemisorption) is the Langmuir equation. This model was originally developed to describe sorption on a set of distinct localized adsorption sites, and it has been used to describe both physical and chemical adsorption. This model is based on the following assumptions [Dechow, 1989] :

- each active site interacts with only one adsorbate molecule.
- sorbate molecules are adsorbed on well defined localized sites.
- there is no interaction between adjacent adsorbed molecules.
- the adsorption sites are all energetically equivalent.

The Langmuir isotherm equation is as follows:

$$q = \frac{Q \cdot b \cdot C}{1 + b \cdot C} \quad (17)$$

Q and b are the Langmuir constants, representing the maximum adsorption capacity and the energy constant related to the heat of adsorption, respectively. The linear form of Langmuir equation is as follows:

$$\frac{1}{q} = \frac{1}{Q} + \frac{1}{Q \cdot b \cdot C} \quad (18)$$

Q and b can be evaluated from the intercept and the slope of the linear plot of the experimental data of $1/q$ vs. $1/C$.

The Langmuir constant b can be used to calculate the change in the apparent enthalpy and entropy of adsorption using following thermodynamic equations (Panday et al., 1985).

$$\ln b = \ln b' - \Delta H / RT \quad (19)$$

$$\ln(1 / b) = -\Delta G / RT \quad (20)$$

$$\Delta S = (\Delta G - \Delta H) / RT \quad (21)$$

where b' is the adsorption energy constant, ΔG is the free energy change for adsorption and T is the absolute temperature of the solution. ΔH is determined from the slope of $\ln b$ vs $1/T$, while ΔG and ΔS can be determined directly from Equations 20 and 21 respectively, for a given temperature.

2.6.2.3 Freundlich Model

This model is derived from Gibbs adsorption equation:

$$q = K_F \cdot C^{1/n} \quad (22)$$

where K_F is a Freundlich constant related to the sorption capacity, and $1/n$ is related to the sorption intensity that is defined as:

$$1 / n = (RT q_m / \sigma_0 - \sigma_1) \quad (23)$$

where q_m is the monolayer capacity of the sorbent for the solute, σ_0 and σ_1 are the free energies of the surface covered with pure solvent and with a monolayer of solute,

respectively. The following linearized form of the Freundlich isotherm model can be used to obtain the values of the Freundlich constants:

$$\ln q = \ln K_F + 1/n \cdot \ln C \quad (24)$$

The intercept and the slope of the linear plot of $\ln q$ vs. $\ln C$ at a given experimental condition provide the values of K_F and $1/n$, respectively. The Freundlich equation, in many ways, is the simplest equation for data representation. It does have a serious defect, namely, it fails to observe Henry's law behaviour in the limiting situations of $C \rightarrow 0$

2.6.2.4 Three-parameter Isotherm

Radke and Prausnitz (1972), developed a three-parameter isotherm model which was a combination of Langmuir and Freundlich isotherms. Three-parameter model can be expressed as :

$$q = \frac{\alpha \cdot C}{1 + \beta \cdot C^\gamma} \quad (25)$$

α , β , and γ are estimated by fitting experimental data to the Equation 25. At low solution concentrations the equation reduces to the linear isotherm of Henry's law; at high solution concentrations, the expression is equivalent to the Freundlich isotherm; and for the special case of $\gamma = 1$, the model becomes the Langmuir isotherm. This isotherm generally describes adsorption data very well.

Chapter Three

Materials and Methods

3.1 Materials

Kinetic and equilibrium experiments were performed for several adsorbents to determine the rate and capacity of adsorption for each adsorbent. Table 4 shows the list of adsorbents which were used in this study.

In this study activated carbon (pellet) and powder adsorbents such as activated alumina, silica gel, and HiSiv (1000, and 3000) were used as is. Filtrasorb 400 which had a large range of particle size was sieved through the mesh (14×20) to obtain the particle size similar to activated carbon particle size. To investigate the effect of particle size on HiSiv 3000, pellet adsorbent was crushed and sieved through the meshes (20×50) and (50×70) to obtain smaller particle sizes. Pretreatment of each adsorbent was performed at 360°C to remove any compounds which might exist in adsorbent pores. All the adsorbents were stored in air-tight bottles until they were used.

Deionized-distilled water filtered through milipore purification system (Zenopure corporation, Quatra 90 LC), was used for preparation of the sorbate solutions. Reagent grade phenol (%99.99 from Aldrich chemical company) was used to prepare phenol solutions.

Table 4: List of adsorbents.

Adsorbent	Particle size	Name of Company
Activated carbon	0.8 mm	Sigma-Aldrich, Canada
Filtrisorb 400 (F-400) [obtained from bituminous coal]	0.55-0.75 mm	Calgon, Mississauga, Ontario, Canada
Activated alumina (Acidic)	63-150 μm	Fisher Scientific, Canada
Activated alumina (Basic)	63-150 μm	Alcan Chemical, Brockville, Ontario, Canada
Silica gel	63-200 μm	Fisher Scientific, Canada
HiSiv 1000 [Zeolite-Y structure]	Powder < 100 μm	UOP Molecular Sieve, USA
HiSiv 3000 [ZSM-5 zeolite structure]	Powder < 100 μm 50 \times 70 mesh (212-297 μm) 20-50 mesh (297- 850 μm) Extrude (1.5 mm)	UOP Molecular Sieve, USA

3.2 Experimental Methods

3.2.1 Kinetic Experiments

200 mg/L phenol solution was prepared and transferred to a 2-L glass vessel. The vessel was submerged in a water bath controlled at a predetermined constant temperature by a thermostat (precision: $\pm 0.5^{\circ}\text{C}$). After the temperature of the adsorbate solution was stabilized at a predetermined level, a known weight adsorbent was immersed in the vessel and agitation was immediately initiated (speed of stirring: 220 rpm). This was time zero for the kinetic experiment. Small-volume liquid samples (6 ml) were withdrawn from the vessel at predetermined time intervals. Then samples were filtered by using glass fiber filter papers (Pore size= 0.5-1 μm , Whatman company). The relation between the adsorbate concentration in the liquid phase and the contact time was determined to generate a concentration decay curve.

3.2.2 Equilibrium Experiments

An adsorption isotherm describes the relationship between the amount of adsorbate that accumulates on the adsorbent and the equilibrium concentration of dissolved adsorbate. Accurately weighed portions of adsorbent were placed into a series of 125-ml bottles. After the addition of 75 ml of phenol solution, bottles were sealed with glass stoppers. Initial concentration of phenol in liquid phase was 200 mg/L for all the experiments. The bottles were placed in an air-bath shaker (Eberbach Corporation, Ann Arbor, Michigan) until they reached equilibrium. The speed of shaker was adjusted to 180 rpm, to let the solutions mix well. Included in each set of bottles, were two control bottles. One of the control bottles

contained just the phenol solution with no adsorbent, and the other one contained just water and adsorbent with no phenol in the solution. The control bottles were used to check for phenol volatilization and/or adsorption onto the walls of the container during the equilibration period. Equilibrium time was determined from the kinetic studies. The bottles were then taken off the shaker and the suspensions were left standing for a while to allow the adsorbent particles to settle. 10 ml of the supernatant were removed from the bottles with syringe and filtered through glass fiber filter paper to remove any remaining adsorbent particles. To minimize the adsorption of the substrate on filters, 2 ml of the sample were filtered and discarded before filtrate samples were taken for analysis. Equilibrium experiments were conducted at room temperature (25 ± 1) for all of the adsorbents. To study the effect of temperature on capacity of adsorption by HiSiv 3000 (50-70 mesh) additional equilibrium experiments were conducted for this adsorbent at 40 and 55 °C. Isotherm curves were determined from changes in liquid concentration in the bottles before and after the tests (a sample solution is shown in Appendix A).

3.2.3 Methods of Analysis

Phenol concentration in liquid phase were measured with either a UV-spectrophotometer (Backman, Model: DU640) or a TOC-analyzer (Rosemount Analytical Inc., Model DC 190). UV-spectrophotometer was used for analyzing the solutions which were clear and colorless, otherwise TOC analyzer was used. However each method had specific errors associated with its measurement. These methods and their possible errors are discussed in the following section.

UV-spectrophotometer

UV wavelength in nanometer, was used for determining concentration of phenol in liquid phase. Each time, a calibration curve for phenol was constructed from a series of standard solutions of known concentration. Samples were measured with UV-silica cells (17×45 mm, Beckman Company). Highly concentrated samples were diluted with deionized-distilled water before measurements. Comparison of the absorbance values to the calibration curves allowed for calculation of the equilibrium adsorbate concentration.

Possible errors associated with UV-spectrophotometer:

1-Light reduction: blank (or reference) cell and sample cell should read the same transmission value when they are filled with the same solution. However, one or both of the cells may be deteriorated by etching (caused by continued use of strong alkali or acid solution). As a result transmission readings might be inaccurate.

2- Inadequate cleaning: UV-silica cells should be rinsed immediately after each use with a mild solvent. However after a long term use, films might be deposited by inadequate cleaning, which may decrease the transmission properties of the cell, and may also cause contamination of subsequent samples.

Total Organic Carbon (TOC) Analyzer

Shell vials (17×160 mm, Kimble glass Inc., USA) were used to determine the amount of TOC in each sample. Phenol solution contained phenol crystals with 99.99% purity, so it was assumed that total organic carbon measured with TOC analyzer was directly related to

concentration of phenol in each sample. Following equations were used to convert the TOC values into phenol concentration values.

$$\text{Conversion Factor} = \frac{(\text{MW})_{\text{Phenol}}}{(\text{MW})_{\text{Carbon}}}$$
$$\Rightarrow \text{Phenol Concentration [mg / L]} = (\text{Conversion Factor}) * (\text{TOC [mg / L]})$$

where:

$(\text{MW})_{\text{Phenol}}$ = molecular weight of phenol

$(\text{MW})_{\text{Carbon}}$ = molecular weight of carbon

Possible errors associated with TOC measurement:

TOC analyzer automatically determines a calibration factor by analyzing one standard solution. This solution should contain exactly a specific amount within the required range of TOC concentration in the sample vials. Small error during preparation of standard solution may change the calibration factor which may considerably affect the analysis.

Comparison between spectrophotometer and TOC analyzer

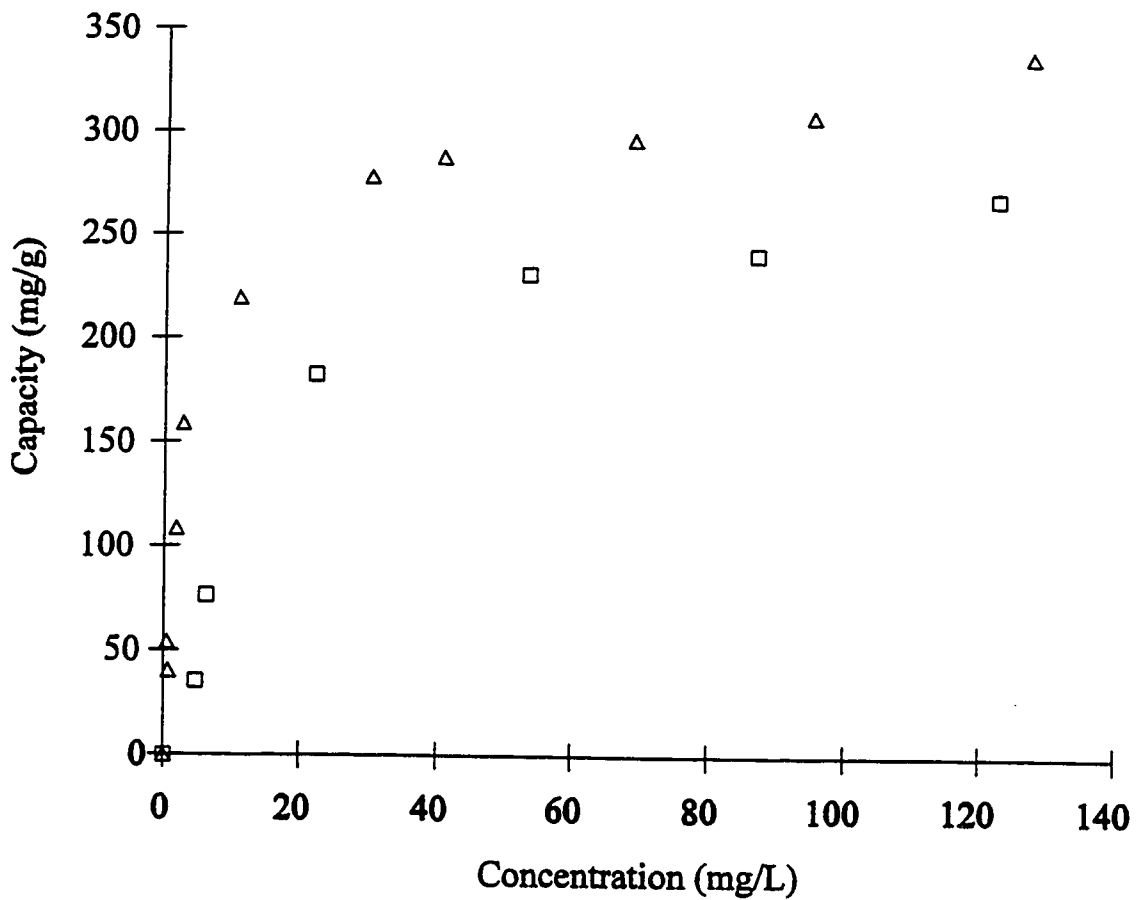
To compare the analyzing results of spectrophotometer with TOC analyzer, two set of equilibrium experiments were performed for activated carbon, under the same initial concentration of phenol. The first test was performed for 14 days , and the second test was carried out for 29 days. The samples from first test (shorter time) were analyzed with spectrophotometer and the samples from second test (longer time) were analyzed with TOC

analyzer. The result of activated carbon isotherms by using spectrophotometer and TOC analyzers are shown in Figure 7. The capacity of adsorption in the first test was supposed to be equal to or smaller than the capacity of adsorption for the second test since it was analyzed after a shorter time. Also, the pretreatment temperature in the first test is lower at 106°C, while the pretreatment temperature for the second test was 360°C. But Figure 7 shows the opposite result. The reason might be related to dilution factor which were used in spectrophotometer analysis. When the spectrophotometer read a value for absorption of a sample, it compared it with a standard curve which related absorption values to concentration of phenol. If this value does not lie in linear portion of the standard curve, the sample should be diluted until its absorption value lies in the linear range of the standard curve. In spite of applying precise dilution method by using micro-pipette, the results of spectrophotometer measurement were still different from those obtained by TOC analyzer measurements. With very small concentration used in this study, it was observed that TOC analyzer results were more reproducible than UV-spectrophotometer analysis. Therefore it was decided to use TOC analyzer for most of the experiments.

Common errors associated with the experimental measurement:

Experimental data are associated with some experimental measurement errors which enter into the overall accuracy of the calculation, making the results less accurate. The most susceptible calculations are those which apply to:

- ***Low adsorbent dosages:*** After measuring small amount of adsorbent, it should be transferred to a container. Meanwhile a small portion of particles may be lost. This small loss



△ Spectrophotometer □ TOC analyzer

Figure 7: Results of phenol adsorption on activated carbon, using spectrophotometer and TOC analyzer at 25 °C.

of particles may not introduce much error in calculations when large amount of adsorbent is used. But for low adsorbent dosage, the loss of small portion of adsorbent during experimental work, will introduce considerable error in any calculation related to the weight of adsorbent.

- **High adsorbent dosages:** In this case, the concentration of solute in liquid will decrease when high amount of adsorbent is used. As a result, solute concentration may be too low to be detected accurately.

In the present work it was observed that when the concentration of phenol in solution was higher than 150 mg/L some errors were introduced to calculation as a result of “low adsorbent dosage”.

3.2.4 Regeneration Method

Regeneration of HiSiv 3000 was studied by using thermal regeneration method. Accurately weighed portions of adsorbent were placed into a series of bottles. Adsorption experiments were performed for 16 hours. Then adsorbent particles in each bottle were filtered through pre-weighed glass filter paper (Pore diameter=0.5 μm). After filtration, filter papers were dried at 110°C and cooled to room temperature. Then adsorbent particles were carefully removed from the filter papers into aluminum foil, and were placed inside a furnace. The temperature controller on the furnace was set to 360°C, and the furnace was turned on for 16 hours. After regeneration, the adsorbent particles were removed from the furnace and placed in a desiccator to cool down. Finally they were measured and replaced in the same bottles that previously used for adsorption. Then another adsorption cycle was performed. This adsorption-regeneration procedure was performed for 14 times and each time the capacity of adsorption and the loss of particles during regeneration were carefully determined. The percentage of loss of adsorbent particles during each adsorption-regeneration cycle was calculated from following equation:

$$\% \text{ loss of adsorbent particles} = \frac{m_n - m_{n+1}}{m_n} \times 100$$

m_n = mass of adsorbent particles used in n^{th} adsorption cycle (g)

m_{n+1} = mass of adsorbent particles used in $(n + 1)^{\text{th}}$ adsorption cycle (g)

Chapter Four

Experimental Results

In this section the results of kinetic and equilibrium isotherms for each adsorbent will be discussed. Experimental results will be compared with literature. Also the effect of temperature and particle size on capacity of adsorption will be demonstrated for HiSiv 3000 (50×70 mesh). Finally regeneration of HiSiv 3000 (50×70 mesh) will be discussed. Appendices B1 and B2 show the raw data for kinetic and equilibrium experiments, respectively. Raw data for regeneration of HiSiv 3000 (50×70 mesh) are shown in Appendix C.

4.1 Silica Gel

Silica gel is a partially dehydrated form of polymeric colloidal silicic acid. The chemical composition can be expressed as $\text{SiO}_2 \cdot n\text{H}_2\text{O}$. Its surface area is in the range of 100-850 m^2/g . It can be used to adsorb water, alcohols, phenols, amines, etc. (Thomas and Crittenden, 1998). The pore size distribution is generally unimodal, as illustrated in Figure 8-a. The pore size of silica gel is between 1 to 40 Å. The most important current application of silica gel is as a desiccant (Ruthven, 1984).

4.1.1 Kinetic Data

Kinetic experiments for phenol adsorption on silica gel were performed at room temperature ($25 \pm 1^\circ\text{C}$) for 24 hours. Figure 9 shows the kinetic results of phenol adsorption on silica gel. This figure illustrates that concentration of phenol did not decrease after 8 hours of contact time. It can be concluded that silica gel can not remove phenol from water. In the literature silica gel has been used for separation of organic molecules from paraffins (Thomas and Crittenden, 1998). The reason silica gel does not adsorb phenol from water might be related to the solvent properties.

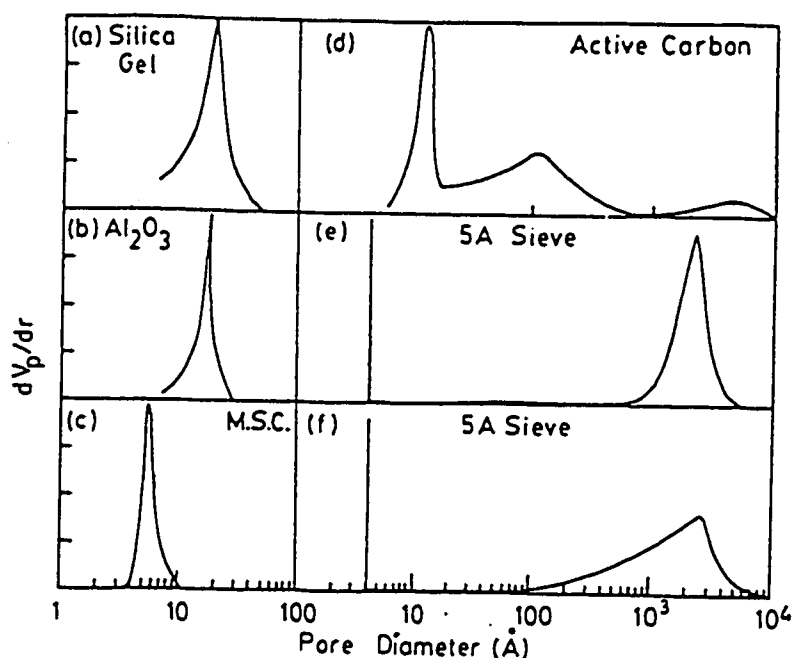


Figure 8: Pore size distribution for (a) silical gel; (b)porous alumina; (c) molecular sieve carbon; (d) activated carbon; (e) Davison binderless 5A molecular sieve type 625; (f) Davison 5A molecular sieve type 525 (Ruthven 1984).

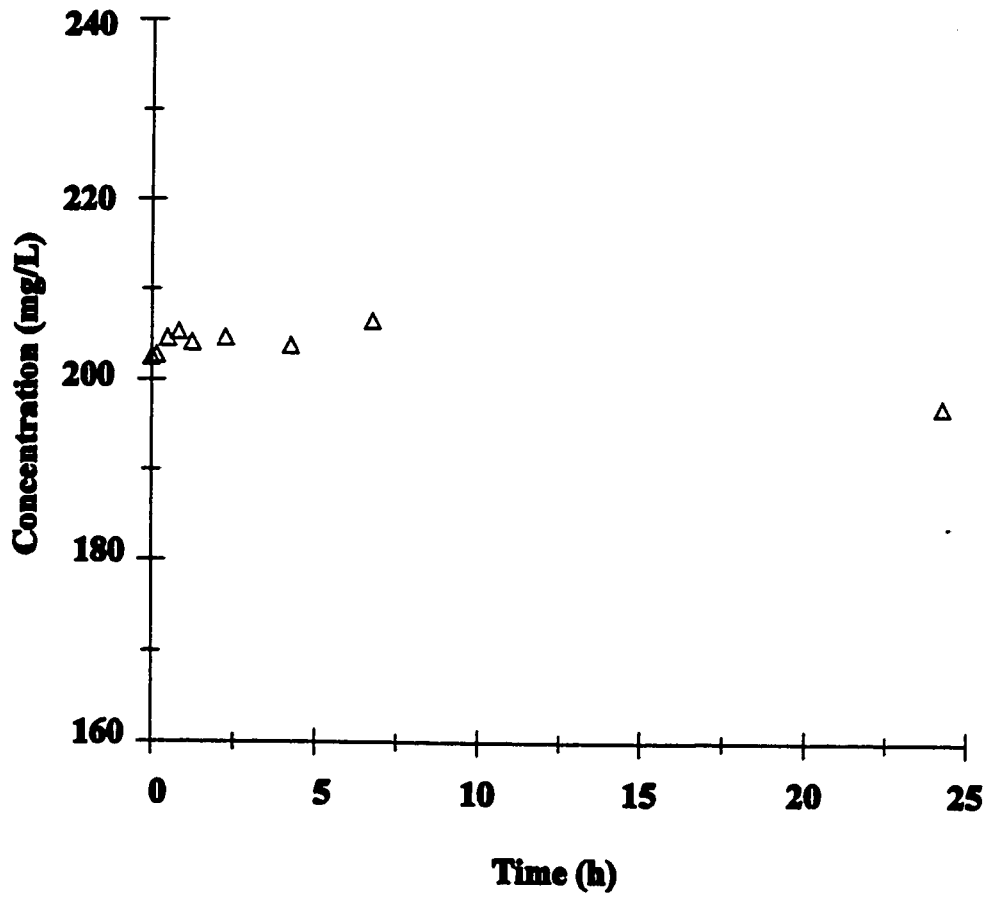


Figure 9: Kinetic data for adsorption of phenol on silica gel at 25°C. Initial concentration of phenol = 202.5 mg/L.

In the present work water was used as the solvent, so there was a high competition between phenol and water for occupying the adsorption sites. Water molecules are smaller than phenol molecules, so water molecules can easily enter the pores of silica gel. Besides, the affinity of silica gel for water might be greater than its affinity for aromatic organic such as phenol. So silica gel may prefer to adsorb water rather than phenol.

Result of kinetic experiments indicated that silica gel is not a good adsorbent for removing phenol from water. As a result no more experiments were conducted for this adsorbent.

4.2 Activated Alumina

Activated alumina is a porous high-area form of aluminum oxide ($\text{Al}_2\text{O}_3 \cdot n\text{H}_2\text{O}$), with a strongly polar surface compared to silica gel and has both acidic and basic character. Surface area is in the range of 250-350 m^2/g (Thomas and Crittenden, 1998). This adsorbent is commonly used as a desiccant for drying warm air or gas streams. The pore size distribution is illustrated in Figure 8-b (Ruthven 1984).

4.2.1 Kinetic data

Kinetic experiments were conducted at room temperature ($25 \pm 1^\circ\text{C}$). Initial concentration of phenol in solution was 201 mg/L, which was reduced to 196 mg/L after 50 hours. Figure 10 indicates that only small portion of phenol was adsorbed on basic-activated alumina (2.5% of initial phenol concentration in solution).

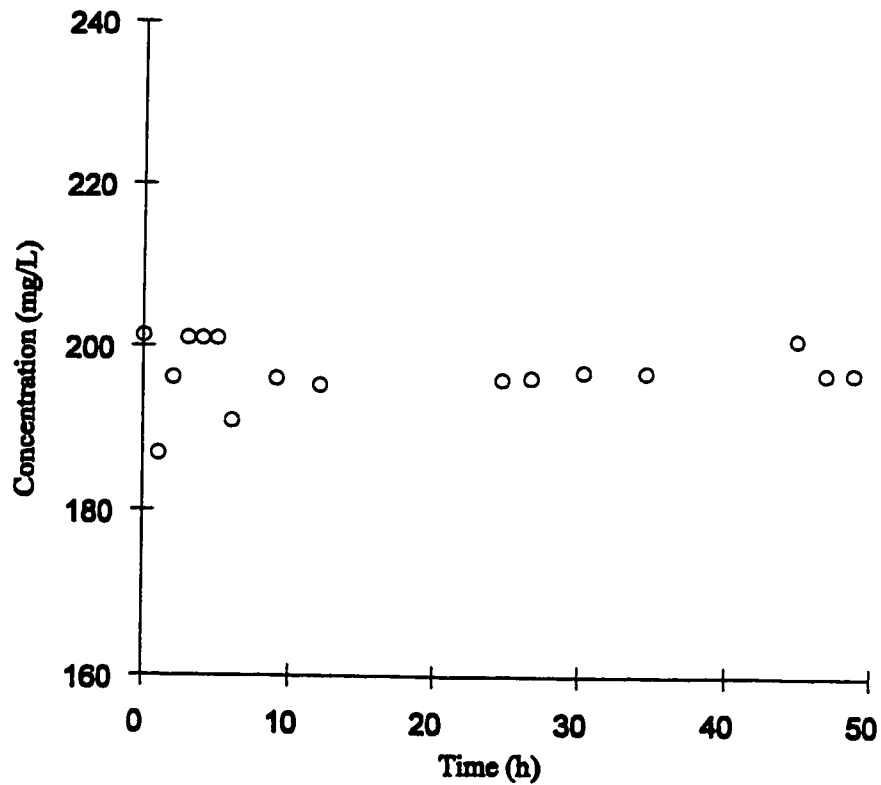


Figure 10: Kinetic data for adsorption of phenol on activated alumina (basic) at 25°C. Initial concentration of phenol = 201 mg/L.

Similar results were obtained for kinetic experiments of acidic-activated alumina at room temperature: $25 \pm 1^\circ\text{C}$ (Figure 11). In this experiment phenol concentration was reduced from 209 mg/L to 202 mg/L after 25 hours. As a result, phenol concentration was decreased by 3.3 % of its initial value in the liquid. This result shows that acidic-activated alumina has slightly better affinity for adsorption of phenol compared to basic-activated alumina. However the amount of removal is not high enough for application purposes.

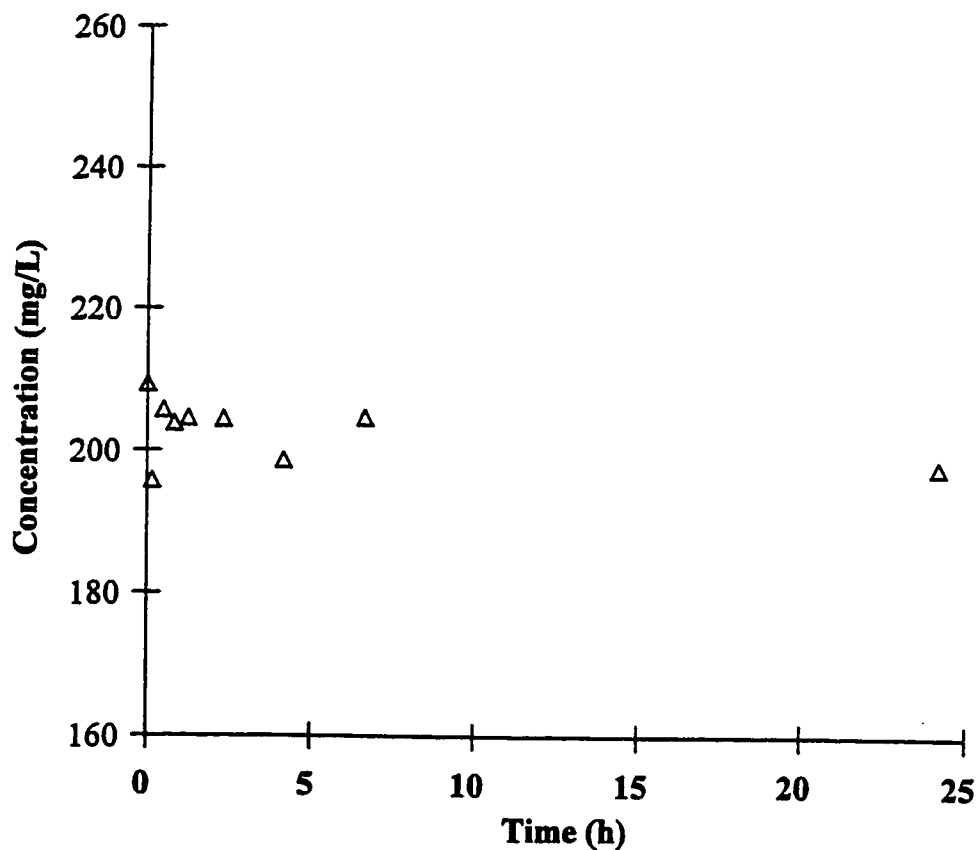


Figure 11: Kinetic data for adsorption of phenol on activated alumina (acidic) at 25°C. Initial concentration of phenol = 209 mg/L.

The results of kinetic experiments indicated that activated alumina is not a good adsorbent for removing phenol from water. As a result no more experiments were conducted for this adsorbent.

4.3 Activated Carbon

The structure of activated carbon consists of elementary microcrystallites of graphite, but these microcrystallites are stacked together in random orientation and it is the spaces between the crystals which form the micropores. The pore size distribution is typically trimodal as illustrated in Figure 8-d. In this figure three specific region of pore size is shown (Thomas and Crittenden, 1998):

- 1) micropores < 2 nm, surface area = 100-1000 m²/g
- 2) mesopores = 2-50 nm, surface area = 10-100 m²/g
- 3) macropore > 50 nm, surface area = 0.5-2 m²/g.

The surface of carbon is essentially non-polar although a slight polarity may arise from surface oxidation. As a result, carbon adsorbents tend to be hydrophobic and organophilic. They are therefore widely used for the adsorption of organics in decolorizing sugar, water purification, and solvent recovery systems (Ruthven 1984).

Activated carbon adsorbents generally show very little selectivity in the adsorption of molecules of different size. However, by special activation procedures it is possible to prepare carbon adsorbents with a very narrow distribution of micropore size which would behave as molecular sieves. Therefore it is possible to prepare carbon sieves with effective micropore diameters ranging from about 4 to 9 Å (Ruthven 1984).

4.3.1 Kinetic data

Kinetic experiments for phenol adsorption on activated carbon were performed at room temperature (25±1 °C) for 29 days. The results are given as normalized concentration vs. time in Figure 12 (Normalized concentration = C_A/C_0). Kinetic results showed that an initial

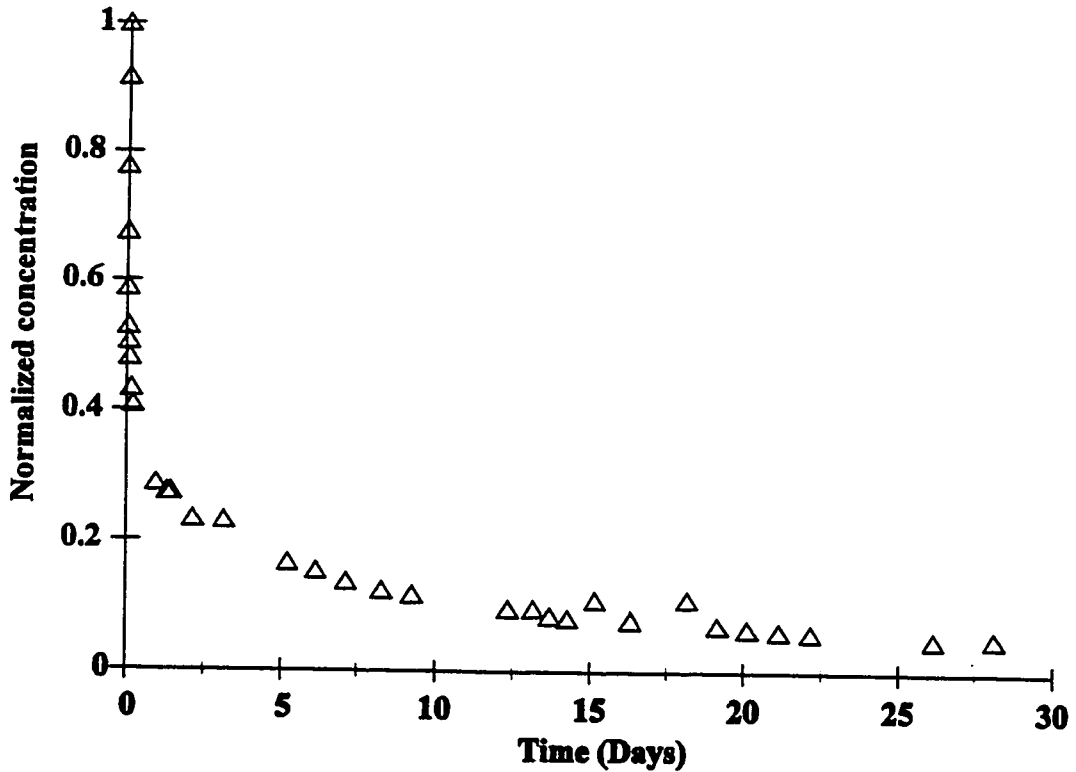


Figure 12: Kinetic data for adsorption of phenol on activated carbon at 25°C.

rapid adsorption occurred within 23 hours. However, the concentration of phenol in liquid phase did not reach final equilibrium within 25 days. Peel and Benedek (1980), observed that adsorption of phenol on activated carbon took up to three weeks to reach equilibrium, however up to 80 % of adsorption equilibrium was reached in the first few hours. Because of rapid initial adsorption, it has often been assumed in the literature that adsorption onto activated carbon occurred rapidly and that chemical equilibrium was obtained in a very short time.

Peel and Benedek demonstrated that adsorption process can be quite slow and that chemical equilibrium approximation from kinetic data may not represent the real equilibrium. They suggested that micropores existing within the carbon particles may require considerable time to reach equilibrium. However, extended contact times introduce the potential for microbial activity which can interfere with adsorption equilibrium studies.

To predict the time required to reach equilibrium, Peel and Benedek carried out equilibrium experiments. They performed equilibrium test for phenol on activated carbon at 14 and 23 days. Because of small change, they concluded that equilibrium appeared to have almost been obtained after 14 days.

Yen (1983), observed the same phenomena when he was investigating the adsorption of phenolic compounds on powder activated carbon (from Amoco research corporation, surface area=2300-2600 m²/g, and average pore size= 20-30 Å). Therefore he decided to perform two sets of kinetic experiments for adsorption of phenol on activated carbon under the same selected condition, i.e., 20°C, 60 rpm, and pH=2.5, but different initial phenol concentrations. Yen observed that the adsorption was completed within one day for both cases. Thus, Yen decided that a two-day contact time should be sufficiently conservative to allow for all the phenolic compounds studied to reach solution concentrations that were analytically undistinguishable from their equilibrium concentrations.

The time required to reach equilibrium in Yen's experiments is much lower than that time in the present study. The reason is related to the type of activated carbon, which was used in Yen's experiments (PX-21 powder activated carbon, from Amoco research corporation, Naperville, Illinois), as well as the difference in particle sizes of activated carbon used.

The particle size of Yen's adsorbent is less than 90 μm, whereas activated carbon used

in the present study has much larger particle size (0.8 mm).

4.3.2 Adsorption Equilibrium Isotherm

The duration of the equilibrium experiments in the isotherm bottles was selected to be 20 days. The results of equilibrium experiments are compared with those data obtained from the literature (Figure 13). Some details are given in Table 5. From this comparison, it is clear that the capacity of adsorption on activated carbon studied in the present work is higher than other activated carbon capacities obtained from literature. The reason for this discrepancy are related to many parameters which are discussed below.

Abuzeid, et al (1995) used lower temperature and moderate pH =7 which was supposed to obtain higher adsorption capacity than that of present study. The reason for lower capacity in their results may be related to contact time between phenol and adsorbent particles. They used larger particle size, but shorter contact time which was not enough for adsorption to reach equilibrium. Since diffusion of adsorbate molecules through the larger particles are slower than diffusion through smaller particles, short contact times will not allow equilibrium to be reached. That, in turn, will reduce the apparent adsorption capacity.

Jankowska, et al (1986), conducted the equilibrium experiments at lower temperature (20°C) compared to present study (25°C). Also the type of adsorbent was different in their experiments (Hydriffin 71). This adsorbent might have been made from different source of activated carbon. As a result its capacity might have been low because of the original base used in its structure. The information about particle size of adsorbent was not available in their study. Lin and Hsu's results showed the lowest capacity of adsorption for phenol on activated carbon, because coconut shell was used as the source of adsorbent structure. Also

particle size of adsorbent in their study is very large which might describe the reason of lower adsorption capacity in their experiments.

In conclusion: particle size and source of activated carbon should be considered during comparison. Larger particle sizes need more contact time to reach adsorption equilibrium. Therefore if the contact time was not enough, the apparent capacity will be lower than the real capacity of adsorption. Lack of enough contact time might affect the temperature comparison as well. For example Abuzeid, et.al (1995) used larger particle size and lower temperature. But the adsorption capacity in their experiments was lower than the related capacity in the present study. That is because Abuzeid, et.al used shorter contact time (14 days) compared to related time in the present work (20 days).

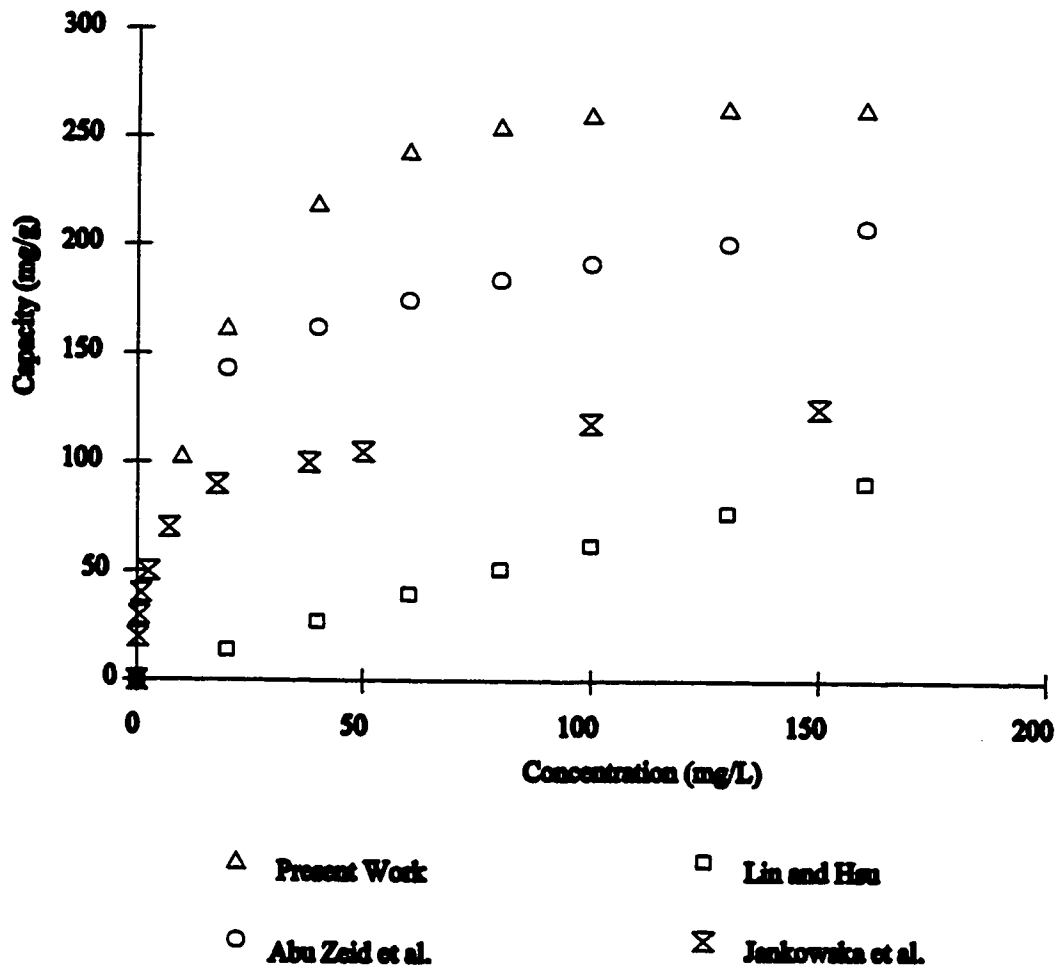


Figure 13: Adsorption isotherm comparison of phenol on activated carbon with literature (details are given in Table 5).

Table 5: Legends for Figure 13

Time Period	Isotherm q (mg/g), C (mg/L)	Particle size(mm)	pH	Temp. °C	Source	Symbol
20 days	$q=13.28C/(1+0.02 \times C^{1.156})$	0.8	7-8.9	25	Present study	△
-	$q=0.733C/(1+0.0018C)$	5	-	20	Lin and Hsu (1995)	□
14 days	$q=83.5C^{0.18}$	1.59	7	23	Abu zeid et al., (1995)	○
14 days	data points were plotted (no isotherm model)	-	-	20	Jankowska, et al. (1986)	+

4.4 Filtrasorb 400

4.4.1 Kinetic Experiments:

Kinetic experiments for phenol adsorption on F-400 were performed at room temperature for 35 days. The results show two stages for adsorption (Figure 14). Rapid initial stage followed by a second slow stage. Peel (1980) proposed a model which divided the particle of adsorbent into macropores and micropores. It is assumed that rapid initial uptake takes place in macropores and slow adsorption occurs in micropores.

4.4.2 Adsorption Equilibrium Isotherm

Kinetic results (Figure 14) showed that the concentration of phenol was still decreasing even after 29 days. By repeating the kinetic experiments the same results were obtained. So there was no observation of adsorption equilibrium attainment from kinetic data. Therefore, it was decided to carry out the adsorption equilibrium experiments for 1 month.

Figure 15 shows the equilibrium isotherms obtained and compares it with those obtained from the literature for F-400. The experimental conditions were similar for “Peel and Benedek” and “Lo and Alok” tests except for contact time which was longer in “Peel and Benedek” test. But in spite of longer contact time, the capacity of adsorption in “Peel and Benedek” test was lower than that of “Lo and Alok” test. This discrepancy can be related to the raw material used as a source of F-400 in their studies.

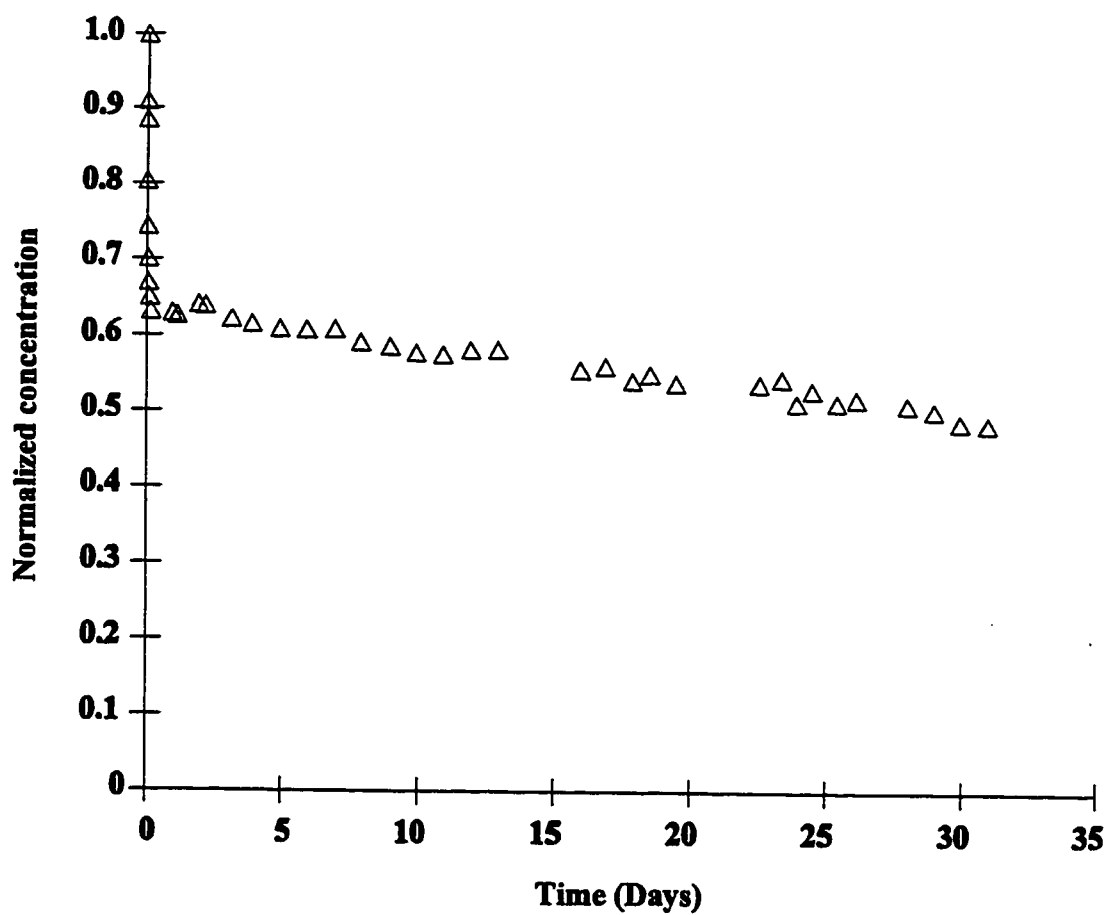


Figure 14: Kinetic data for adsorption of phenol on F-400 at 25°C.

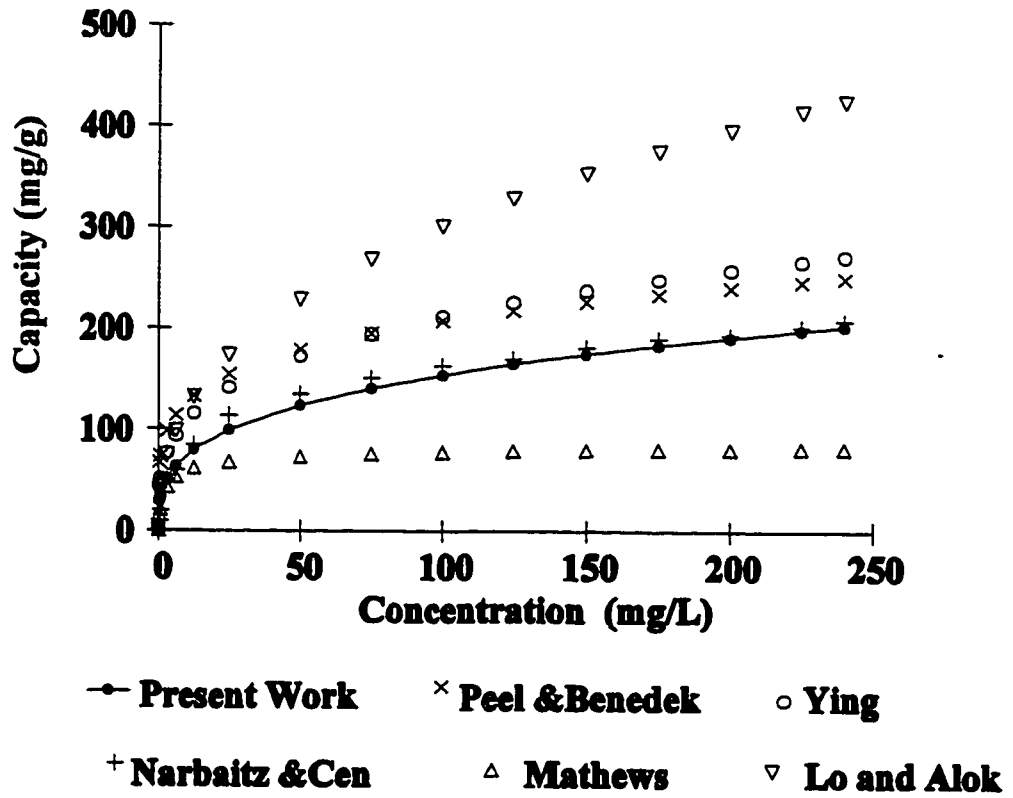


Figure 15: Literature comparison for adsorption isotherms of phenol on F-400 at 26.5°C (legend on Table 6).

Table 2: Legends for Figure 15.

Time Period	Isotherm q (mg/g), C (mg/L)	Particle (mesh size)	pH	Temp. °C	Source	Symbol
30 days	$q=386.54C/(1+10.27C^{0.69})$	14×20	5.3-6.6	25	Present work (1999)	•
23-40 days	$q=78.1C^{0.212}$	16×30, 200	7	20	Peels and Benedek (1980)	×
6 days-6 weeks	$q=56C^{0.288}$	30×35	-	Room	Ying (1978)	○
N/A	$q=43.29C/(1+C^{0.7942})$	30×35, 60×100	7	Room	Mathews (1975)	△
6-7 days	$q=46.76C^{0.2584}$	12×16, 16×18	7	21±2	Narbaitz and Cen (1994)	+
4 days	$q=48.473C^{0.3959}$	16×30	7	20	Lo and Alok (1996)	▽

Figure 15 clearly depicts the results of temperature effect on adsorption capacity. Therefore by decreasing the temperature from 25 °C (present work) to 20 °C (Peel & Benedek and Lo & Alok) the capacity of adsorption is decreased.

The results of Narbaitz and Cen experiments are very close to the results obtained in the present study since both of them used the same adsorbent prepared from the same raw material (F-400, Calgon). Also their results shows that one week is enough for adsorption equilibrium to be reached.

In general, the reason for discrepancy of adsorption capacities in different experiments is due to differences in temperatures, contact times, and sources of raw materials. Shorter contact time will affect the equilibrium isotherms only if equilibrium is not reached during this period of time. As a result the apparent capacity will be lower than the real capacity of the adsorbent.

4.5 HiSiv 1000

HiSiv 1000 adsorbent is a crystalline, inorganic silica-alumina structure which is developed from high silica molecular sieve, also referred to as “high silica zeolites” (UOP, 1998a).

Zeolites are porous crystalline aluminosilicates. The Zeolite framework consists of an assemblage of SiO_4 and AlO_4 tetrahedra, joined together in various regular arrangements through shared oxygen atoms, to form an open crystal lattice containing pores of molecular dimensions into which guest molecules can penetrate. Since the micropore structure is

determined by the crystal lattice it is precisely uniform with no distribution of pore size. It is this feature which distinguishes the zeolites from the traditional microporous adsorbents (Ruthven, 1984).

In considering zeolite framework it is convenient to regard the structures as built up from assemblage of secondary building units, which are themselves polyhedra made up of several SiO_4 and AlO_4 tetrahedra. The secondary building unit of HiSiv 1000 is similar to those of zeolite-Y, with Si/Al ratio less than 100 (UOP, 1998a).

4.5.1 Kinetic Results

Kinetic experiments of phenol adsorption on HiSiv 1000 were carried out at room temperature (25 ± 1 °C) for 6 days. From kinetic results, it was observed that the rate of adsorption was fast and equilibrium reached within 10 hours (Figure 16).

4.5.2 Adsorption Equilibrium Isotherm

Equilibrium experiments for adsorption of phenol on HiSiv 1000 were carried out at room temperature (25 ± 1 °C) for 8 days. It was observed that capacity of adsorption was very low (Figure 17). Therefore HiSiv 1000 was not considered as an effective adsorbent for removal of phenol from water.

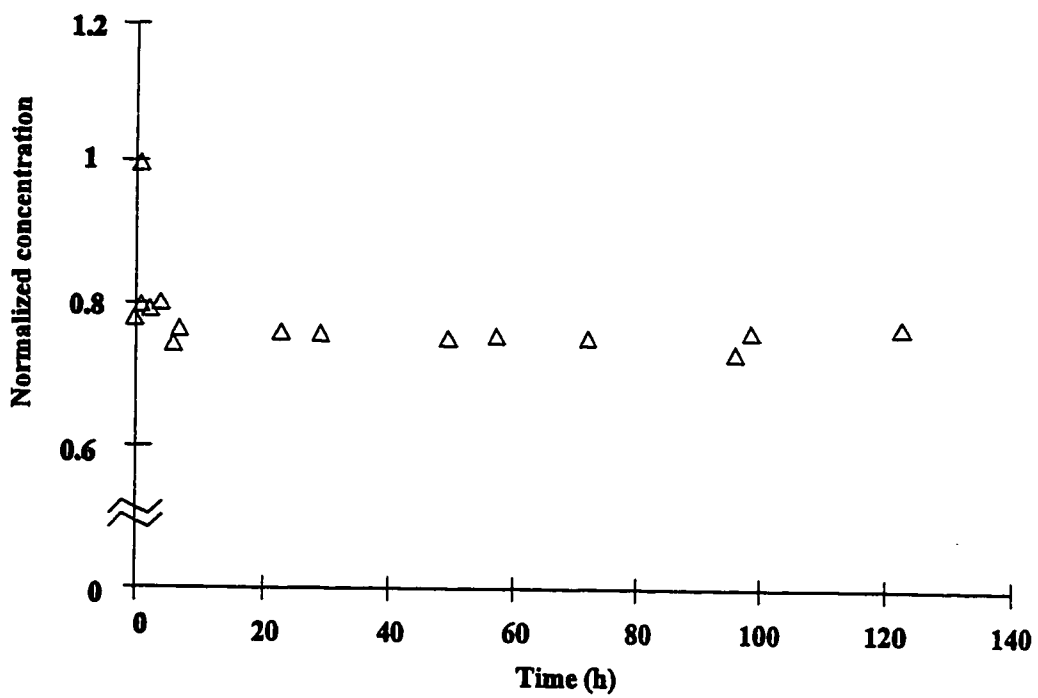


Figure 16: Kinetic data for adsorption of phenol onto HiSiv 1000 at 25°C.

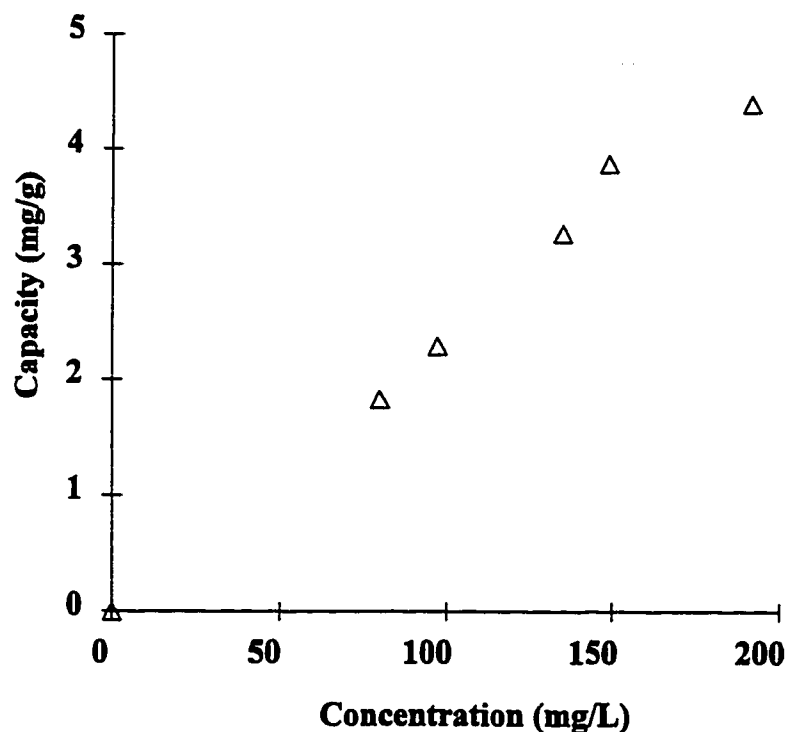


Figure 17: Equilibrium isotherm for adsorption of phenol onto HiSiv 1000 at 25°C.

4.6 HiSiv 3000

HiSiv 3000 is a zeolite adsorbent which its secondary building units are silicalite/ZSM-5. The Si/Al ratio of HiSiv 3000 is in the range of thousands. HiSiv 3000 is preferred adsorbent for adsorbing molecules which are smaller than 0.6 nm, while HiSiv 1000 adsorbs larger molecules in the range of 0.6-0.8 nm (UOP, 1998b).

4.6.1 Kinetic Results

Kinetic experiment for phenol adsorption on HiSiv 3000 powder was performed at room temperature for 2 hours. Kinetic experiments showed a rapid rate of phenol adsorption on HiSiv 3000 powder (Figure 18). As a result of comparison the rapid adsorption region of

kinetics for HiSiv 3000 powder, F-400 and activated carbon were observed to be 15 minutes, 2.5 hours (150 minutes), and more than 5 hours (300 minutes), respectively. So it can be concluded that removal rate of HiSiv 3000 powder is higher than F-400 and activated carbon. This advantage for HiSiv 3000 was a good point for further investigation in this work.

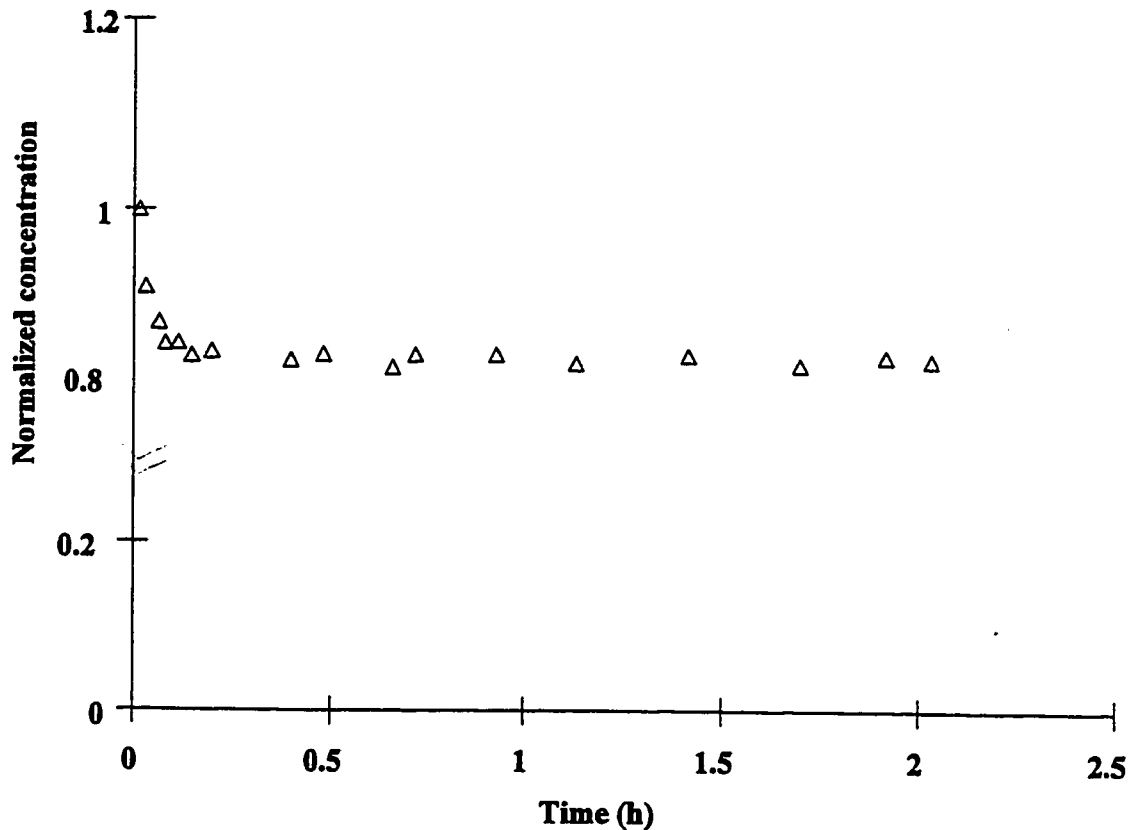


Figure 18: Kinetic data for adsorption of phenol on HiSiv 3000 powder at 25°C.

4.6.2 Adsorption Equilibrium Isotherm

Equilibrium experiments for adsorption of phenol on HiSiv 3000 powder were carried out at room temperature ($25\pm 1^\circ\text{C}$) for 11 days. Figure 19 illustrates the equilibrium isotherm

for adsorption of phenol on HiSiv 3000 powder. The capacity of adsorption is not as high F-400 and activated carbon, but it is higher than the rest of the adsorbents studied in this work. Since the adsorption rate on HiSiv 3000 powder was much faster than that for the other adsorbents studied in this work, this adsorbent was chosen for further study in this work.

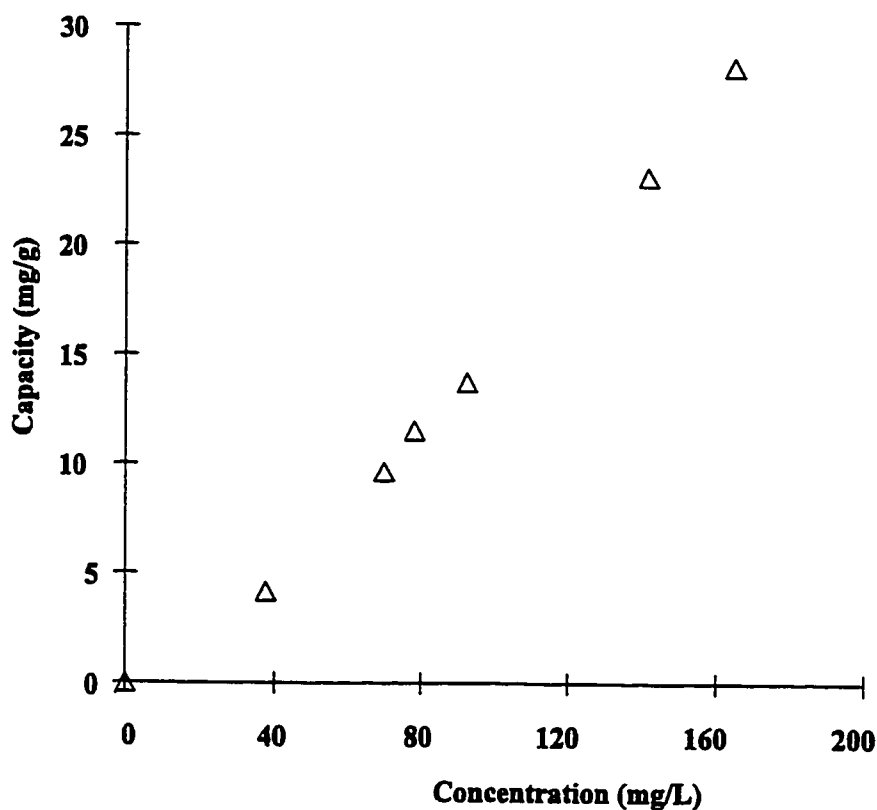


Figure 19: Equilibrium isotherm for HiSiv 3000 powder at 25°C.

4.6.3 Comparison between HiSiv 3000 and HiSiv 1000

HiSiv 3000 and HiSiv 1000 are zeolite type adsorbents with a different micropore sizes as a result of different intracrystalline channel structures. The intracrystalline diffusivity and

hence the kinetic selectivity and, in extreme cases, the molecular sieve properties are determined mainly by the free diameters of the windows in the intracrystalline channel structure. ZSM-5 zeolites including HiSiv 3000 are characterized by 5.7 Å channel size formed by 10-membered oxygen rings where as zeolite-Y adsorbents including HiSiv 1000 are characterized by 12-membered oxygen rings which have free diameters of 7.0 -7.4 Å (Ruthven, 1984). Therefore the size of micropores in HiSiv 3000 is smaller than those of HiSiv 1000.

The size of phenol can be approximately found by determining the volume of phenol molecule (Appendix A1). If phenol molecule was considered spherical, then the diameter of phenol molecule would be about 6.6Å. Then phenol molecule could not be able to enter the pores of HiSiv 3000. But phenol molecule is not spherical since it contains a hydroxyl group on one side of the molecule. So phenol is smaller than the pore size of HiSiv 3000, on one side. Therefore it is possible for phenol to be adsorbed by HiSiv 3000.

On the other hand, the Si/Al ratio play a very important role in determining the adsorptive properties of zeolites. The Si/Al ratio in a zeolite is never less than 1.0 but there is no upper limit and pure silica analogs of some of the zeolite structures have been prepared. The adsorptive properties show a systematic transition from the aluminum-rich sieves, which have very high affinities for water and other polar molecules, to the microporous silicas such as silicalite which are essentially hydrophobic and adsorb *n*-paraffins in preference to water (Ruthven, 1984). The Si/Al ratio of HiSiv 3000 is in the range of thousands, where as this ratio for HiSiv 1000 is less than 100. As a result of high affinity of Hisiv 1000 for water there will be a competition between water molecules and phenol molecules for occupying the adsorption sites. Therefore the adsorption capacity of phenol on HiSiv 1000 will be less than related capacity of phenol on HiSiv 3000.

4.6.4 Problem Associated Working With HiSiv 3000 Powder:

During experimental work powdered adsorbent caused many problems. For example at the end of each test, adsorbent particles formed a sticky structure which was hardly separated from the wall of the container. So it was impossible to recover the adsorbent for further investigation. As a result it was decided to work with larger particle size. The effect of particle size was studied to find the optimum size of particle. As a result particle size in the range of 50×70 mesh was chosen and the rest of experiments were performed by using this particle size.

4.6.5 Effect of Particle Size on Adsorption Equilibrium Capacity

HiSiv 3000 was received in two forms: 1) Powder with particle size less than 100 μm , and 2) Extrude with particle size: 1.5 mm. The extrude adsorbent was crushed and sieved through 20×50 (297-850 μm) and 50×70 (212-297 μm) meshes. Then equilibrium experiments were performed by using these four particle sizes. Results of isotherm experiments is shown in Figure 20.

Considering experimental errors associated with concentration measurement (refer to section 3.2.3), data points related to the phenol concentrations higher than 150 mg/L were not considered in the results. Therefore for the concentration region less than 150 mg/L, it can be concluded that particle size do not affect the adsorption isotherms. This is to be expected for an adsorbent with high microporosity like HiSiv 3000. By crushing the particles into smaller sizes, the access area of the phenol into the micropores are increased. As a result, the rate of

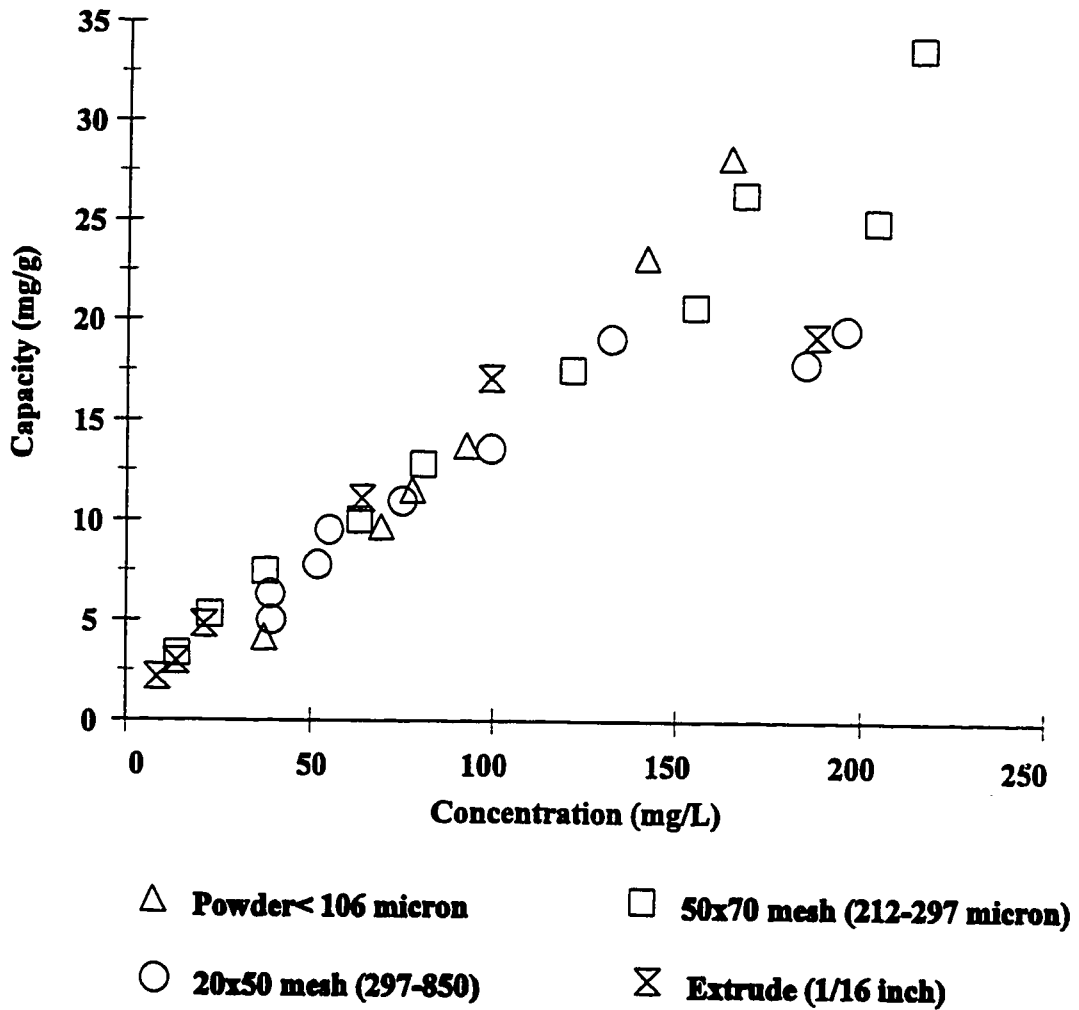


Figure 20: Effect of particle size on adsorption capacity of HiSiv 3000 for phenol at 25°C.

adsorption increases by decreasing the particle size. But the capacity of adsorption does not change because it is the surface area of the micropores that eventually determine the adsorption capacity, and this surface area is almost the same for all different sizes of adsorbent particles. Therefore by measuring the adsorption capacity of different particle sizes after giving enough time for equilibrium to be achieved (e.g.: 12 days contact time for largest particles of Hisiv 3000), the capacity of adsorption should be the same for all of them.

contact time for largest particles of Hisiv 3000), the capacity of adsorption should be the same for all of them.

Peel and Benedek (1980), reported similar results by using two particle size of activated carbon (granular and powder). They concluded that particle size has no effect on the equilibrium relationship. Randtke and Snoeyink (1983) also found the similar result when they were studying the effect of particle size on adsorption of low-molecular-weight adsorbates, such as *p*-nitrophenol. Singh and Rawat (1994), studied the effect of particle size on adsorption of phenol on fly ash and impregnated fly ash. They showed that by decreasing the adsorbent particle size from 150 μm to 45 μm , the capacity of adsorption was increased.

Weber and Morris (1964) pointed out a decrease in adsorptive capacity with increasing particle size, and they argued that, this is because the rate of saturation of large particles is much slower than that of small particles. Tests that do not allow enough time for the entire particles to reach equilibrium with the bulk solution will show that the small particles have higher adsorptive capacities.

4.6.6 Effect of Particle Size on Rate of Adsorption

Kinetic experiments were performed with the same particle sizes used in equilibrium experiments. The results illustrated that, the smaller the particle size the faster it can reach equilibrium (Figures 21 and 22). It was observed that powder adsorbent reached equilibrium in 15 minutes, followed by 50 \times 70 mesh size adsorbent which reached equilibrium within 2.5 hours. Equilibrium obtained after 23 hours for adsorbent with 20 \times 50 mesh size. Finally the adsorbent with largest particle size (extrude) had the slowest kinetic rate by reaching

equilibrium after 75 hours. Chatzopoulos and Varma (1993) explained this phenomena as a result of particle grinding which can expose adsorbate molecules to the large surface area of adsorbent leading to a rapid adsorption rate and slight increase in specific surface area.

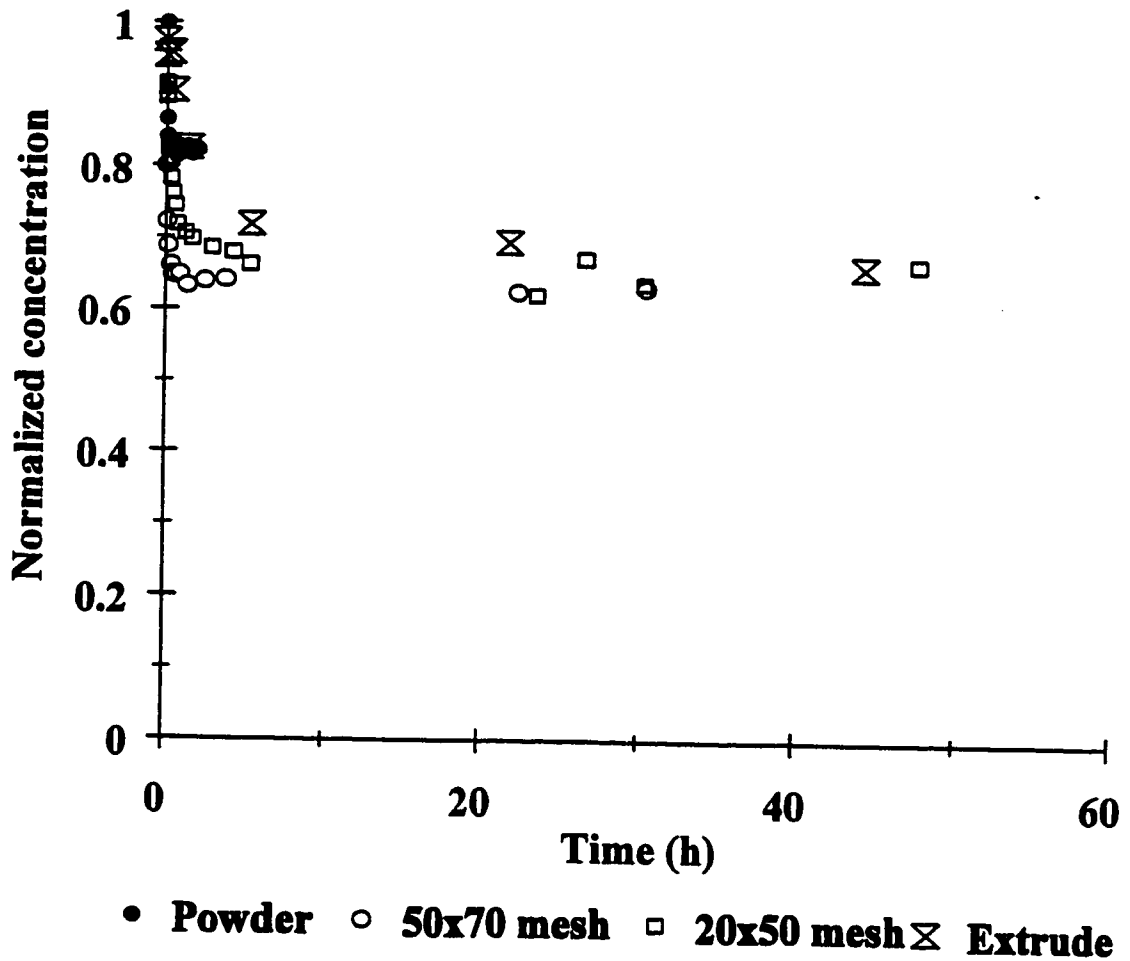


Figure 21: Effect of particle size on rate of adsorption of phenol on HiSiv 3000 at 25°C (X-axis: up to 60 hours).

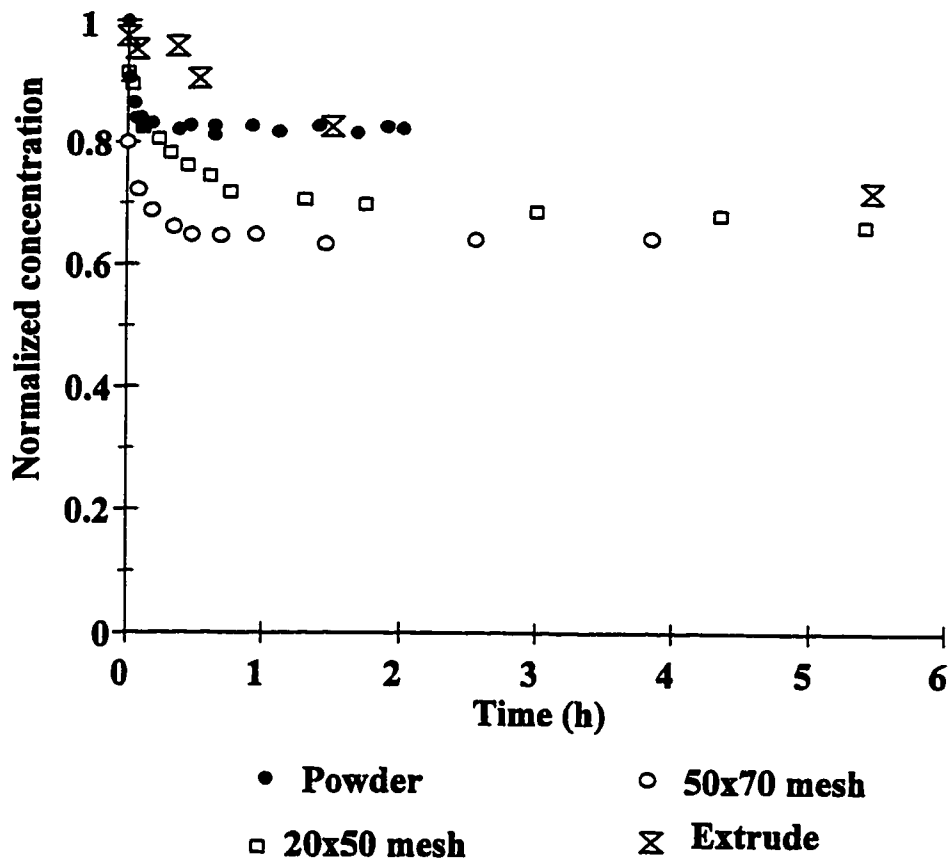


Figure 22: Effect of particle size on rate of adsorption of phenol on HiSiv 3000 at 25°C (X-axis: up to 6 hours).

4.7 HiSiv 3000 (50×70 mesh)

Working with powdered particles was not easy (refer to section 4.6.4, “problem associated working ...”), so it was decided to work with the next smallest size (50×70 mesh).

The results of kinetic and equilibrium experiments of phenol adsorption on HiSiv 3000 (50×70 mesh) are shown in the following part.

4.7.1 Kinetic Experiments

Kinetic experiments for phenol adsorption on HiSiv 3000 (50×70 mesh) were performed at room temperature ($25 \pm 1^\circ\text{C}$) for 47 hours (Figure 23). The results showed that

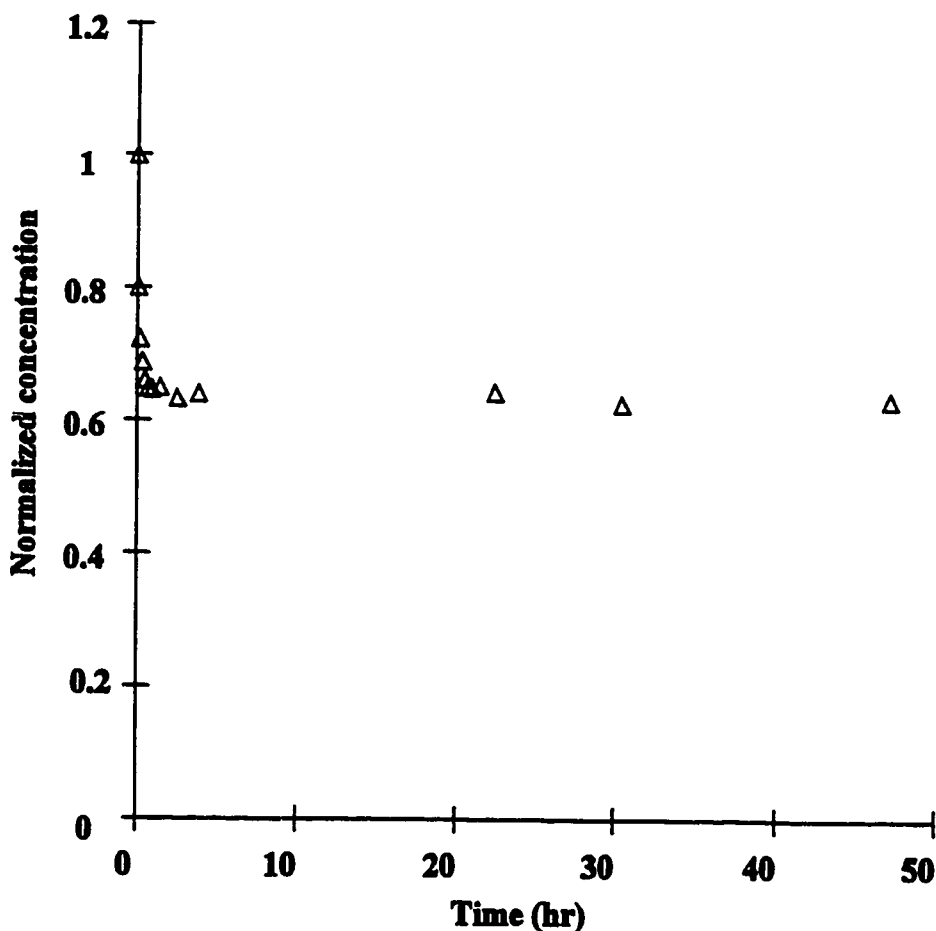


Figure 23: Kinetic data for adsorption of phenol on HiSiv 3000 (50x70) at 25°C .

equilibrium was reached after 2.5 hours.

The results of kinetic experiments for HiSiv 3000 (50×70) were compared to those results obtained for activated carbon and F-400 in Figures 24 and 25 as long term and short term results, respectively. It was found that removal of phenol by HiSiv 3000 (50×70) was very fast and equilibrium was obtained in less than 3 hours (Figure 23), where activated carbon reached equilibrium after 25 days and F-400 did not reach equilibrium even after 30 days (Figure 24).

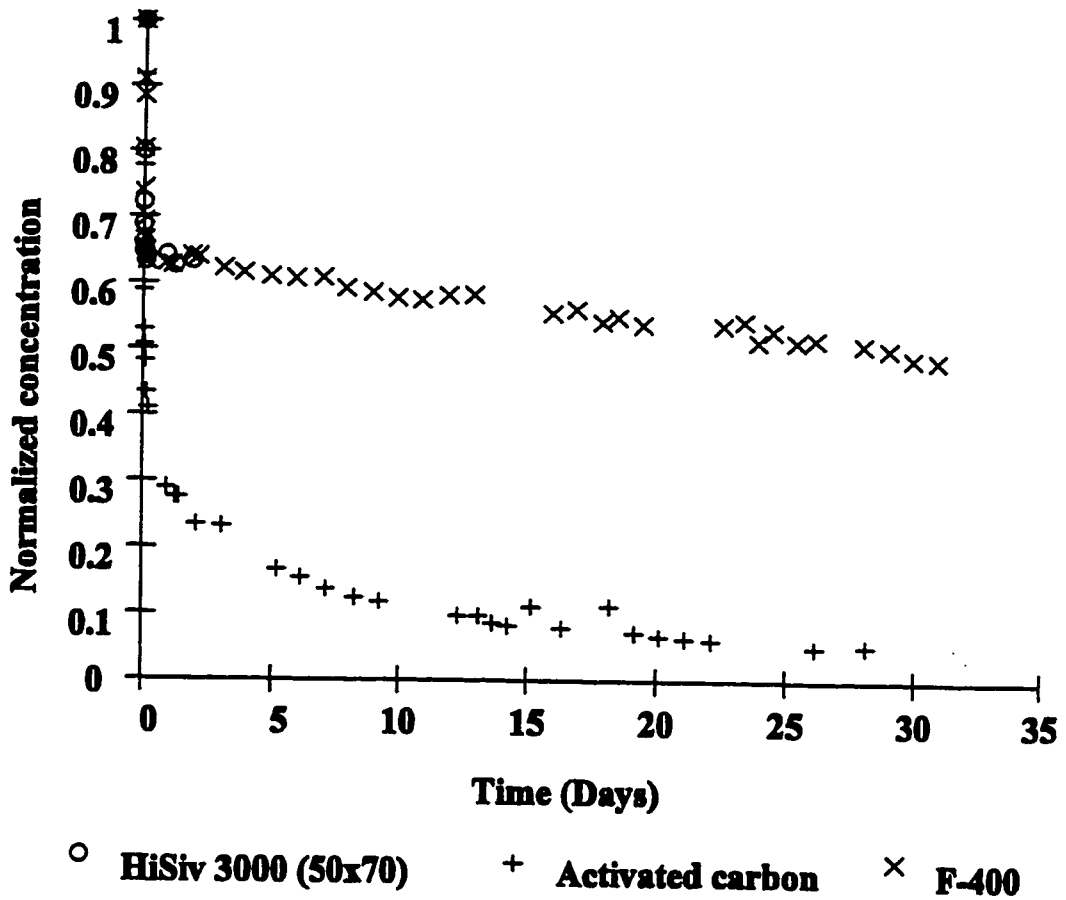


Figure 24: Kinetic rate comparison for adsorption of phenol on HiSiv 3000 (50x70mesh), F-400 and activated carbon at 25°C (x-axis: up to 35 days).

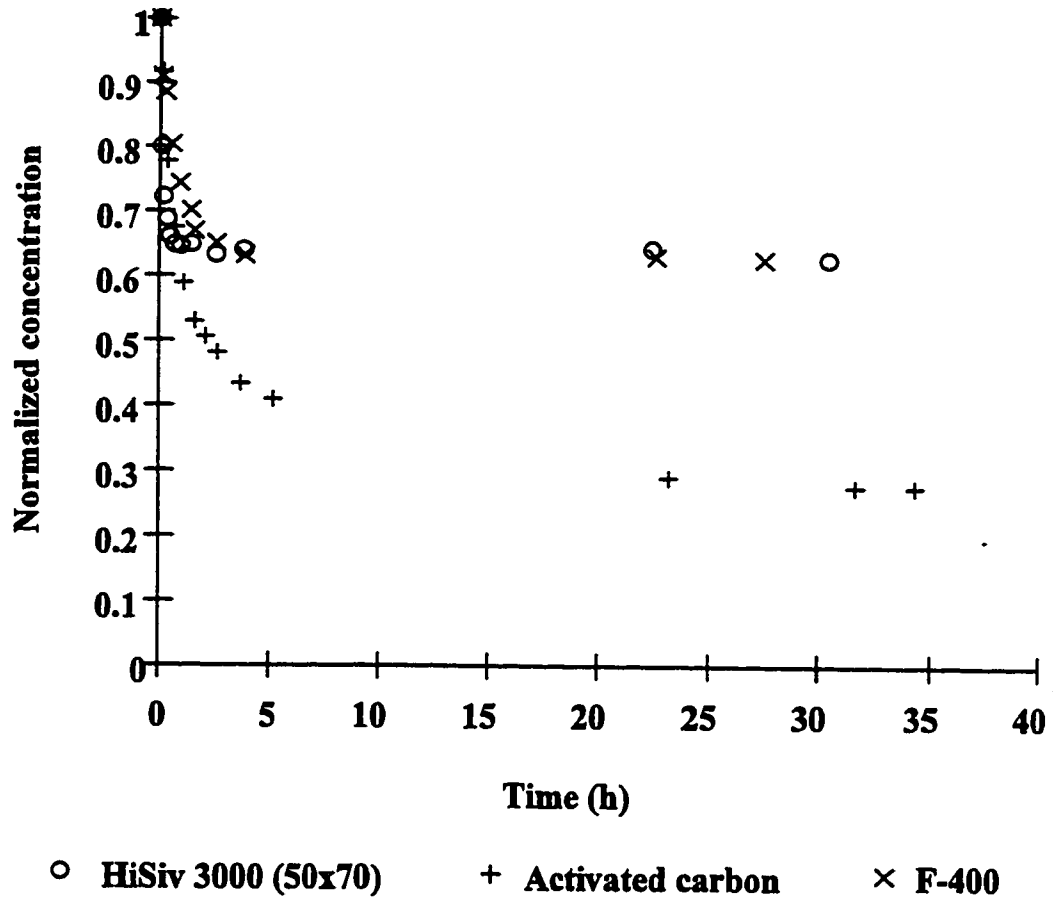


Figure 25: Kinetic rate comparison for adsorption of phenol on HiSiv 3000 (50×70mesh), F-400 and activated carbon at 25°C (x-axis: up to 40 hours).

4.7.2 Adsorption Equilibrium Isotherm

The results of equilibrium experiments for adsorption of phenol on HiSiv 3000 (50×70mesh) are shown in Figure 26. Also the results of adsorption equilibrium comparison for HiSiv 3000 (50×70mesh), activated carbon, and F-400 are shown in Figure 27. It was found

that when the concentration of phenol in solution was 150 mg/L, the capacity of activated carbon and F-400 were 14 and 9 times higher than the capacity of HiSiv 3000, respectively.

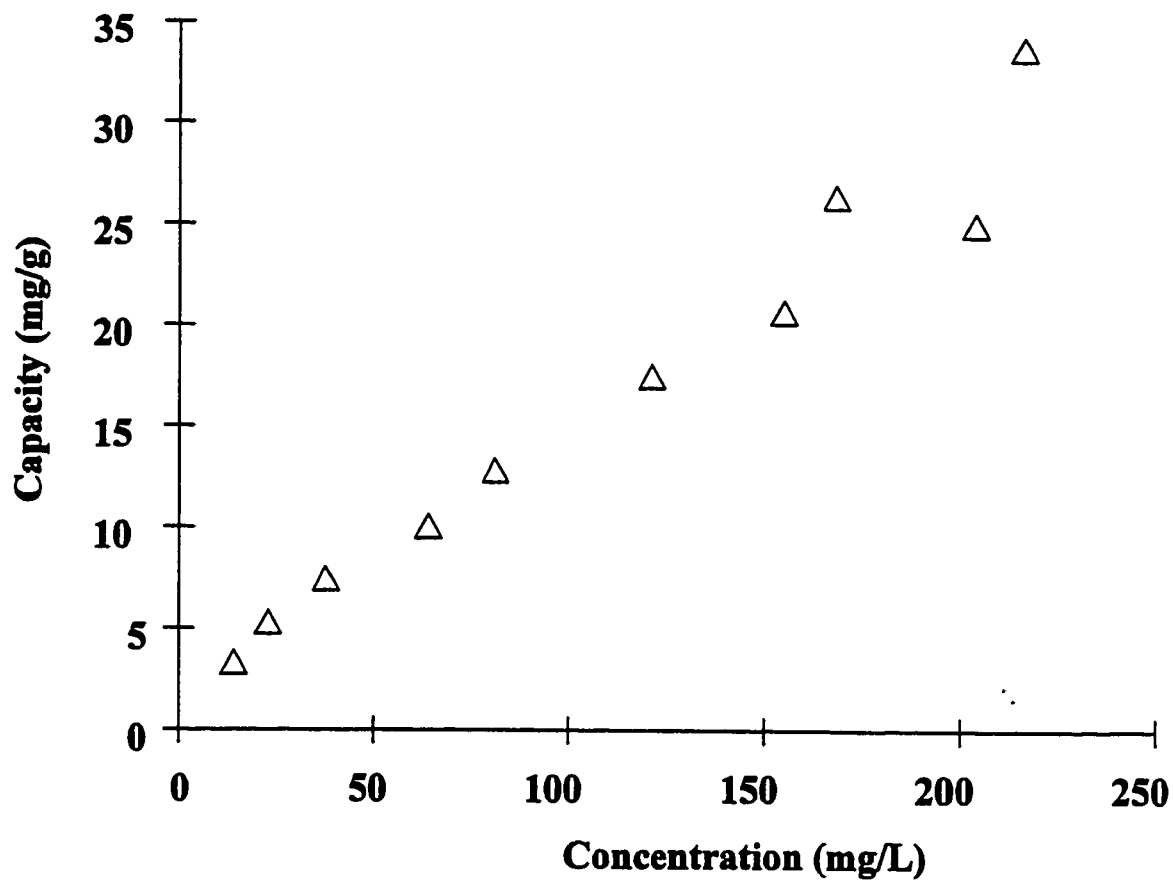


Figure 26: Adsorption isotherm of phenol on HiSiv 3000 (50×70 mesh) at 25°C.

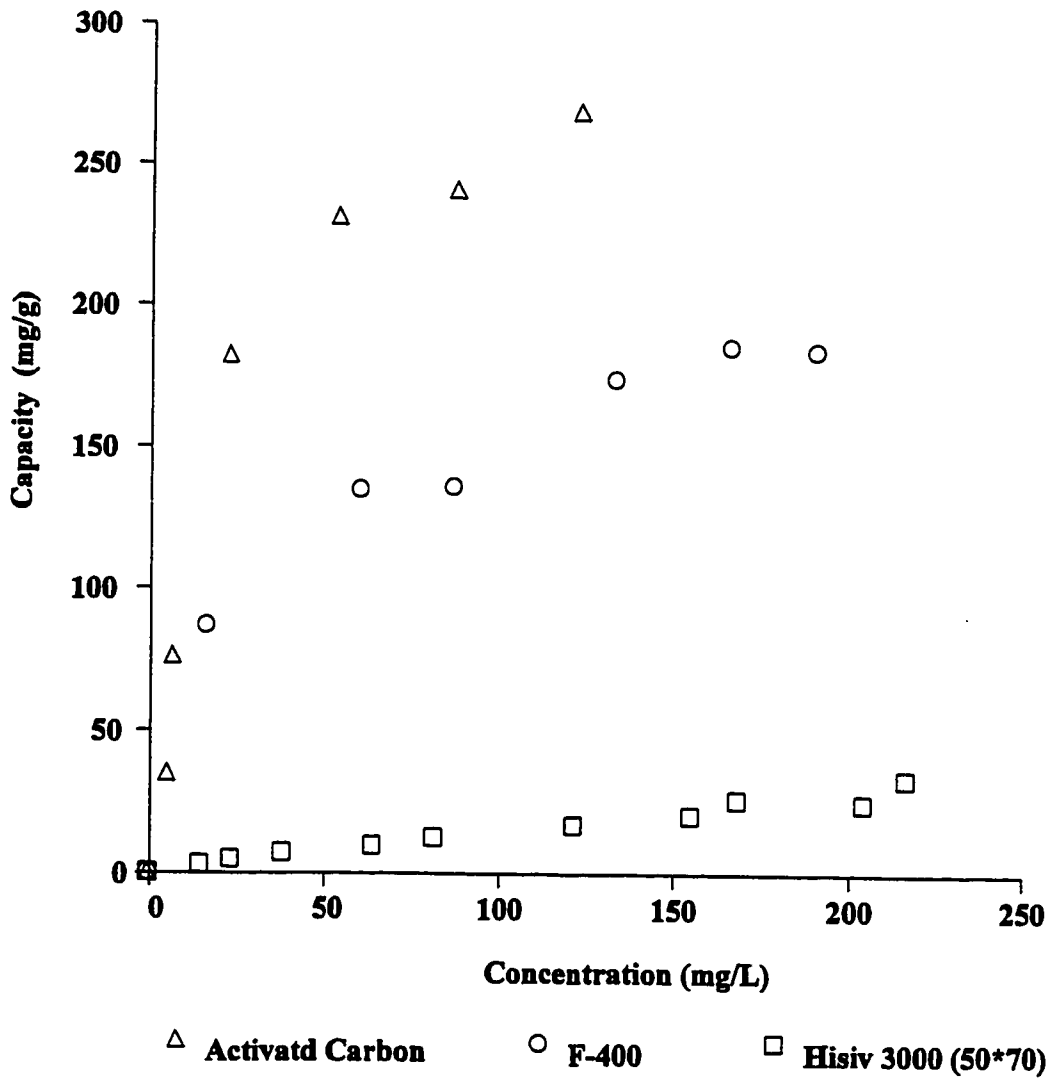


Figure 27: Equilibrium isotherm comparison for adsorption of phenol on activated carbon, F-400, and HiSiv 3000 (50x70 mesh), at room temperature (25°C ±1).

4.7.3 Effect of Temperature

To investigate the effect of temperature on adsorption capacity of HiSiv 3000 (50x70 mesh), isotherm experiments were conducted at 25, 40, and 55°C. The results indicated that adsorption capacity was decreased as temperature was increased (Figure 28).This observation explains that adsorption onto HiSiv 3000 is an exothermic process which means adsorption takes place upon releasing heat to the surrounding.

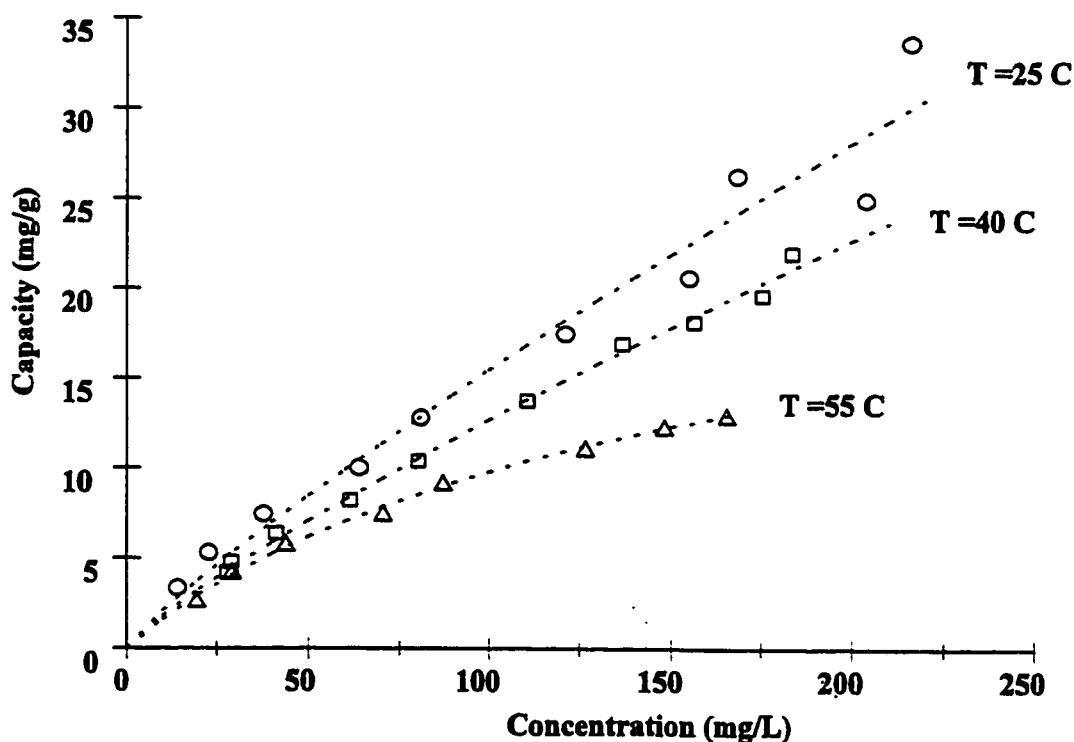


Figure 28: Adsorption isotherms for phenol onto HiSiv 3000 (50×70 mesh), at different temperatures.

Ma et al. (1996), observed the same phenomenon when they were investigating the influence of temperature on the adsorption of phenol on GH-82 powder activated carbon. But Radeke and Hartmann (1992) found different results during their studies. They reported that adsorption of phenol on Filtrasorb 400 (USA), at 20, 30, 40, 50 and 60°C did not decrease monotonically with increasing temperature but has a maximum over the temperature range 40-50°C (Figure 29).

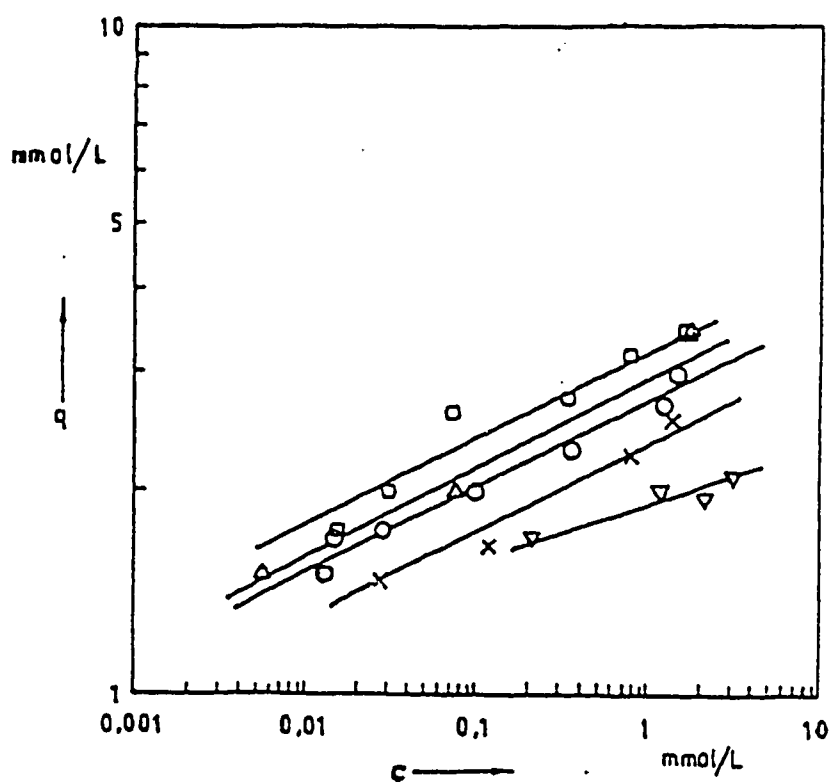


Figure 29: Adsorption isotherms for phenol on Filtrasorb 400 at different temperatures. (○): 20°C; (▽):30°C; (△):40°C; (□):50°C; (×):60°C (Radeke and Hartmann, 1992).

4.7.4 Regeneration

In this study, HiSiv 3000 (50x70 mesh) was regenerated at 360°C for 16 hours. Meytal et al. (1997) reported that oxidation of adsorbed phenol onto activated carbon occurred in the range of 320-350°C. Therefore regeneration of HiSiv 3000 at 360°C completely converts the adsorbed phenol into carbon dioxide and water vapor and small amount of graphite. Also regeneration of HiSiv 3000 at 360°C will not damage the structure of the adsorbent, since this adsorbent is thermally stable up to 500°C (UOP company, 1998b). Therefore a temperature of 360°C was chosen for regeneration temperature.

After regeneration another adsorption experiment was performed to determine the capacity of adsorption after regeneration. This process was repeated up to fourteen times to investigate the effect of regeneration on capacity of adsorption and also to determine the loss of adsorbent particles during regeneration experiments.

Figure 30 shows the result of fourteen regeneration-adsorption cycles. The scatter in the data above 150 mg/L of phenol concentration is due to the increased experimental error above this concentration. It was observed that there was no apparent change in adsorption capacity after regeneration up to 14 cycles. Data for each regeneration-adsorption cycle is detailed in Appendix C1.

Loss of adsorbent particles during regeneration was also determined for each regeneration adsorption cycle (Sample calculation in Appendix C2, also refer to section 3.2.4). The average loss of particles during regeneration was about 2.5-5 % per cycle for HiSiv 3000 while the same amount for activated carbon was 5-10% per cycle due to oxidation and attrition (Cen, 1994). Comparing Hisiv 3000 particles with activated carbon particles it was observed

that HiSiv 3000 particles were more rigid than activated carbon particles. As a result activated carbon lost more particles during adsorption-regeneration cycles.

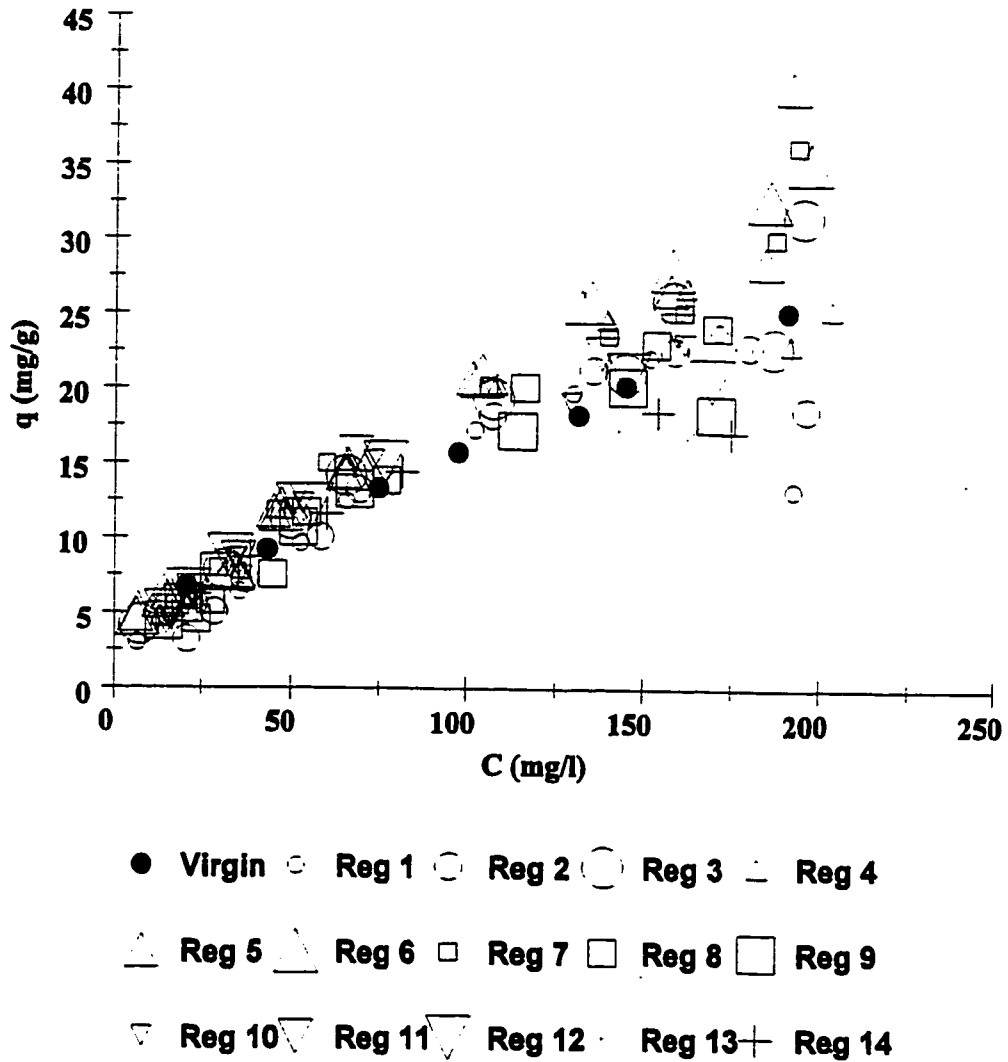


Figure 30:Effect of regeneration on adsorption of phenol on HiSiv 3000 (50x70 mesh), temperature=25°C.

4.8 Modeling

4.8.1 Kinetic Modeling

4.8.1.1 First Order Reversible Model

In the present work, the “first order reversible adsorption” model (see section 2.6.1.1) was applied to the data obtained from batch kinetic adsorption of phenol on different adsorbents. In this study it was assumed that adsorbents were initially free of phenol ($C_{B0} = 0$). By plotting $\ln[1-U(t)]$ vs. contact time (Equation 8), the value of rate constant (k') was determined for activated carbon, F-400, and HiSiv 3000 (50x70 mesh), respectively (Figures 31 to 33). In each curve fitting the confidence interval was more than 95%. In addition the same modeling results for different particle size of HiSiv 3000 are shown in Appendix D1.

The value of rate constants and diffusion coefficients for above mentioned adsorbents are shown in Table 7. Comparing the value of k' for HiSiv 3000 it is shown that this value is decreased when the particle size of the adsorbent is increased. This observation was previously discussed in section 4.6.6.

Comparing k' values for HiSiv 3000 and activated carbon and F-400 it is concluded that in general HiSiv 3000 has the highest rate constant. For different particle size of HiSiv 3000 the value of k' increases as the particle size is decreased. The same result can be obtained by comparing the diffusional time constant ($\frac{\bar{D}}{r_0^2}$) for different particle size of HiSiv 3000. As a result it takes more time for adsorbate molecules to diffuse into the larger particles.

Diffusion within the adsorbent particle will be much slower than movement of adsorbate molecules from solution to the external surface, because of the greater mechanical obstruction to movement presented by the surface molecules or surface layers. As a result pore diffusion coefficient (\bar{D}) is smaller than film diffusion coefficient (D_f). This phenomenon can be observed by comparing the pore diffusion coefficient (\bar{D}) with film diffusion coefficient (D_f) for each adsorbent (Table 7).

Table 7: The values of rate constants and diffusion coefficients for different adsorbents

Adsorbent	k' (1/h)	$t_{1/2}$ (hr)	r_0 (cm)	\bar{D} (cm ² /s)	$\frac{\bar{D}}{r_0^2}$ (1/s)	D_f (cm ² /s)
HiSiv 3000 (powder)	25.51	0.0271	0.005	2.76E-05	1.104	1.84E-03
HiSiv 3000 (50×70 mesh)	5.194	0.133	0.0123	3.40E-05	0.224	1.02E-03
HiSiv 3000 (20×50 mesh)	2.19	0.316	0.0286	7.75E-05	0.094	3.85E-04
HiSiv 3000 (extrude)	0.141	4.914	0.075	3.43E-05	0.006	2.36E-05
Activated carbon	0.625	1.108	0.04	4.33E-05	0.02	3.90E-03
F-400	0.926	0.748	0.0325	4.23E-05	0.04	3.02E-04

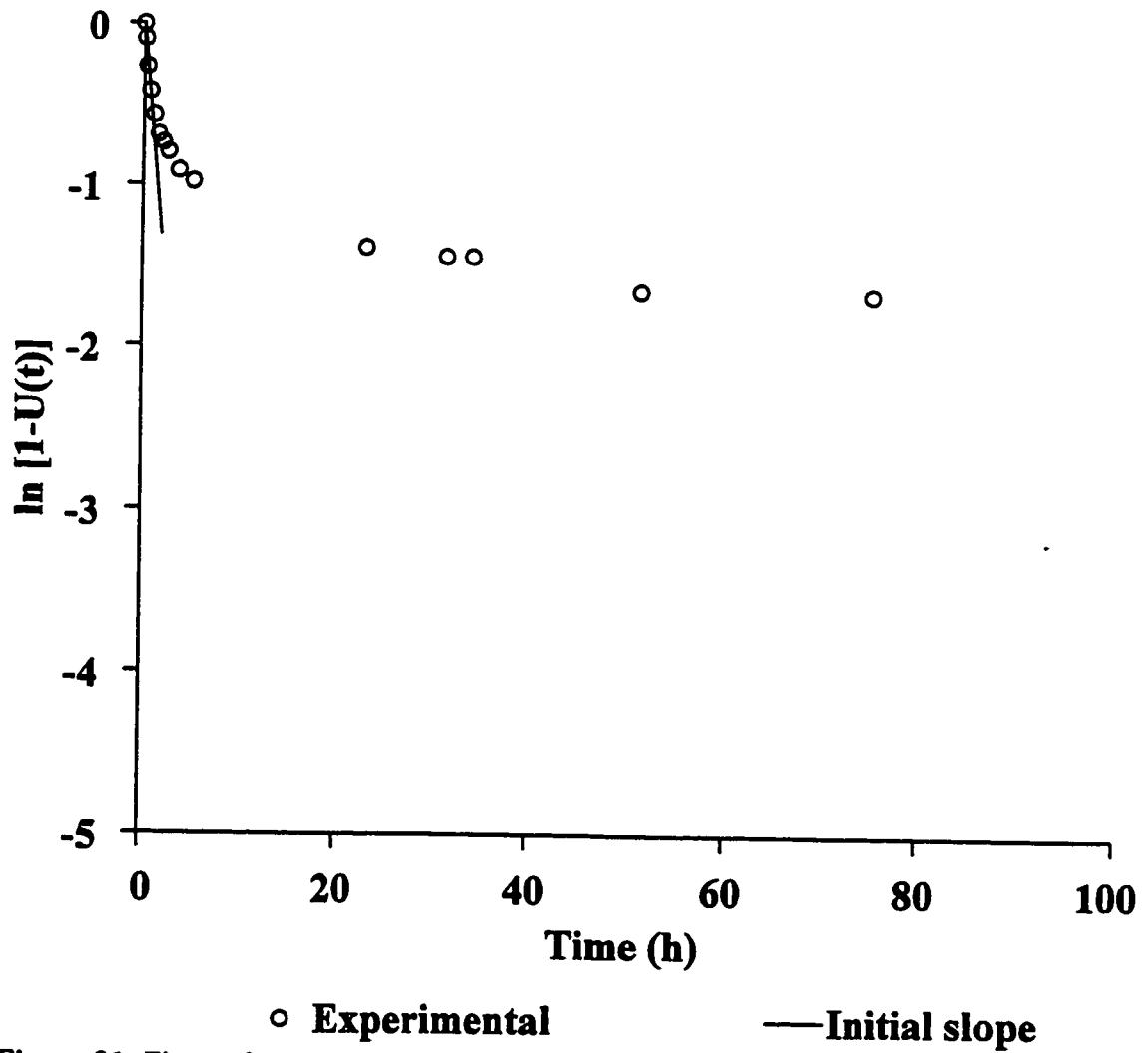


Figure 31: First order reversible kinetic fit of phenol adsorption data on activated carbon, at 25°C.

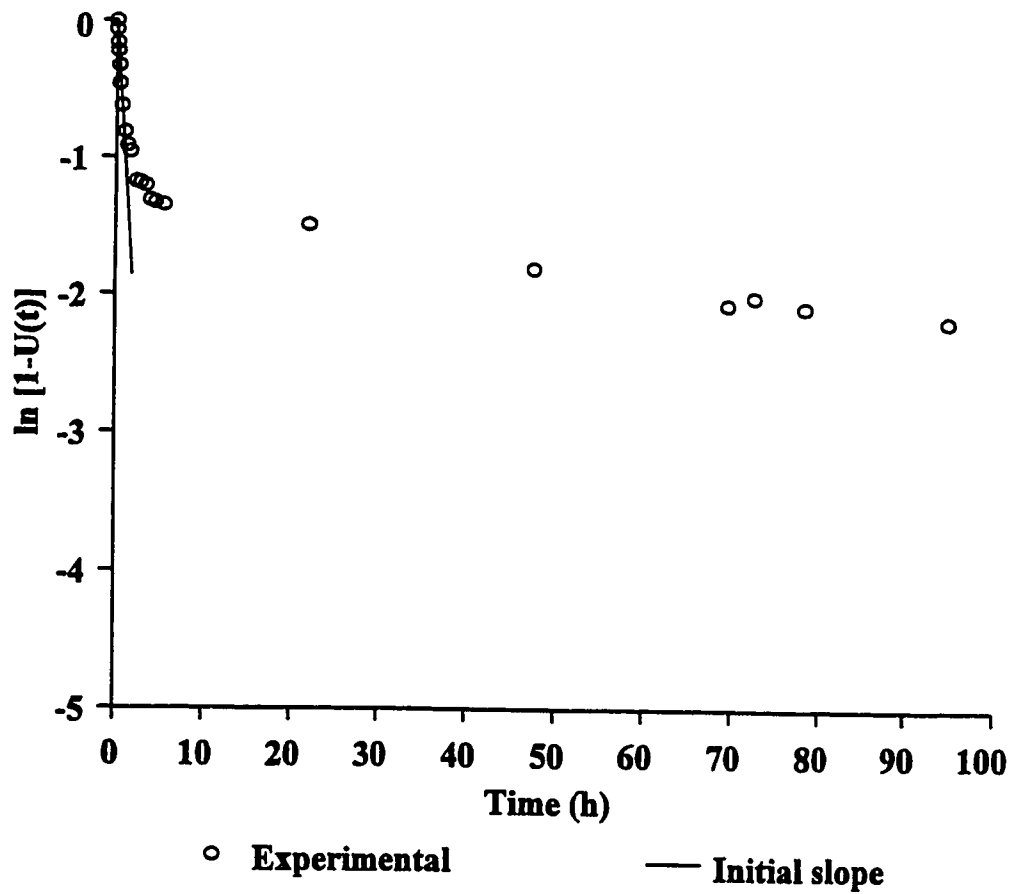


Figure 32: First order reversible kinetic fit of phenol adsorption data on F400, at 25°C.

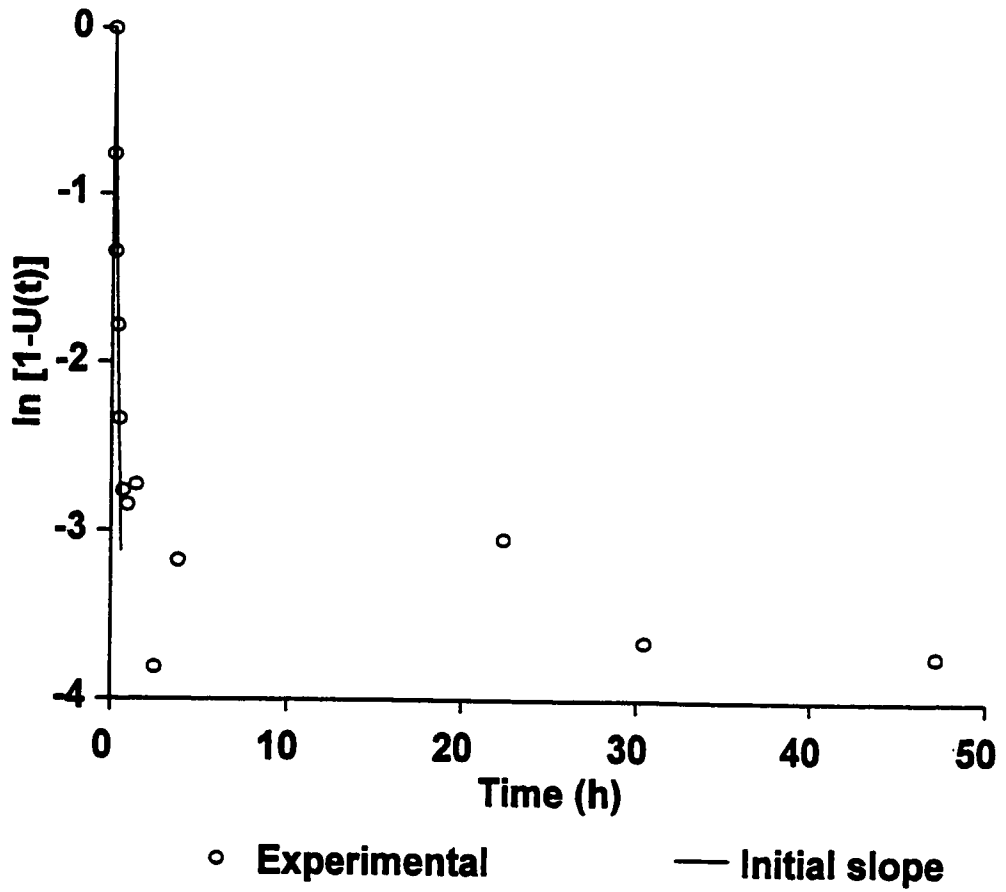


Figure 33: First order reversible kinetic fit of phenol adsorption data on HiSiv 3000 (50 × 70 mesh size), at 25°C.

4.8.1.2 Isothermal Diffusion Model

Isothermal diffusion model was the second model which was applied to the data obtained from kinetic experiments for phenol adsorption on different adsorbents studied in this work (refer to section 2.6.1.2). Figures 34 to 36 show the plots of phenol uptake against $t^{1/2}$ for activated carbon, F-400, and HiSiv 3000. The confidence interval for all the curve fittings were more than 95% for these figures. Results of isothermal diffusion modeling for HiSiv 3000 with different particle sizes are shown in Appendix D2. The linear portion of the plots is due to intraparticle diffusion being predominant as the rate controlling step, and as the bulk phenol concentration and surface phenol concentration start to decrease, the final portion of the figures begin to curve due to a decrease in the rate of diffusion.

The rate parameter, k (mg of phenol/g of adsorbent. $\text{min}^{1/2}$), is determined from the slope of the linear region of the plots of phenol uptake against $t^{1/2}$. In isothermal diffusion model it is assumed that film diffusion is not rate controlling because the solution is well agitated. Table 8 shows the value of k for different adsorbents as well as different particle sizes of HiSiv 3000.

These results show that as the particle size of HiSiv 3000 increases the rate parameter decreases, as a result diffusion in adsorbent with larger particle size is much slower than that of smaller particle size (See section 4.6.4). Comparing the rate parameter of HiSiv 3000, activated carbon, and F-400 it is clear that intraparticle diffusion of phenol into F-400 is higher than that of the other two adsorbents. Also F-400 and activated carbon show much higher intraparticle diffusion than HiSiv 3000, which is related to their structures.

Table 8: Rate parameters obtained from isothermal diffusion model for phenol adsorption at 25 °C

Adsorbent	k, Rate parameter mg/(g.min ^{1/2})
HiSiv 3000 (powder)	10.67
HiSiv 3000 (50×70 mesh)	5.23
HiSiv 3000 (20×50 mesh)	2.71
HiSiv 3000 (extrude)	0.58
F- 400	853.82
Activated carbon	675

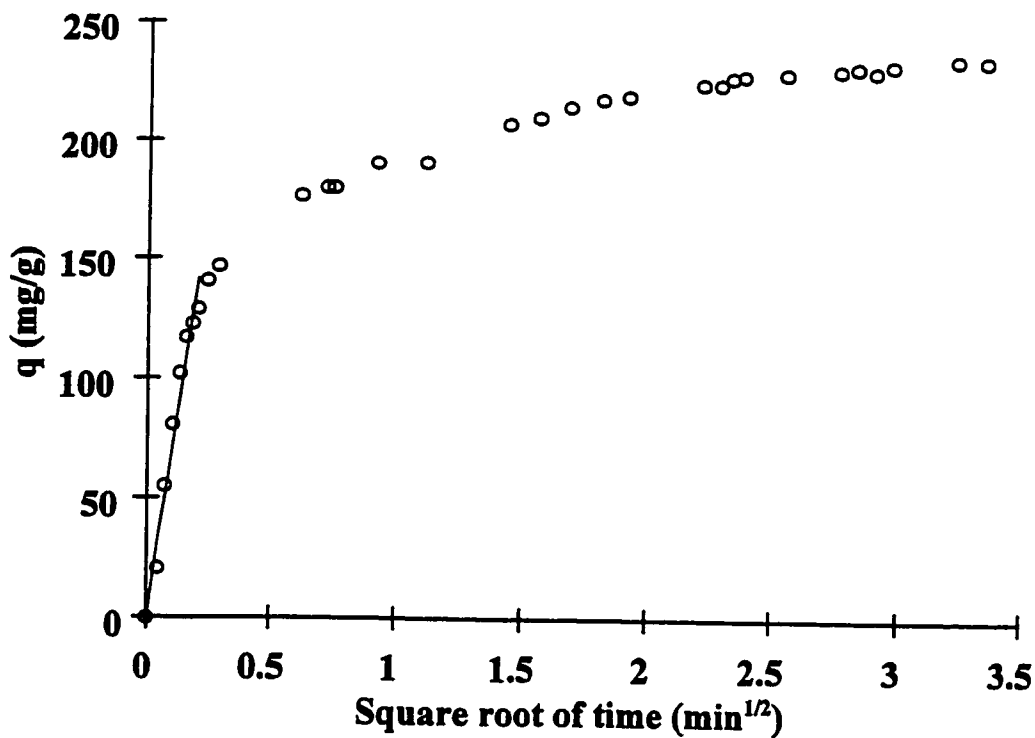


Figure 34: Plot of q against $t^{1/2}$ for adsorption of phenol on activated carbon at 25°C.

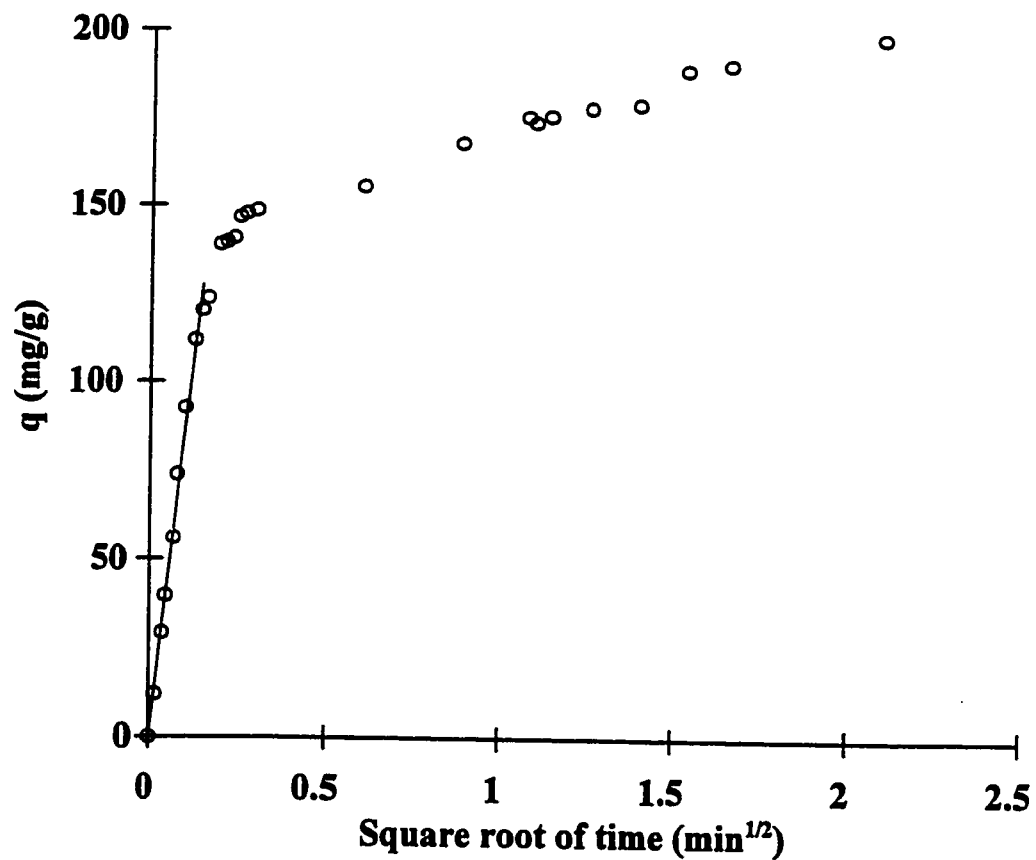


Figure 35: Plot of q against $t^{1/2}$ for adsorption of phenol on F-400 at 25°C.

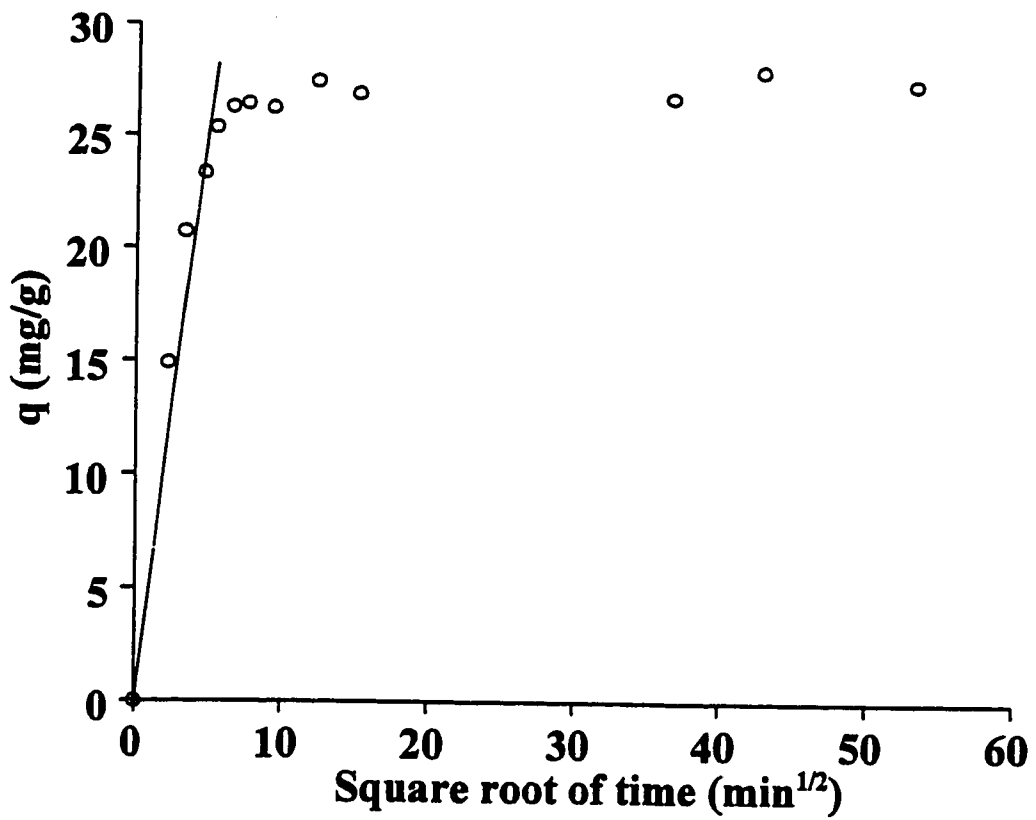


Figure 36: P lot of q against $t^{1/2}$ for adsorption of phenol on HiSiv 3000 (particle size =50×70 mesh) at 25°C.

4.8.2 Equilibrium Modelling

In the present work, three equilibrium models (Langmuir, Freundlich, and 3-parameter isotherm models) were applied to adsorption equilibrium data obtained experimentally. The unknown parameters in each model were determined by using optimization method (Quattro Pro, Microsoft package, 1995). Table 9 shows the values of these parameters for 95 % confidence interval. Figures 37 to 39 show the results of equilibrium modelling for activated carbon, F-400, and HiSiv 3000 (50×70 mesh) respectively. The results of equilibrium modelling for other experiments such as particle size effect and temperature effect are shown in Appendix E. The results of equilibrium modelling shows that 3-parameter isotherm model has the best fit for most of the adsorption isotherms.

Table 9: Equilibrium model's parameters.

Adsorbent	3-parameter			Freundlich		Langmuir	
	α (L/mg)	β (L/mg) $^\gamma$	γ (-)	k (mg/g)(L/mg) $^{1/n}$	1/n (-)	Q_b (mg/g)	b (L/mg)
Activated Carbon	13.28	0.02	1.156	41.66	0.40	308.91	0.052
F-400	186.70	4.756	0.699	36.32	0.314	205.035	0.037
HiSiv3000(powder)	0.119	0.005	0.819	0.05	1.242	322.58	0.0005
HiSiv 3000 (50x70 mesh)	13.78	46.87	0.140	0.289	0.865	322.6	0.0005
HiSiv 3000 (20-50 mesh)	0.189	0.001	1.289	0.602	0.667	322.63	0.0004
HiSiv 3000 (extrude)	0.834	0.615	1.289	0.834	0.615	322.63	0.0004
HiSiv 3000 (50-70 mesh), T=40°C	1.944	6.489	0.171	0.266	0.840	322.133	0.0004
HiSiv 3000 (50x70mesh), T=55°C	0.183	0.016	0.860	0.480	0.650	322.553	0.0003

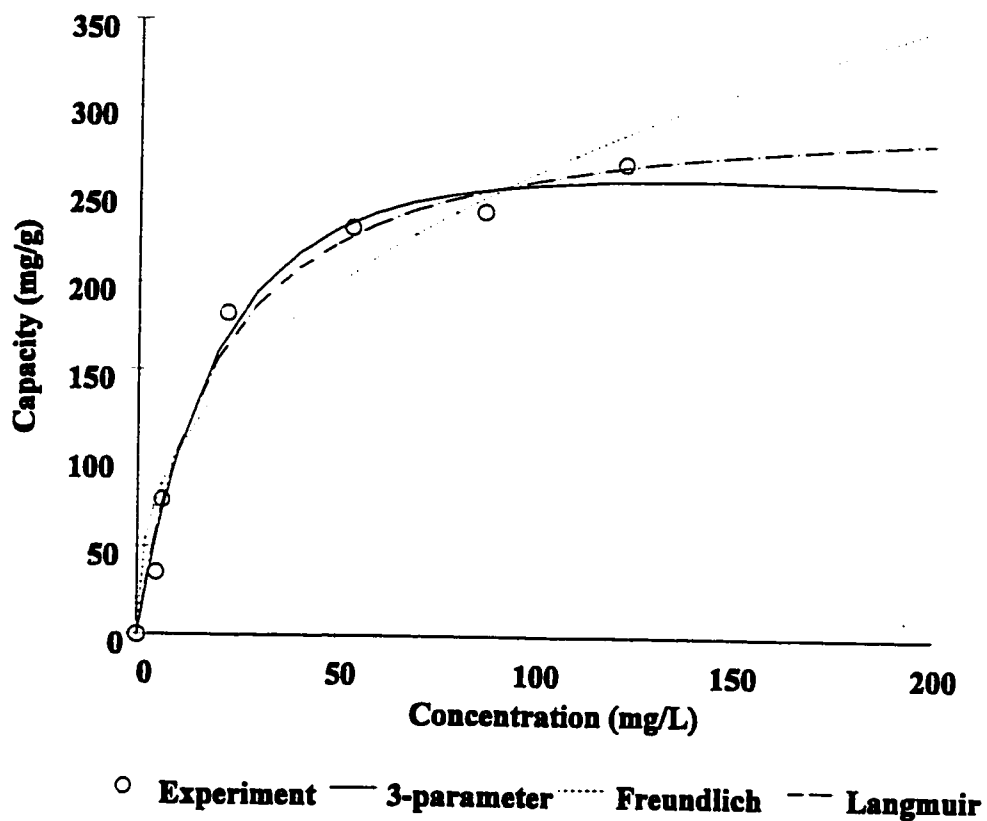
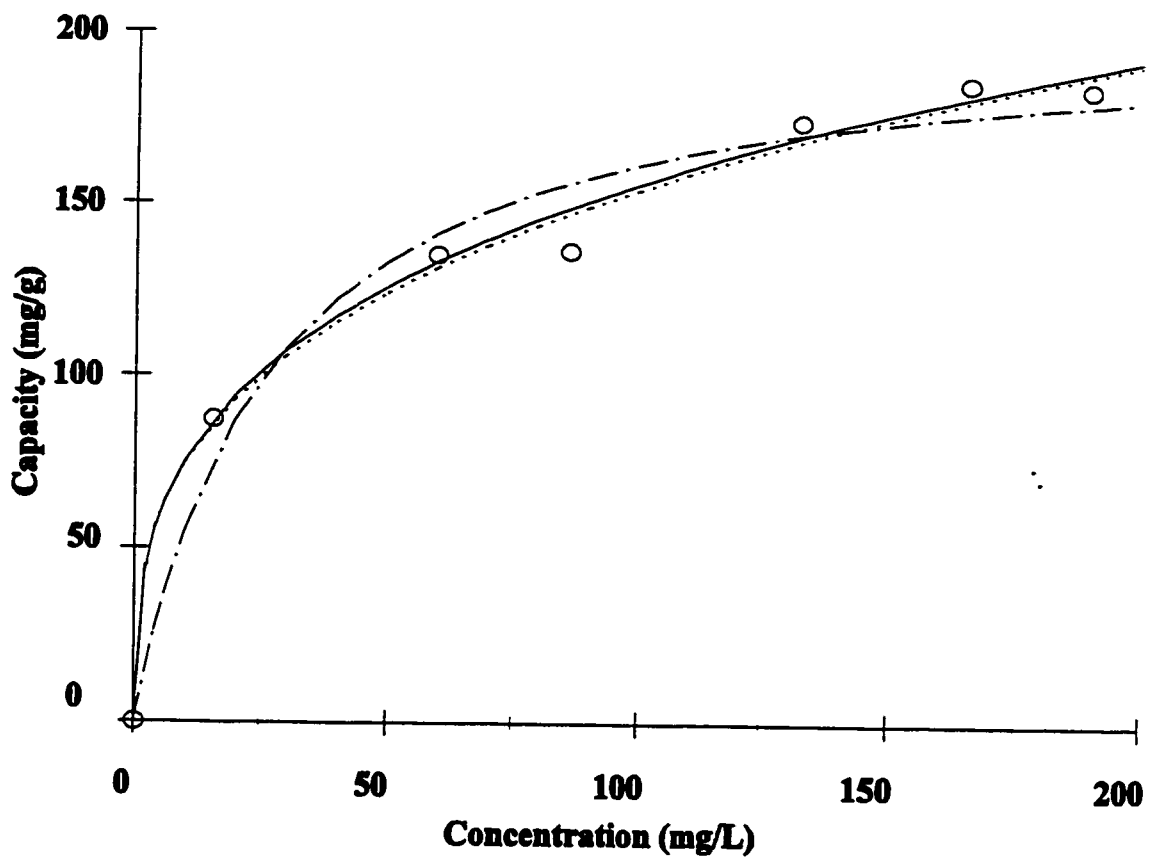
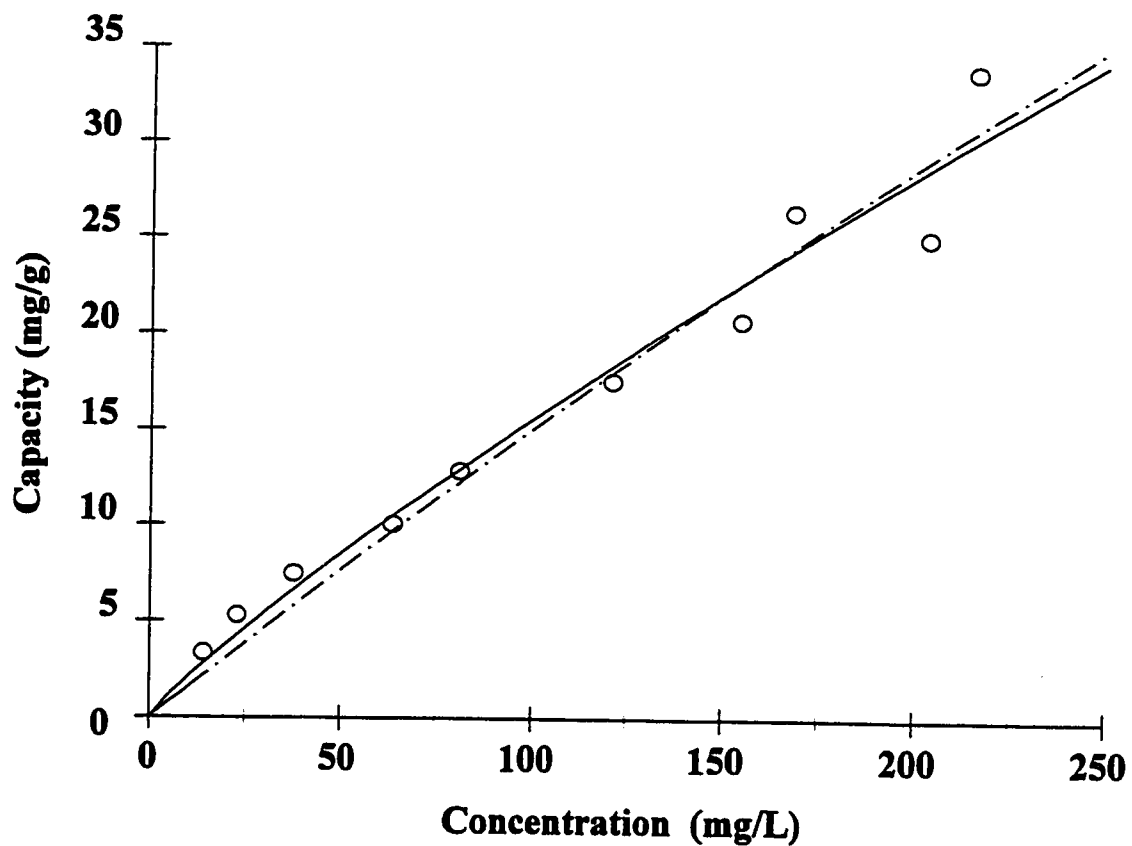


Figure 37: Isotherm models applied to phenol adsorption data with activated carbon at 25°C .



○ Experiment — 3-parameter Freundlich - - - Langmuir

Figure 38: Isotherm models applied to phenol adsorption data with F-400, at 25°C.



○ Experiment — 3- parameter Freundlich - - - Langmuir

Figure 39: Isotherm models applied to phenol adsorption data with HiSiv 3000 (50×70 mesh), at 25°C. In this figure Freundlich model coincides with 3- parameter model.

Chapter Five

Conclusions

In the present work the rate and capacity of phenol adsorption on different adsorbents were studied. Results of the equilibrium experiments indicated that phenol adsorption capacity of activated alumina, silica gel, and HiSiv 1000 are very low compared to HiSiv 3000, activated carbon, and filtrisorb 400. Although adsorption capacity of phenol on HiSiv 3000 was not as high as the capacity of phenol adsorption on activated carbon and filtrisorb 400, results of kinetic experiments showed that HiSiv 3000 reached equilibrium much faster than activated carbon and filtrisorb 400.

Results of regeneration experiments showed that phenol adsorption capacity of HiSiv 3000 did not change after 14 regeneration cycles. Particles of HiSiv 3000 had more resistance against attrition than activated carbon, therefore, loss of adsorbent particles during regeneration-adsorption cycles was lower for HiSiv 3000. Another advantage for HiSiv 3000 regeneration is that it can be regenerated at 360° C while activated carbon regeneration is generally performed at 800° C.

Decreasing the particle size of HiSiv 3000 did not change the capacity of adsorption, but it increased the rate of phenol adsorption.

Adsorption capacity of phenol on HiSiv 3000 was decreased by increasing temperature.

Chapter Six

Recommendations

Following recommendations were made after the completion of the present work:

6.1 Continuous Systems

1) Continuous-Flow Tank:

In this research batch adsorption experiments were carried out to study the adsorption of phenol from water. The same method and procedures discussed in this work can be adopted for continuous-flow tanks. The only distinguishing feature of adsorption in continuous-flow tanks arises from the fact that, if the pellets enter and leave the tank together with the solution, the residence time the pellets present in a continuous-flow tank is, in general, not constant but follows a distribution function (Tien, 1994). Future study should investigate the effect of continuous flow on adsorption capacity of phenol.

2) Fixed-bed Column

Practical applications of adsorption are most commonly carried out in the fixed-bed mode. Therefore it is necessary to investigate the adsorption equilibrium relationship and rate mechanisms as well as predicting breakthrough curves for specified conditions in a fixed-bed operation.

6.2 Multi-component Adsorption

The micro-pollutants generally enter drinking water supplies by water runoff, through waste discharge, or by chemical spills. Among the micro-pollutants, phenolic compounds are considered to be one of the main groups of contaminants in polluted waters (Ma, et al., 1996). In this work single adsorption of phenol from water was studied. However there are other phenolic compounds in water such as 2,4 -chlorophenol, o-cresol, p-nitrophenol. The influence of these compounds on adsorption of phenol from water should be studied as a multi-component adsorption process.

6.3 Enhancing the Adsorption Capacity

Considering HiSiv 3000 as a zeolite adsorbent, it has aluminosilicate skeleton which contains an excess of negative charges which are balanced by alkali metal Me^+ or alkaline earth Me^{+2} ions not included in the skeleton but loosely bound in the channels of the crystal lattice. These ions can be displaced and therefore substituted by other ions such as those from the surrounding solution. So by finding a suitable solution in ion exchange process the adsorption capacity of HiSiv 3000 can be increased.

6.4 Regeneration Time

In this project, regeneration of HiSiv 3000 was conducted over night for 16 hours. But it is necessary to find the minimum time for regeneration. The advantages of minimum regeneration time are:

- 1) Minimum cost of energy required for regeneration.

2) Preventing adsorbent structure from being destroyed by exposing it to high temperature for shorter periods of time.

References

Abdo, M.S.E., Nosier, S.A., El-Tawil, Y.A., Fadl, S.M., and El-Khaiary, M. I., "Removal of phenol from aqueous solutions by mixed adsorbents: Maghara Coal and Activated carbon", *J. Environ. Sci. Health*, **A32(4)**, 1159-1169 (1997).

Abuzaid, N., Nakhla ,G., Farooq S., and Osei-Twum E., "Activated carbon adsorption in oxidizing environments", *Water Resource*, **29**, No. 2 , 653-660, (1995).

Abuzaid, N., Nakhla ,G., "Effect of pH on the kinetics of phenolics uptake on granular activated carbon", *Hazardous Materials*, **49**, 217-230, (1996).

Baharat, G. K., Yenkie M., and Natarajan, G.S., "Influence of Physico-chemical characteristics of adsorbent and adsorbate on competitive adsorption equilibrium and kinetics", *Fundamental of adsorption* , Kluwer Academic Publishers, Boston, 91-98, (1996).

Bhattacharya, A. K, and Venkobachar, C., "Removal of cadmium (II) by low cost adsorbents", *Environm. Eng.* **110**, No. 1, (1984).

Bishop, D. J., Kenezovich, J. P., and Harrison Florencel L., "Behavior of phenol and aniline on selected sorbents and energy-related solid wastes", *Water, Air, Soil Pollution*, **49**, 93-106, (1990).

Cen, J., "Electrochemical regeneration of granular activated carbon", M.A.Sc. Thesis, Dep. of Civil Eng., University of Ottawa, (1994).

Chiang, P.C., and Wu, J.S., "Evaluation of chemical and thermal regeneration of activated carbon", *Water Sci. Tech.*, **21**, 1697-1700, (1989).

Chatzopoulos, D. and Varma, A., "Activated carbon adsorption and desorption of toluene in the aqueous phase", *AIChE journal*, **39**, No. 12, 2027-2041, (1993).

Cooke, S. and Labes, M. M., "Destruction of the environmentally hazardous monochlorinated phenols via pyrolysis in an inert atmosphere" *Carbon*, **32**, 1055-1058, (1994).

CRC Handbook of Chemistry and physics, 66th edition, CRC Press, Cleveland, Ohio, (1985).

Crittenden, H. C.M. and Weber, W. J. Jr., *J. Envir. Engrg. Div. ASC*, **104**, 433 (1978).

Crute, T. D., "Phenol and the importance of dose", *J. Chemical Education*, **69**, No. 7, 553, (1992).

Dechow, F. H.M. "Separation and purification techniques in biotechnology", Noyes Publications, Park Ridge, New Jersey (1989).

EPA (United States Environmental Protection Agency), "Quality criteria for water, office of water and hazardous materials/ office of water planning and standards: Washington, DC.(1976).

Faust, S., and Ali, O., "Adsorption process for water treatment", Butterworths Publication, (1987).

Goto, M., Hayashi, N., Goto, S., "Adsorption and desorption of phenol on an ion-exchange resin and activated carbon", *Envir. Sc. and Tech.*, **20**, 463-467, (1986).

Helfferich, F., "Ion exchange", McGraw Hill book company Inc., New York, (1962).

Hutchinson, D. H. and Robinson, C.W., "A microbial regeneration process for granular activated carbon-I, Process modeling", *Water Research*, **24**, 1209-1215, (1990a).

Hutchinson, D. H. and Robinson, C.W., "A microbial regeneration process for granular activated carbon-II, Process modeling", *Water Research*, **24**, 1217-1223, (1990b).

Jankowska, H., Swiatkowski, A., Gelbin, D., Radeke, K.H., and Seidel, A., "Influence of porous structure and surface properties of active carbons on the adsorption of phenol from aqueous solutions", 4th International Carbon Conference, Beden, Germany, 397-399, (1986).

Juang, R. S., Tseng, R. L., Wu, F.C., and Lee, S. H., "Liquid-phase adsorption of phenol and its derivatives on activated carbon fibers," *Separation Science and Technology*, **31**(14), 1915-1931, (1996).

Jüntgen, H., "Phenomena of activated carbon regeneration, translation of reports on special problems of water technology", -600/9-76-03 Cincinnati, Ohio, (1976).

Lin, S.H., and Hsu, F.M., "Liquid-phase adsorption of organic compounds by granular activated carbon and activated carbon fibers", *Ind. Eng. Chem. Res.*, **34**, 2110-2116, (1995).

Lo, M.C., Irene, A., and Pota A. "Computer simulation of activated carbon adsorption for multi-component systems", *Environment International*, **22**, No. 2, 239-252, (1996).

Ma, J., Li, G., and Graham, N.J.D., "A study of the factors affecting the removal of phenolic compounds from water by PAC," *Water Supply*, **14**, n: 2, Amsterdam, 209-221, (1996).

Mathews, A.P., "Mathematical modeling of multicomponent adsorption in batch reactors", Ph.D. Thesis, University of Michigan, pp 207, (1975).

- McKay, G, "The adsorption of dye stuff from aqueous solutions using activated carbon. III. Intraparticle diffusion processes", *J. Chem. Tech. Biotechnol.*, **33A**, 196-204, (1983).
- Meytal, Y. I., Sheintuch, M., Shter G. E., and Grader, G. S., "Optimal temperature for catalytic regeneration of activated carbon", *Carbon*, **35**, No. 10, 1527-1531, (1997).
- Narbaitz, R. M., Cen, J., "Electrochemical regeneration of granular activated carbon", *Wat. Res.*, **28**, No. 8, 1771-1778, (1994).
- Narbaitz, R.M. and Cen, J., "Alternative methods for determining the percentage regeneration of activated carbon", *Wat. Res.*, **31**, No. 10, 2532-2542, (1997).
- Ościk, J., "Adsorption", Ellis Horwood Ltd. publication, New York, (1982) .
- Panday, K., Prasad, G., and Singh V.N., "Copper (II) removal from aqueous solution by fly ash", *Wat. Res.*, **19**, 869-873, (1985).
- Parfitt, G.D., and Rochester, C.H., "Adsorption from solution at solid/liquid interface", Academic Press, Inc. New York, (1983).
- Peel, R.G., "The roles of slow adsorption and biological activity in activated carbon kinetic modeling", Ph.D. Thesis, Dept. of Chemical Engineering, McMaster university, Hamilton, Ontario (1980).

- Peel, R.G., and Benedec, A., "Attainment of Equilibrium in activated carbon isotherm studies," *Environmental Science & Technology*, **14**, No. 1, 66-71, (1980).
- Radeke, K.H., and Hartmann, G., "On the temperature dependence of adsorption of organic materials from aqueous solution", *Adsorption Science and Technology*, **8**, No. 3, 153-156 (1992).
- Radke, C.J., and Prausnitz, J.M., "Thermodynamics of Multi-solute adsorption from dilute liquid solutions", *AIChE J.*, **18**, 761 (1972).
- Randtke, S.J. and Snoeyink, V.L. "Evaluating GAC adsorptive capacity", *J. of American Water Works Association*, **75**, 406-413, (1983).
- Robeck, E.G., Dostal, K.A., Cohen, J.M., and Kreiss J.F. (1965). "Effectiveness of water treatment processes in pesticide removal." *J. of Am. Water Works Assoc.*, **57**, 181-199, (1965).
- Ruthven, D.M., "Principles of adsorption and adsorption processes", Wiley publication, New York, (1984).
- Salvador, F. and Merchán, M.D., "Study of the desorption of phenol and phenolic compounds from activated carbon by liquid-phase temperature-programmed desorption", *Carbon*, **34**, 1543-1551, (1992).
- Sigurdson, S. P. and Robinson, C.W. "Substrat-inhibited microbiological regeneration of granular activated carbon", *The Canadian Journal of Chemical Engineering*, **56**, 330-339, (1978).

- Singh, B. K., and Rawat, N. S., "Comparative sorption equilibrium studies of toxic phenols on fly ash and impregnated fly ash", *J. Chem. Tech. Biotechnol.*, **61**, 307-313, (1994).
- Snoeyink, V.L., Weber, W. J., Jr. and Mark, H. B., Jr., "Sorption of phenol and nitrophenol by active carbon.". *Environmental Science and Technology*, **3**, 918-926., (1969).
- Suzuki, M., "Adsorption Engineering", Elsevier publication, New York, (1990).
- Sveshnikova, D. A., Ramazanov, A. Kh., Aliev, Z .M., Shakhnazarov, T.A., Hamalurdinova, I. A. and Babaev, M. S. "Electrochemical regeneration of carbons" *Kimiyai Teknologiya Vody*, **9**, No. 5, 466-467, (1987).
- Thomas, W.J., and Crittenden, B. "Adsorption Technology and Design", Butterworth-Heinemann Publication, Oxford, U.K. (1998).
- Tien, C. , "Adsorption calculation and modeling", Butter worth-Heinemann, Boston, (1994).
- UOP company, "Product information sheet of HiSiv 1000", Molecular sieve Department, Mt. Laurel, NJ, USA, (1998a).
- UOP company, "Product information sheet of HiSiv 3000", Molecular sieve Department, Mt. Laurel, NJ, USA, (1998b).
- van, Vliet, B. M. and Venter, L., "Infrared thermal regeneration of spend carbon from water reclamation.", *Water Science and Technology*, **17**, 1029-1042, (1984).
- Vidic, R.D. and Suidan, M.T., "Role of dissolved oxygen on the adsorptive capacity of activated carbon for synthetic and natural organic matter", *Environ. Sci. Technol.*, **25**, No. 9, 1612-1618 (1991)

- Viraraghavan, T. and Alfaro, F. "Removal of phenol from wastewater by adsorption on peat, fly ash and bentonite," *J. of Environmental Engineering*, **5**, 311-317, (1992).
- Waer, M.A., Snoeyink, V.L. and Mallon, K. L., "Carbon regeneration dependence in time and temperature.", *J. American Water Works Association*, **84**, 3, 82-91, (1992).
- Wallis, D. A. and Bolton E. E., "Biological regeneration of activated carbon", *AICHE Symposium Series*, **78**, No. 219, 64-70, (1982).
- Weber, T.M., and Getzen, F.W., "Influence of pH on the adsorption of aromatic acids on activated carbon", *Environmental Science and Technology*, **4**, No. 1, 64-67, (1970).
- Yen, C.Y., "The adsorption of phenol and substituted phenols on activated carbon in single- and multi-component systems". Ph.D. Thesis, University of North Carolina, Chapel Hill, N.C., USA (1983).
- Weber, W. J., Jr. and Morris, J.C., "equilibria and capacities for adsorption on carbon", *J. of the Sanitary Engineering Division, ASCE*, **90**, EE2, 185-197, (1964).
- Ying, W., Ph.D. Thesis, University of Michigan, Ann Arbor, Michigan, (1978).
- Zogorski, J.S.M., Faust, S. D. and Haas, J. H., Jr., "The kinetics of adsorption of phenols by granular activated carbon.", *J. of Colloid and Interface Science*, **55**, No.2, 329-341, (1976).
- Zogorski, J. S., and Faust, S. D., "Equilibria of adsorption of phenols by granular activated carbon.", Chapter 9 in *Chemistry of Wastewater Technology*, A. J. Rubin (ed.), Ann Arbor Science Publishers, Ann Arbor, Michigan, (1978).

Zogorski, J. S., "The adsorption of phenol onto granular activated carbon from aqueous solution", Ph.D. Thesis, Dept. of Environmental Sciences, Rutgers University, New Brunswick, New Jersey, (1975).

Appendices

A1. Phenol Structure and Size

Phenol is an aromatic organic compounds with a hydroxyl group (Figure 40).

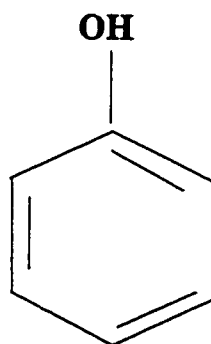


Figure 40: Phenol structure

To calculate the volume of phenol molecule:

The density of phenol (D) is divided by the molecular weight of phenol (MW). The result has the unit of mole/cc. By multiplying this value with Avogadro No., the number of molecules per cubic centimetre will be found. By inverting this value the volume of 1 molecule of phenol will be found as following:

Density of phenol =D = 1.071 g/cm³ , at room temperature, and solid phase¹

No. of phenol moles per unit volume =D/MW =1.071/94.11 =0.01138 Mole/cm³

1. Sigma-Aldrich product information, catalog No. 431516, phenol purity =99.99%

Avogadro no. = 6.023×10^{23} molecules/mole

No. of molecules per unit of volume = $0.01138 \times 6.023 \times 10^{23}$

= 6.854×10^{21} molecules/cm³

Volume of 1 molecule = $1/6.854 \times 10^{21} = 1.4589 \times 10^{-22}$ cm³/ molecule

A2. Adsorption Isotherm Curve

The relation between amount adsorbed, q , and concentration in liquid phase, C , at constant temperature, T , is called the adsorption isotherm which can be determined from following equation:

$$V(C_0 - C) = m(q - q_0)$$

V = Volume of solution in each bottle (L)

C_0 = initial concentration of phenol in liquid phase (mg/L).

C = concentration of phenol in liquid phase after reaching equilibrium (mg/L).

m = amount of adsorbent used in each bottle (g).

q = concentration of phenol in adsorbed phase after reaching equilibrium (mg/g).

q_0 = Initial concentration of phenol in adsorbed phase (mg/g).

The equilibrium tests were conducted with virgin adsorbent ($q_0 = 0$), as a result the above equation can be rearranged to :

$$q = (C_0 - C) \cdot V/m$$

By plotting q vs C for each bottle point the adsorption isotherm can be determined (Figure 41).

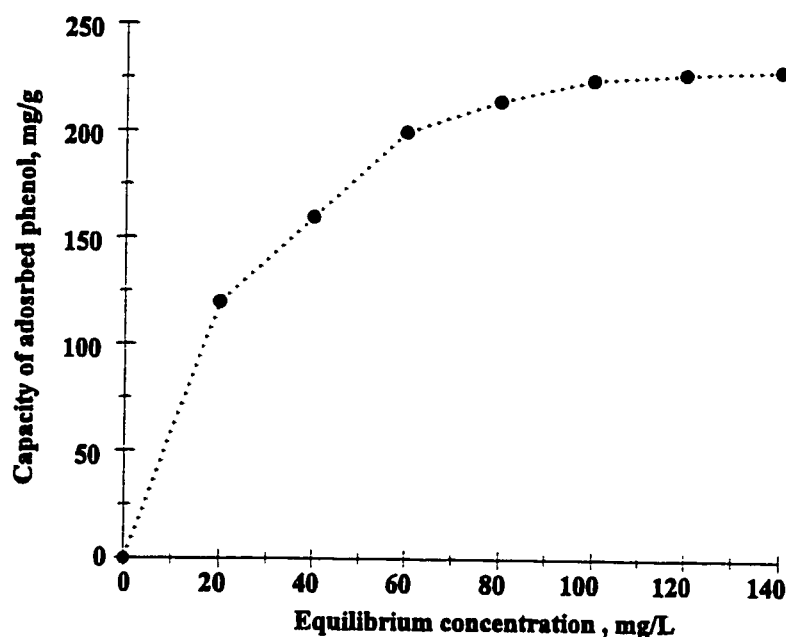


Figure 41: An example for plotting adsorption isotherm curve.

B. Raw Data from Adsorption Experiments

B.1 Kinetic Experiments

Adsorbent name	Silica gel
weight of adsorbent	5.205 g
Initial concentration of phenol in solution	202.52 mg/L
Initial pH of phenol in solution	5.6
Volume of phenol solution	1944 ml
Analyzing method	Spectrophotometer

Date (1998)	Time of sampling	Δt (h)	Phenol concentration in liquid phase (mg/L)
May 27	08:45 AM	0.00	202.52
May 27	08:55 AM	0.17	202.81
May 27	09:15 AM	0.50	204.69
May 27	09:35 AM	0.83	205.33
May 27	10:00 AM	1.25	204.19
May 27	11:00 AM	2.25	204.73
May 27	01:00 PM	4.25	203.88
May 27	03:30 PM	6.75	206.60
May 28	09:00 AM	24.25	197.21

Adsorbent name	Activated alumina (acidic)
weight of adsorbent	5.189 g
Initial concentration of phenol in solution	209.4 mg/L
Initial pH of phenol in solution	5.6
Volume of phenol solution	1944 ml
Analyzing method	Spectrophotometer

Date (1998)	Time of sampling	Δt (h)	Phenol concentration in liquid phase (mg/L)
May 27	08:50 AM	0.00	209.40
May 27	09:00 AM	0.17	195.87
May 27	09:20 AM	0.50	205.79
May 27	09:40 AM	0.83	203.87
May 27	10:05 AM	1.25	204.63
May 27	11:10 AM	2.33	204.46
May 27	01:00 PM	4.17	198.71
May 27	03:30 PM	6.67	204.71
May 28	09:00 AM	24.17	197.94

Adsorbent name	Activated alumina (basic)
Weight of adsorbent	2.6 g
Initial concentration of phenol in solution	201.3 mg/L
Initial pH of phenol in solution	8.3
Volume of phenol solution	1950 ml
Analyzing method	Spectrophotometer

Date (1998)	Time of sampling	Δt (h)	Phenol concentration in liquid phase (mg/L)
19-Jan	09:10 AM	0.00	201.3
19-Jan	10:15 AM	1.08	187.0
19-Jan	11:10 AM	2.00	196.2
19-Jan	12:10 PM	3.00	201.0
19-Jan	01:10 PM	4.00	201.0
19-Jan	02:10 PM	5.00	201.0
19-Jan	03:10 PM	6.00	191.0
19-Jan	06:15 PM	9.08	196.1
19-Jan	09:15 PM	12.08	195.3
20-Jan	09:45 AM	24.75	196.0
20-Jan	11:45 AM	26.75	196.3
20-Jan	03:18 PM	30.30	197.0
20-Jan	07:30 PM	34.50	196.9
21-Jan	07:50 AM	44.83	201.0
21-Jan	10:50 AM	46.83	196.8
21-Jan	0.53125	48.75	196.9

Adsorbent name	Activated carbon
weight of adsorbent	1.553 g
Initial concentration of phenol in solution	198.18 mg/L
Initial pH of phenol in solution	6.41
Volume of phenol solution	1950 ml
Analyzing method	TOC

Date (1998)	Time of sampling	Δt (h)	Phenol concentration in liquid phase (mg/L)
Nov 4	09:56 AM	0.00	198.18
Nov 4	10:02 AM	0.13	181.79
Nov 4	10:14 AM	0.33	154.18
Nov 4	10:35 AM	0.68	133.84
Nov 4	11:00 AM	1.10	116.84
Nov 4	11:30 AM	1.60	105.07
Nov 4	12:00 PM	2.10	100.42
Nov 4	12:32 PM	2.63	95.54
Nov 4	01:36 PM	3.70	86.04
Nov 4	03:05 PM	5.18	81.27
Nov 5	09:08 AM	23.23	57.41
Nov 5	01:33 PM	31.65	54.82
Nov 5	04:15 PM	34.35	54.82
Nov 6	09:20 AM	51.43	46.52
Nov 7	09:20 AM	75.43	46.07
Nov 9	11:34 AM	125.67	33.06
Nov 10	09:40 AM	147.77	30.73
Nov 11	09:30 AM	171.60	27.33
Nov 12	12:50 PM	198.93	24.77
Nov 13	12:05 PM	222.18	23.50
Nov 16	02:20 PM	296.43	19.42
Nov 17	09:50 AM	315.93	19.45
Nov 18	11:00 AM	329.10	17.11
Nov 19	12:30 PM	342.60	16.54
Nov 20	10:05 AM	364.18	22.17
Nov 21	02:00 PM	392.10	15.84
Nov 23	10:20 AM	436.43	22.30
Nov 24	10:05 AM	460.18	14.38
Nov 25	09:00 AM	483.10	13.40
Nov 26	09:00 AM	507.10	12.78
Nov 27	09:30 AM	531.60	12.29
Dec 1	09:50 AM	627.93	10.34
Dec 3	10:10 AM	675.27	10.71

Adsorbent name	Filtrisorb-400
Weight of adsorbent	1.04095 g
Initial concentration of phenol in solution	195.83 mg/L
Initial pH of phenol in solution	7.01
Volume of phenol solution	1950 ml
Analyzing method	TOC

Date (1998)	Time of sampling	Δt (h)	Phenol concentration in liquid phase (mg/L)
Oct-21	10:12 AM	0	195.83
Oct-21	10:19 AM	0.12	178.39
Oct-21	10:27 AM	0.25	173.46
Oct-21	10:44 AM	0.53	157.58
Oct-21	11:06 AM	0.9	145.79
Oct-21	11:37 AM	1.42	137.49
Oct-21	12:47 PM	1.58	131.23
Oct-21	01:47 PM	2.58	127.51
Oct-21	03:06 PM	3.9	123.90
Oct-22	09:50 AM	22.63	123.42
Oct-22	02:45 PM	27.55	122.81
Oct-23	09:45 AM	46.55	125.66
Oct-23	04:00 PM	52.8	125.33
Oct-24	03:00 PM	75.8	121.95
Oct-26	09:15 AM	94.05	120.67
Oct-27	10:00 AM	118.8	119.53
Oct-28	09:30 AM	142.3	119.10
Oct-29	10:45 AM	167.55	119.28
Oct-30	09:00 AM	189.8	116.05
Nov-02	10:00 AM	214.8	114.88
Nov-03	09:30 AM	238.3	113.20
Nov-04	09:00 AM	261.8	112.76
Nov-05	09:10 AM	285.97	114.04
Nov-06	09:20 AM	310.13	114.22
Nov-09	11:34 AM	382.37	108.83
Nov-10	09:40 AM	404.47	110.00
Nov-11	09:40 AM	428.47	106.23
Nov-12	12:50 PM	443.63	107.76
Nov-13	12:05 PM	466.88	105.52
Nov-16	02:20 PM	541.13	105.41
Nov-17	09:50 AM	560.63	106.77
Nov-18	11:05 AM	573.88	100.62
Nov-19	12:35 AM	587.38	103.92

Filtrisorb 400 kinetic data (continued) :

Date (1998)	Time of sampling	Δt (h)	Phenol concentration in liquid phase (mg/L)
Nov-20	10:10 AM	608.97	100.76
Nov-21	02:00 PM	626.80	101.55
Nov-23	10:15 AM	671.05	100.08
Nov-24	10:05 AM	694.88	98.72
Nov-25	09:00 AM	717.80	95.77
Nov-26	09:00 AM	741.80	95.34

Adsorbent name	HiSiv 1000
Weight of adsorbent	26.679 g
Initial concentration of phenol in solution	215.29 mg/L
Initial pH of phenol in solution	6.66
Volume of phenol solution	1950 ml
Analyzing method	TOC

Date (1998)	Time of sampling	Δt (h)	Phenol concentration in liquid phase (mg/L)
July 2	08:40 AM	0	215.29
July 2	08:50 AM	0.17	167.06
July 2	09:50 AM	1.17	170.83
July 2	11:20 AM	2.67	169.66
July 2	01:00 PM	4.33	171.61
July 2	03:00 PM	6.33	159.24
July 2	04:00 PM	7.33	163.8
July 3	08:15 AM	23.58	162.78
July 3	02:30 PM	29.83	162.4
July 4	11:00 AM	50.33	161.01
July 4	06:45 PM	58.08	161.77
July 5	09:30 AM	72.83	161.14
July 6	09:30 AM	96.83	156.58
July 7	12:00 PM	99.33	163.17
July 8	12:00 PM	123.33	164.60

Adsorbent name	HiSiv 3000 (powder)
Weight of adsorbent	3.012 g
Initial concentration of phenol in solution	224.2 mg/L
Initial pH of phenol in solution	7.35
Volume of phenol solution	1950 ml
Analyzing method	TOC

Date (1998)	Time of sampling	Δt (h)	Phenol concentration in liquid phase (mg/L)
Aug 6	10:54 AM	0	224.2
Aug 6	10:55 AM	0.02	203.58
Aug 6	10:57 AM	0.05	194.21
Aug 6	10:58 AM	0.07	188.59
Aug 6	11:00 AM	0.1	188.72
Aug 6	11:02 AM	0.13	185.38
Aug 6	11:05 AM	0.18	186.58
Aug 6	11:17 AM	0.38	184.25
Aug 6	11:22 AM	0.47	185.87
Aug 6	11:33 AM	0.65	182.36
Aug 6	11:39 AM	0.71	185.73
Aug 6	11:49 AM	0.92	185.73
Aug 6	12:01 PM	1.12	183.44
Aug 6	12:18 PM	1.4	185.6
Aug 6	12:35 PM	1.68	183.17
Aug 6	12:48 PM	1.9	185.33
Aug 6	12:55 PM	2.02	184.52

Adsorbent name	HiSiv 3000 (50×70 mesh)
Weight of adsorbent	5.627 g
Initial concentration of phenol in solution	215.95 mg/L
Initial pH of phenol in solution	7.15
Volume of phenol solution	1950 ml
Analyzing method	TOC

Date (1998)	Time of sampling	Δt (h)	Phenol concentration in liquid phase (mg/L)
Oct 6	10:33 AM	0.00	215.95
Oct 6	10:38 AM	0.08	172.91
Oct 6	10:44 AM	0.18	156.19
Oct 6	10:54 AM	0.35	148.66
Oct 6	11:02 AM	0.48	142.83
Oct 6	11:15 AM	0.70	140.11
Oct 6	11:30 AM	0.95	139.72
Oct 6	12:00 PM	1.45	140.31
Oct 6	01:06 PM	2.55	136.80
Oct 6	02:24 PM	3.85	138.39
Oct 7	09:00 AM	22.45	138.85
Oct 7	05:00 PM	30.45	135.38
Oct 8	09:45 AM	47.20	136.95

Adsorbent name	HiSiv 3000 (20×50 mesh)
weight of adsorbent	6.0064 g
Initial concentration of phenol in solution	204.73 mg/L
Initial pH of phenol in solution	6.29
Volume of phenol solution	1950 ml
Analyzing method	TOC

Date (1998)	Time of sampling	Δt (h)	Phenol concentration in liquid phase (mg/L)
Dec 16	09:19 AM	0	204.73
Dec 16	09:21 AM	0.03	187.33
Dec 16	09:26 AM	0.12	183.56
Dec 16	09:33 AM	0.23	169.00
Dec 16	09:38 AM	0.32	164.97
Dec 16	09:46 AM	0.45	160.29
Dec 16	09:56 AM	0.62	156.00
Dec 16	10:05 AM	0.77	152.49
Dec 16	10:37 AM	1.3	147.16
Dec 16	11:04 AM	1.75	144.69
Dec 16	12:19 PM	3	143.00
Dec 16	01:40 PM	4.35	140.53
Dec 16	02:43 PM	5.4	139.36
Dec 17	09:00 AM	23.68	135.85
Dec 17	12:00 PM	26.68	127.54
Dec 17	03:40 PM	30.35	138.01
Dec 18	09:00 AM	47.68	131.00
Dec 19	09:20 AM	72.02	137.34
Dec 21	09:40 AM	96.35	135.08
Dec 22	08:20 AM	119.02	134.03

Adsorbent name	HiSiv 3000 (extrude)
weight of adsorbent	5.696 g
Initial concentration of phenol in solution	206.77 mg/L
Initial pH of phenol in solution	6.79
Volume of phenol solution	1950 ml
Analyzing method	TOC

Date (1998)	Time of sampling	Δt (h)	Phenol concentration in liquid phase (mg/L)
Aug 10	11:40 AM	0.00	206.77
Aug 10	11:44 AM	0.07	201.67
Aug 10	12:02 PM	0.37	197.20
Aug 10	12:12 PM	0.53	198.09
Aug 10	01:08 PM	1.50	187.11
Aug 10	05:05 PM	5.45	170.78
Aug 11	09:30 AM	21.87	148.82
Aug 12	08:00 AM	44.37	143.97
Aug 13	08:30 AM	68.87	137.47
Aug 14	08:10 AM	92.53	137.60
Aug 15	08:10 AM	116.53	137.34
Aug 18	10:30 AM	214.87	134.64

B.2 Equilibrium Experiments:

Adsorbent name	Activated carbon
Initial concentration of phenol in solution	200.59 mg/L
Volume of phenol solution in each bottle	75 ml
Start at	5:20 p.m. Dec 10, 1998
End at	10 :00 a.m. Dec 29, 1998
Analyzing method	TOC

Bottle's code	Amount of adsorbent (g)	pH	Temperature (°C)	Equilibrium concentration (mg/L)
1	0.02016	7.94	26.9	122.57
2	0.03357	8.23	26.1	86.98
3	0.04578	8.93	27	53.59
4	0.07079	9.19	26.8	22.37
5	0.18458	8.94	27.1	6.17
6	0.40272	8.67	28	4.74
7	Phenol blank (Just phenol solution)	7.02	28	194.77
8	Control blank 0.22 g of adsorbent +water	8.63	27.5	Total organic carbon=9.28

Adsorbent name	F-400
Initial concentration of phenol in solution	205.13 mg/L
Volume of phenol solution in each bottle	75 ml
Start at	12:50 p.m. Oct 19, 1998
End at	3:10 p.m. Nov 17, 1998
Analyzing method	TOC

Bottle's code	Amount of adsorbent (g)	pH	Temperature (°C)	Equilibrium concentration (mg/L)
1	0.00552	6.63	26.6	155.6
2	0.0153	6.55	26.6	136.1
3	0.03052	6.18	27.1	109.7
4	0.06469	5.88	26.5	72.89
5	0.07983	5.61	26.6	51.96
6	0.1612	5.31	26.7	18.63
7	Phenol blank (Just phenol solution)	5.83	26.4	166.5
8	Control blank 0.148 g of adsorbent +water	5.3	27.3	Total organic carbon=5.33

Adsorbent name	HiSiv 1000
Initial concentration of phenol in solution	199.3 mg/L
Volume of phenol solution in each bottle	75 ml
Start at	12:30 p.m. July 14, 1998
End at	10:30 a.m. July 22, 1998
Analyzing method	TOC

Bottle's code	Amount of adsorbent (g)	pH	Temperature (°C)	Equilibrium concentration (mg/L)
1	5.35	6.08	25.4	87.32
2	3.6978	6.07	25.4	104.47
3	1.7099	6.21	25.5	142.22
4	1.1703	6.08	25.4	156.13
5	0.30039	6.36	25.5	198.77
6	Phenol blank (Just phenol solution)	6.78	25.4	216.32
7	Control blank 0.3108 g of adsorbent +water	6.79	25.4	Total organic carbon= 1.761
8	Control blank 5.366 g of adsorbent +water	6.39	25.4	Total organic carbon= 0.604

Adsorbent name	HiSiv 3000 (powder)
Initial concentration of phenol in solution	207.5 mg/L
Volume of phenol solution in each bottle	75 ml
Start at	9:05 a.m. June 29, 1998
End at	9:30 a.m. July 10, 1998
Analyzing method	TOC

Bottle's code	Amount of adsorbent (g)	pH	Temperature (°C)	Equilibrium concentration (mg/L)
1	0.1092	8.75	25.2	164.55
2	0.2074	9.26	25.1	141.52
3	0.6158	9.81	24.8	92.72
4	0.8283	9.95	25	78.12
5	1.052	10.06	25.7	69.74
6	3.0122	10.4	24.8	37.55
7	Phenol blank (Just phenol solution)	9.07	25.2	205.62
8	Control blank 0.108 g of adsorbent +water	9.35	25	Total organic carbon= 3.142
9	Control blank 5.03 g of adsorbent +water	10.67	24.9	Total organic carbon=2.147

Adsorbent name	HiSiv 3000 (50×70 mesh)
Initial concentration of phenol in solution	200.77 mg/L
Volume of phenol solution in each bottle	75 ml
Start at	3:10 p.m. Sep 11, 1998
End at	9:00 a.m. Oct 3, 1998
Analyzing method	TOC

Bottle's code	Amount of adsorbent (g)	pH	Temperature (°C)	Equilibrium concentration (mg/L)
1	0.05022	7.46	25.6	216.04
2	0.1045	7.98	25.9	203.8
3	0.20022	8.82	25.8	168.29
4	0.30394	9.01	26.1	154.82
5	0.503	9.35	26.1	121.22
6	0.92109	9.48	25.9	81.06
7	1.30322	9.43	26.4	63.79
8	2.01569	9.48	26.2	37.73
9	3.0322	9.5	25.9	22.87
10	5.01466	9.45	26.7	14.04
11	Phenol blank (Just phenol solution)	8.61	25.9	238.63
12	Control blank 2.55 g of adsorbent +water	9.47	26.4	Total organic carbon= 0.80

Adsorbent name	HiSiv 3000 (20×50 mesh)
Initial concentration of phenol in solution	203.39 mg/L
Volume of phenol solution in each bottle	75 ml
Start at	Start @ 2:30 p.m. Sep 1st, 1998
End at	End @ 9:00 a.m. Sep 8th, 1998
Analyzing method	TOC

Bottle's code	Amount of adsorbent (g)	pH	Temperature (°C)	Equilibrium concentration (mg/L)
1	0.0503	6.68	27	195.64
2	0.10036	8.41	26.6	184.80
3	0.30187	8.96	26.5	131.91
4	0.603	9.23	27.5	99.28
5	0.90889	9.33	27.6	75.54
6	1.20451	9.38	27	55.17
7	1.509	9.37	28.9	51.99
8	2.00271	9.39	26.5	39.19
9	2.50416	9.41	27	39.46
10	Phenol blank (Just phenol solution)	7.93	27.3	208.76
11	Control blank 1.321 g of adsorbent +water	9.47	28.1	Total organic carbon= 5.74

Adsorbent name	HiSiv 3000 (extrude)
Initial concentration of phenol in solution	206 mg/L
Volume of phenol solution in each bottle	75 ml
Start at	Start @ 2:30 p.m. Aug 14, 1998
End at	End @ 1:30 p.m. Aug 26, 1998
Analyzing method	TOC

Bottle's code	Amount of adsorbent (g)	pH	Temperature (°C)	Equilibrium concentration (mg/L)
1	0.10265	7.59	25.1	187.69
2	0.504	8.8	24.9	99.20
3	1.0106	9.07	25.3	64.33
4	3.003	9.62	25.3	21.35
5	5.0173	9.67	25.4	13.91
6	7.026	9.66	25.3	8.56
11	Phenol blank (Just phenol solution)	8.39	25.4	214.07
12	Control blank 3.548 g of adsorbent +water	9.8	25.3	Total organic carbon= 1.5

Adsorbent name	HiSiv 3000 (50×70 mesh), Working Temp.=40°C
Initial concentration of phenol in solution	204.13 mg/L
Volume of phenol solution in each bottle	75 ml
Start at	Start @ 10:45 a.m. Feb-10, 1999
End at	End @ 4:00 p.m. Feb-11, 1999
Analyzing method	TOC

Bottle's code	Amount of adsorbent (g)	pH	Temperature (°C)	Equilibrium concentration (mg/L)
1	0.07607	7.7	41	183.37
2	0.11598	8.59	40	175.27
3	0.20428	9.05	40	156.18
4	0.30493	9.22	40.5	136.74
5	0.51714	9.24	40.2	110.74
6	0.90378	9.38	40	80.32
7	1.31503	9.66	40	61.52
8	1.92734	9.68	40.5	41.34
9	2.75804	9.69	40.6	29.10
10	3.14409	9.83	40.1	28.02
11	Phenol blank (Just phenol solution)	6.69	40.5	205.69
12	Control blank 0.559 g of adsorbent +water	7.42	40.2	Total organic carbon= 8.74

Adsorbent name	HiSiv 3000 (50×70 mesh), Working Temp.=55°C
Initial concentration of phenol in solution	204.75 mg/L
Volume of phenol solution in each bottle	75 ml
Start at	Start @ 10:30 a.m. Feb-17, 1999
End at	End @ 3:30 p.m. Feb-18, 1999
Analyzing method	TOC

Bottle's code	Amount of adsorbent (g)	pH	Temperature (°C)	Equilibrium concentration (mg/L)
1	0.06243	7.96	54	199.00
2	0.13645	8.68	56	183.53
3	0.20597	8.89	53	165.55
4	0.32196	9.03	53	148.17
5	0.5011	9.21	54	126.71
6	0.92558	9.3	54	87.17
7	1.30344	9.28	55	70.50
8	2.01074	9.23	55	43.95
9	3.00626	9.35	55	29.25
10	5.01684	9.21	57	19.42
11	Phenol blank (Just phenol solution)	7.19	57	201.27
12	Control blank 2.533 g of adsorbent +water	9.27	57	Total organic carbon= 1.5

C. Raw Data from Regeneration Experiments

C.1 Result of adsorption cycles performed after each regeneration cycle

Adsorption after first regeneration:

Initial concentration of phenol in solution	200.55 mg/L
Initial pH of phenol solution	7.69
Volume of phenol solution in each bottle	75 ml
Start at	5:00 p.m. Oct 15, 1998
End at	11:30 a.m. Oct 16, 1998
Analyzing method	TOC

Bottle's code	amount of adsorbent (g)	pH	T (°C)	Equilibrium concentration (mg/L)
1	0.0439	7.18	25.1	192.59
2	0.09114	7.57	24.9	171.38
3	0.165	7.59	25.2	151.82
4	0.26702	8.04	25	130.17
5	0.4263	8.39	25	102.47
6	0.80899	8.83	25	65.90
7	1.14622	8.97	25.2	52.94
8	1.9165	8.94	25	35.42
9	2.91073	9.23	25.1	16.31
10	4.83855	9.37	25	6.68
11	Phenol blank	7.53	25	200.67

Adsorption after second regeneration:

Initial concentration of phenol in solution	217.36 mg/L
Initial pH of phenol solution	7.61
Volume of phenol solution in each bottle	75 ml
Start at	12:15 p.m. Oct 19, 1998
End at	8:30 a.m. Oct 20, 1998
Analyzing method	TOC

Bottle's code	amount of adsorbent (g)	pH	T (°C)	Equilibrium concentration (mg/L)
1	0.04213	7.11	24.9	196.17
2	0.08789	7.4	24.9	179.86
3	0.15922	7.4	24.9	158.83
4	0.24979	7.56	24.8	135.83
5	0.40895	7.99	24.9	107.53
6	0.77763	8.34	24.9	69.50
7	1.10403	8.62	24.9	58.56
8	1.75121	8.74	24.8	37.12
9	2.62423	8.98	24.9	28.64
10	4.3105	9.05	24.8	20.81
11	Phenol blank	7.77	24.9	224.03

Adsorption after third regeneration:

Initial concentration of phenol in solution	212.16 mg/L
Initial pH of phenol solution	7.09
Volume of phenol solution in each bottle	75 ml
Start at	12: p.m. Oct 28, 1998
End at	10:45 a.m. Oct 29, 1998
Analyzing method	TOC

Bottle's code	amount of adsorbent g	pH	T (°C)	Equilibrium concentration (mg/L)
1	0.04068	7.93	24.6	195.03
2	0.08417	8.02	24	186.63
3	0.15592	8.09	24	158.34
4	0.239	8.18	24.5	145.15
5	0.40616	8.32	24	107.74
6	0.77486	8.51	24.6	65.73
7	1.08139	8.5	24	50.03
8	1.72946	8.79	24.2	31.46
9	2.55351	8.95	24	20.86
10	3.6716	9.12	24	7.29
11	Phenol blank	8.25	24	212.11

Adsorption after fourth regeneration:

Initial concentration of phenol in solution	215.28 mg/L
Initial pH of phenol solution	5.18
Volume of phenol solution in each bottle	75 ml
Start at	1:40 p.m. Nov 9, 1998
End at	12:00 p.m. Nov 10, 1998
Analyzing method	TOC

Bottle's code	amount of adsorbent g	pH	T (°C)	Equilibrium concentration (mg/L)
1	0.04057	7.65	24.4	203.22
2	0.08238	8.05	24.3	191.67
3	0.15367	8.09	24.1	162.05
4	0.23572	8.19	24	139.60
5	0.4003	8.35	24.5	108.68
6	0.76405	8.45	24	65.89
7	1.064	8.56	24.6	48.25
8	1.71362	8.85	24	36.36
9	2.50327	8.9	24	20.90
10	3.1956	9	24.2	13.52
11	Phenol blank	8.25	24	216.91

Adsorption after fifth regeneration:

Initial concentration of phenol in solution	212.94 mg/L
Initial pH of phenol solution	7
Volume of phenol solution in each bottle	75 ml
Start at	12:00 p.m. Nov 12, 1998
End at	10:00 a.m. Nov 13, 1998
Analyzing method	TOC

Bottle's code	amount of adsorbent g	pH	T (°C)	Equilibrium concentration (mg/L)
1	0.0364	7.81	24.8	191.79
2	0.07088	8.22	24 .3	184.41
3	0.15124	8.19	24	157.62
4	0.23219	8.16	24	132.47
5	0.397	8.25	24 .2	101.83
6	0.76115	8.55	25	65.31
7	1.05851	8.5 2	24	45.19
8	1.70939	8.99	24	35.20
9	2.47357	9.1	25.1	15.04
10	3.18306	9.12	24 .8	6.57
11	Phenol blank	8.05	24	211.33

Adsorption after sixth regeneration:

Initial concentration of phenol in solution	217.4 mg/L
Initial pH of phenol solution	6.83
Volume of phenol solution in each bottle	75 ml
Start at	5:00 p.m. Nov 16, 1998
End at	10:30 a.m. Nov 17, 1998
Analyzing method	TOC

Bottle's code	amount of adsorbent g	pH	T (°C)	Equilibrium concentration (mg/L)
1	0.03586	7.25	25	196.85
2	0.06444	7.42	24.9	185.59
3	0.14868	7.85	25	158.16
4	0.228145	8.22	25.1	135.16
5	0.39213	8.16	25	104.44
6	0.75761	8.35	25.4	66.17
7	1.05207	8.46	25	47.22
8	1.703635	8.77	24.7	33.69
9	2.46065	8.87	25	14.23
10	3.17322	9.01	24.9	6.88
11	Phenol blank	7.19	25	213.66

Adsorption after seventh regeneration:

Initial concentration of phenol in solution	212.94 mg/L
Initial pH of phenol solution	6.84
Volume of phenol solution in each bottle	75 ml
Start at	7:00 p.m. Nov 18, 1998
End at	12:30 p.m. Nov 19, 1998
Analyzing method	TOC

Bottle's code	amount of adsorbent g	pH	T (°C)	Equilibrium concentration (mg/L)
1	0.03532	6.99	25.5	193.4
2	0.058	7.15	25.1	187.25
3	0.14612	7.49	25	161.56
4	0.2241	7.98	25	140.12
5	0.38726	8.05	25.3	106.40
6	0.75407	8.24	25	60.15
7	1.04563	8.35	25.2	45.75
8	1.69788	8.72	25	29.70
9	2.44773	8.88	25.4	22.40
10	3.16338	8.96	25	14.66
11	Phenol blank	7.19	25	210.48

Adsorption after eighth regeneration:

Initial concentration of phenol in solution	203.94 mg/L
Initial pH of phenol solution	6.96
Volume of phenol solution in each bottle	75 ml
Start at	9:50 a.m. Dec 8, 1998
End at	9:30 a.m. Dec 9, 1998
Analyzing method	TOC

Bottle's code	amount of adsorbent g	pH	T (°C)	Equilibrium concentration (mg/L)
1	0.13832	7.34	25.3	170.94
2	0.20122	7.58	25	153.72
3	0.36944	8.01	25.5	116.51
4	0.74755	8.46	25	77.42
5	1.03245	8.65	25	54.57
6	1.68829	8.82	25.1	45.07
7	2.4266	8.99	25	27.64
8	3.14832	9.17	25	23.53
9	Phenol blank	7.19	25.7	173.4

Adsorption after ninth regeneration:

Initial concentration of phenol in solution	215.28 mg/L
Initial pH of phenol solution	6.54
Volume of phenol solution in each bottle	75 ml
Start at	10:00a.m. Dec 10, 1998
End at	9:30 a.m. Dec 11, 1998
Analyzing method	TOC

Bottle's code	amount of adsorbent g	pH	T (°C)	Equilibrium concentration (mg/L)
1	0.11493	6.84	27	170.67
2	0.19795	6.98	27.5	145.62
3	0.36777	7.25	27	114.49
4	0.74018	7.66	26	68.22
5	1.03042	8.12	26	52.06
6	1.64393	8.42	26.5	30.19
7	2.41159	8.76	27	20.06
8	3.14486	8.95	26.5	14.34
9	Phenol blank	7.1	27.5	198.79

Adsorption after tenth regeneration:

Initial concentration of phenol in solution	218.79 mg/L
Initial pH of phenol solution	6.64
Volume of phenol solution in each bottle	75 ml
Start at	4:30p.m. Dec 12, 1998
End at	8:30 a.m. Dec 14, 1998
Analyzing method	TOC

Bottle's code	amount of adsorbent g	pH	T (°C)	Equilibrium concentration (mg/L)
1	0.19371	7.16	25.2	161.63
2	0.35961	7.23	26	129.59
3	0.72955	7.54	26	73.51
4	1.02374	8.26	25.3	53.58
5	1.62335	8.39	26.1	34.91
6	2.39074	8.85	25.2	22.37
7	3.10981	8.99	26	17.40
8	Phenol blank	7.16	26.1	221.11

Adsorption after eleventh regeneration:

Initial concentration of phenol in solution	217.62 mg/L
Initial pH of phenol solution	6.65
Volume of phenol solution in each bottle	75 ml
Start at	10:30 a.m. Dec 15, 1998
End at	9:30 a.m. Dec 16 , 1998
Analyzing method	TOC

Bottle's code	amount of adsorbent g	pH	T (°C)	Equilibrium concentration (mg/L)
1	0.18835	7.16	25.9	159.64
2	0.27419	7.29	26.5	138.20
3	0.72374	7.45	25.9	68.55
4	1.02002	8.34	26.5	50.43
5	1.61308	8.46	26.5	35.38
6	2.318	8.73	26.5	22.78
7	3.08736	8.93	26.8	16.17
8	Phenol blank	7.16	26.5	219.9

Adsorption after twelfth regeneration:

Initial concentration of phenol in solution	213.9 mg/L
Initial pH of phenol solution	6.17
Volume of phenol solution in each bottle	75 ml
Start at	5:00 p.m. Dec 18, 1998
End at	9:00 a.m. Dec 19, 1998
Analyzing method	TOC

Bottle's code	amount of adsorbent g	pH	T (°C)	Equilibrium concentration (mg/L)
1	0.18374	7.167	26.2	169.48
2	0.2651	7.29	26.2	145.69
3	0.71381	7.45	26.1	76.94
4	1.01354	8.34	26.1	55.86
5	1.59914	8.46	26.1	32.99
6	2.3321	8.73	25.7	21.26
7	3.06838	8.93	25.5	15.05
8	Phenol blank	7.16	25.6	220.29

Adsorption after thirteenth regeneration:

Initial concentration of phenol in solution	217.62 mg/L
Initial pH of phenol solution	6.17
Volume of phenol solution in each bottle	75 ml
Start at	10:00 a.m. Jan 13, 1999
End at	9:00 a.m. Jan 14 , 1999
Analyzing method	TOC

Bottle's code	amount of adsorbent g	pH	T (°C)	Equilibrium concentration (mg/L)
1	0.18069	7.17	25.2	162.58
2	0.25973	6.9	25	143.08
3	0.69999	6.98	25.1	75.76
4	1.00422	7.13	26	53.71
5	1.54138	7.41	25.9	32.20
6	2.26056	7.54	25.8	23.84
7	3.05249	7.62	25.8	15.57
8	Phenol blank	6.74	25.8	202.88

Adsorption after fourteenth regeneration:

Initial concentration of phenol in solution	211.77 mg/L
Initial pH of phenol solution	6.17
Volume of phenol solution in each bottle	75 ml
Start at	10:50 a.m. Jan 15, 1999
End at	9:20 am Jan 19, 1999
Analyzing method	TOC

Bottle's code	amount of adsorbent (g)	pH	T (°C)	Equilibrium concentration (mg/L)
1	0.16944	6.77	24.7	174.86
2	0.2401	6.87	25	154.25
3	0.68746	7.05	24.9	81.67
4	0.99413	7.41	25.7	60.23
5	1.50563	7.61	25.8	38.63
6	2.27855	7.77	25.2	23.14
7	3.03383	7.89	25.4	16.79
8	Phenol blank	6.54	25.5	213.39

C.2 Loss of adsorbent particles during filtration.

Sample calculation:

Sample code	W_0 (g)	$W_0 + \text{ads.}$ (g)	W_{end} (g)	$(W_{\text{end}} - W_0)$ Loss of particles (g)
1	0.44494	0.63483	0.44904	0.00410
2	0.44906	0.71799	0.45252	0.00346
3	0.44702	1.1597	0.44767	0.00065
4	0.43955	1.46063	0.44098	0.00143
5	0.44579	2.04573	0.44761	0.00182
6	0.43873	2.78149	0.44129	0.00256
7	0.445	3.5255	0.44802	0.00302
8	0.44439	2.37089	0.44595	0.00156

W_0 = Weight of filter paper before it was used, g

$W + \text{ads.}$ = Weight of filter paper containing adsorbent particles, g

W_{end} = Weight of filter paper after removing the adsorbent particles, g

Sample code is referred to the written code in each container.

C.3 Total Loss of adsorbent particles during each adsorption and regeneration cycle.

Referring to section 3.2.4, the loss of particles were determined by using data from adsorption cycles which performed after 12th and 13th regeneration cycles. Sample code is referred to the written code in each container.

Sample calculation:

Sample code	Mass of adsorbent after regeneration # 12 th	Mass of adsorbent after regeneration # 13 th	% Loss of particles
1	0.18374	0.18069	1.66
2	0.2651	0.25973	2.03
3	0.71381	0.69999	1.94
4	1.01354	1.00422	0.92
5	1.59914	1.54136	3.61
6	2.3321	2.26056	3.07
7	3.06838	3.05249	0.52
8	1.95246	1.91477	1.93

D. Kinetic Models

D.1 First Order Reversible model Applied to Kinetic Data

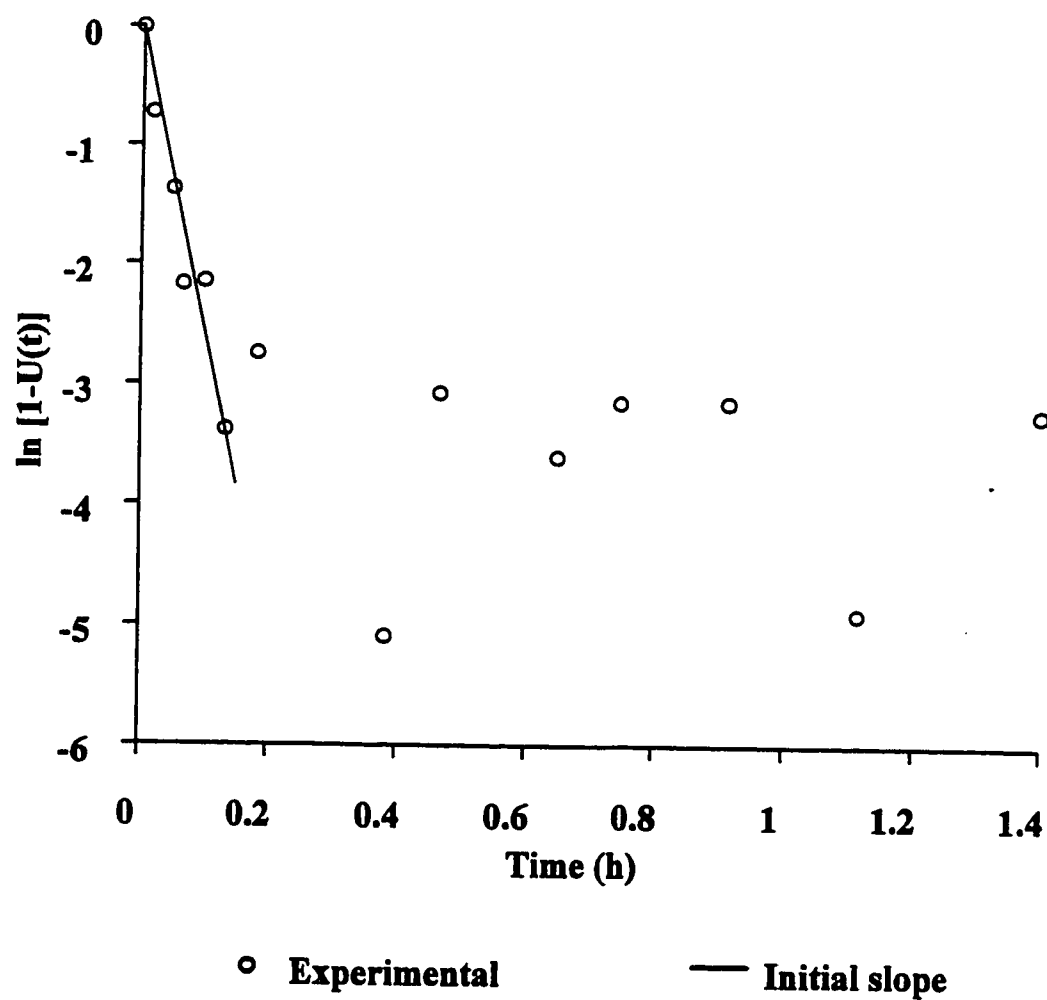


Figure 42: First order reversible kinetic fit of phenol adsorption data on HiSiv 3000 (powder particles), at $T=25^{\circ}\text{C}$.

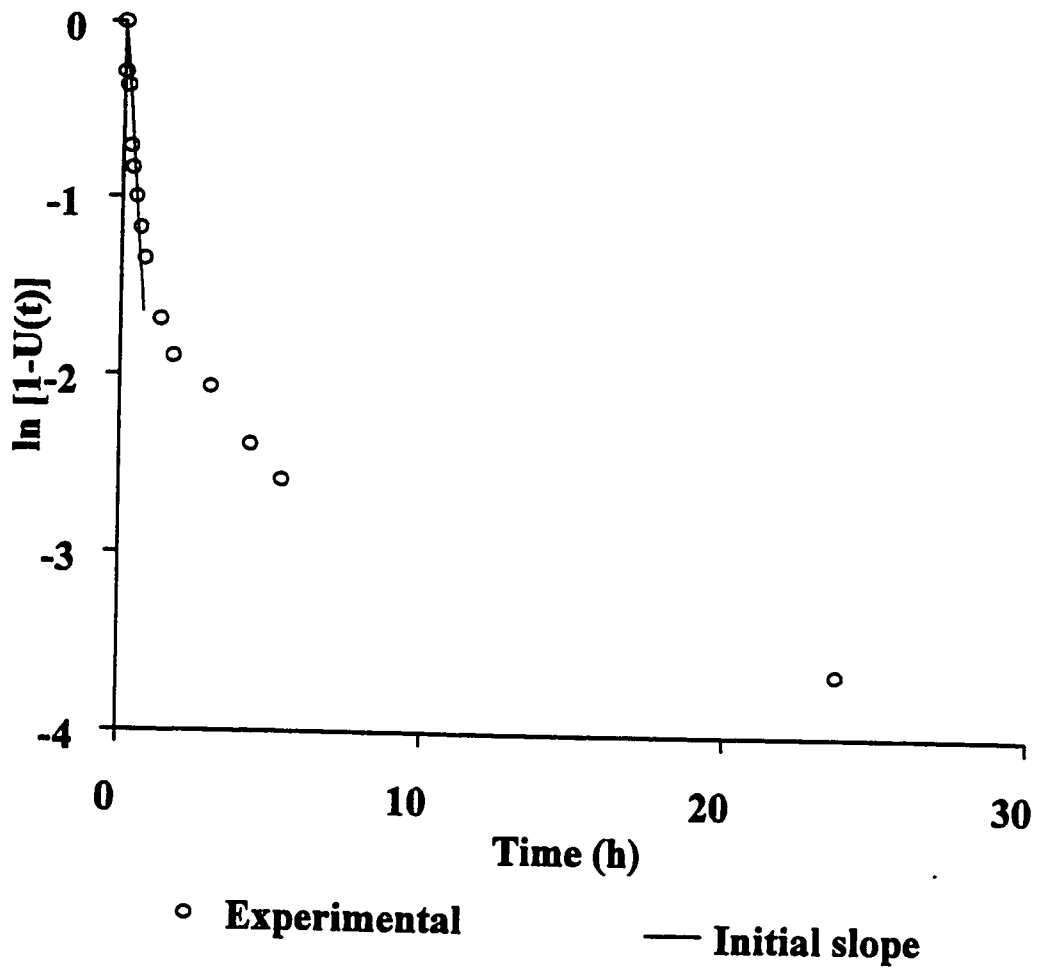
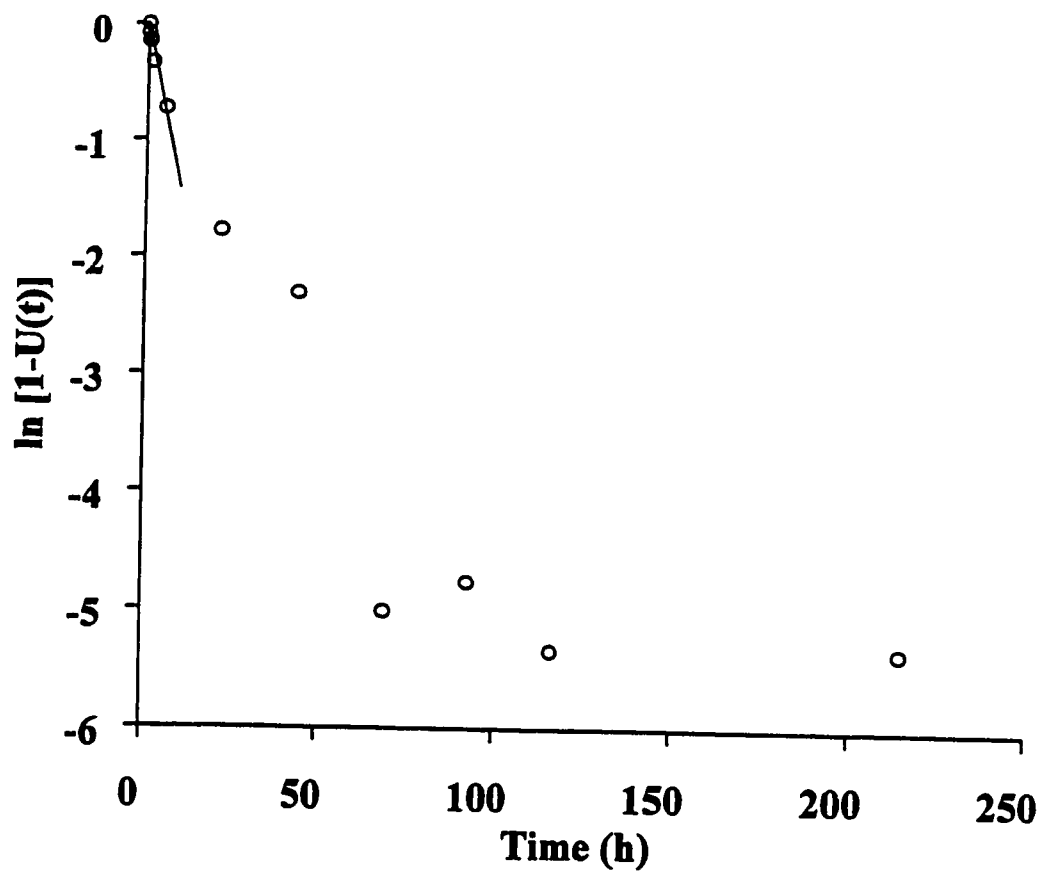


Figure 43: First order reversible kinetic fit of phenol adsorption data on HiSiv 3000 (20 × 50 mesh size), at T=25°C.



○ Experimental — Initial slope

Figure 44: First order reversible kinetic fit of phenol adsorption data on HiSiv 3000 (extrude, particle size =1.5 mm), at T=25°C.

D.2 Isothermal Diffusion Model

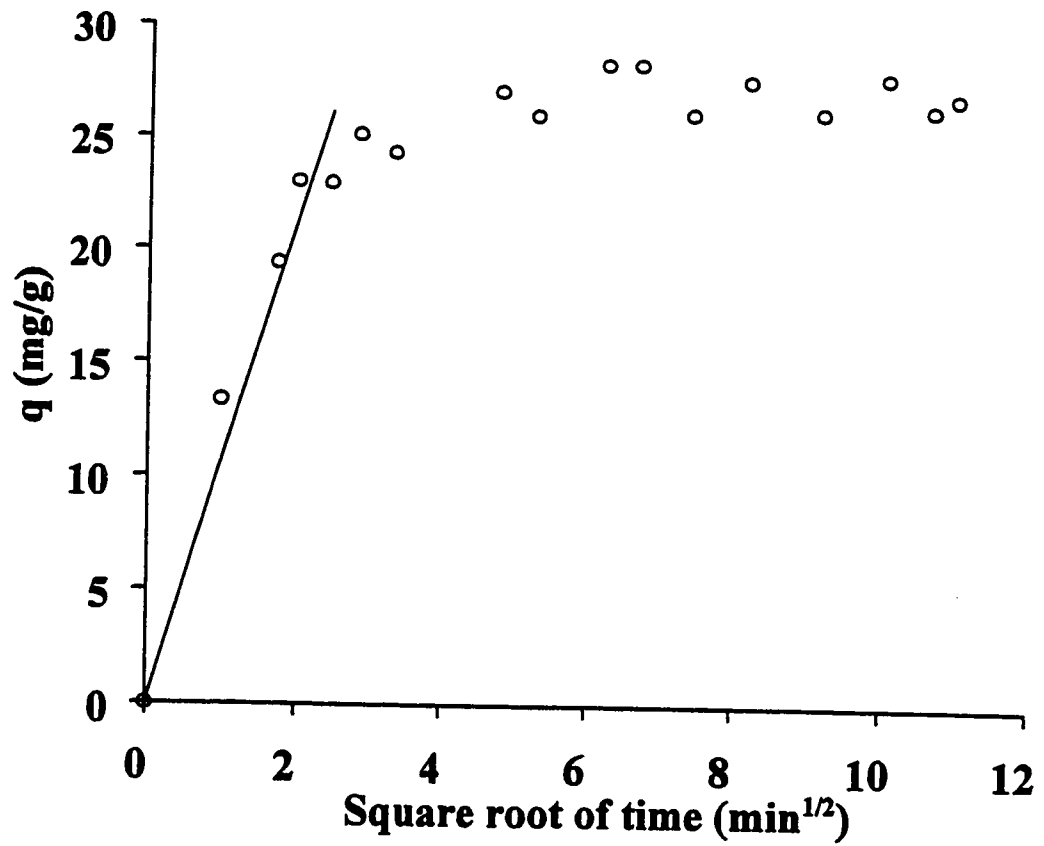


Figure 45: Plot of q against $t^{1/2}$ for adsorption of phenol on HiSiv 3000 (powder particle size) at 25°C.

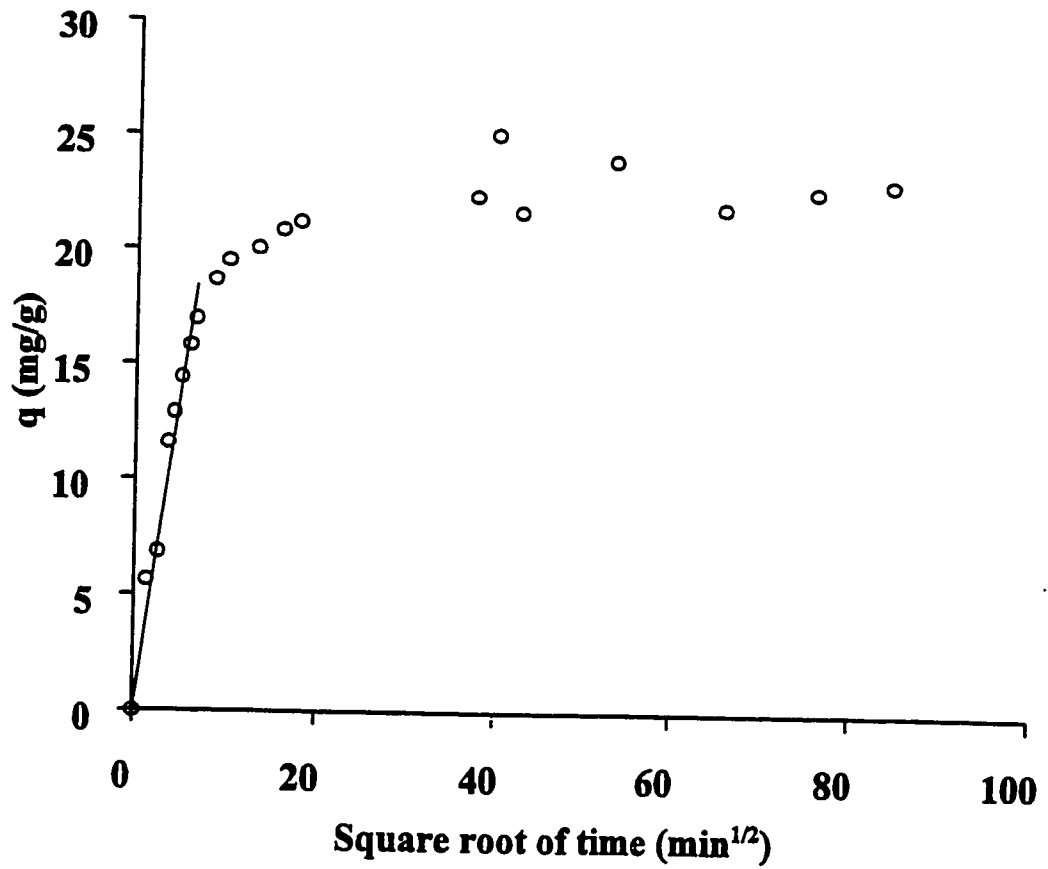


Figure 46: plot of q against $t^{1/2}$ for adsorption of phenol on HiSiv 3000 (particle size =20×50 mesh) at 25°C.

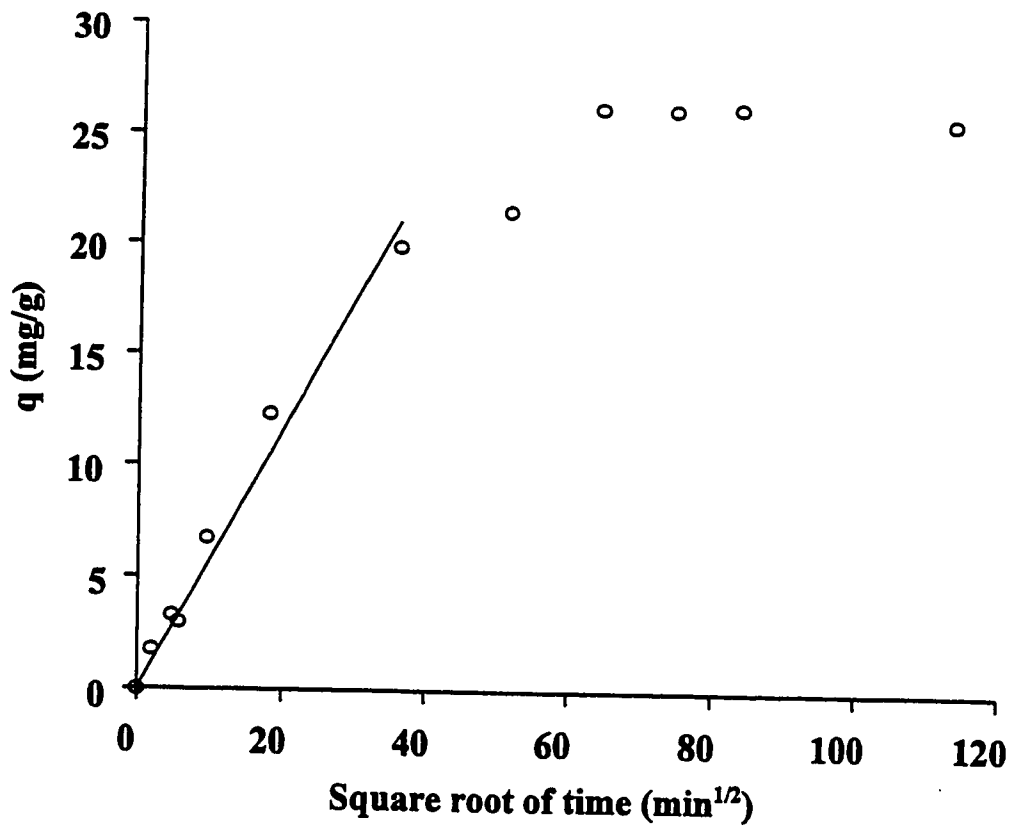


Figure 47: plot of q against $t^{1/2}$ for adsorption of phenol on HiSiv 3000 (particle size =1.5 mm, extrude) at 25°C.

E. Equilibrium Models

The results of applying equilibrium models to data obtained from adsorption of phenol on HiSiv 3000 (50-70 mesh) at 40 and 55°C are shown in Figures 48 and 49, respectively.

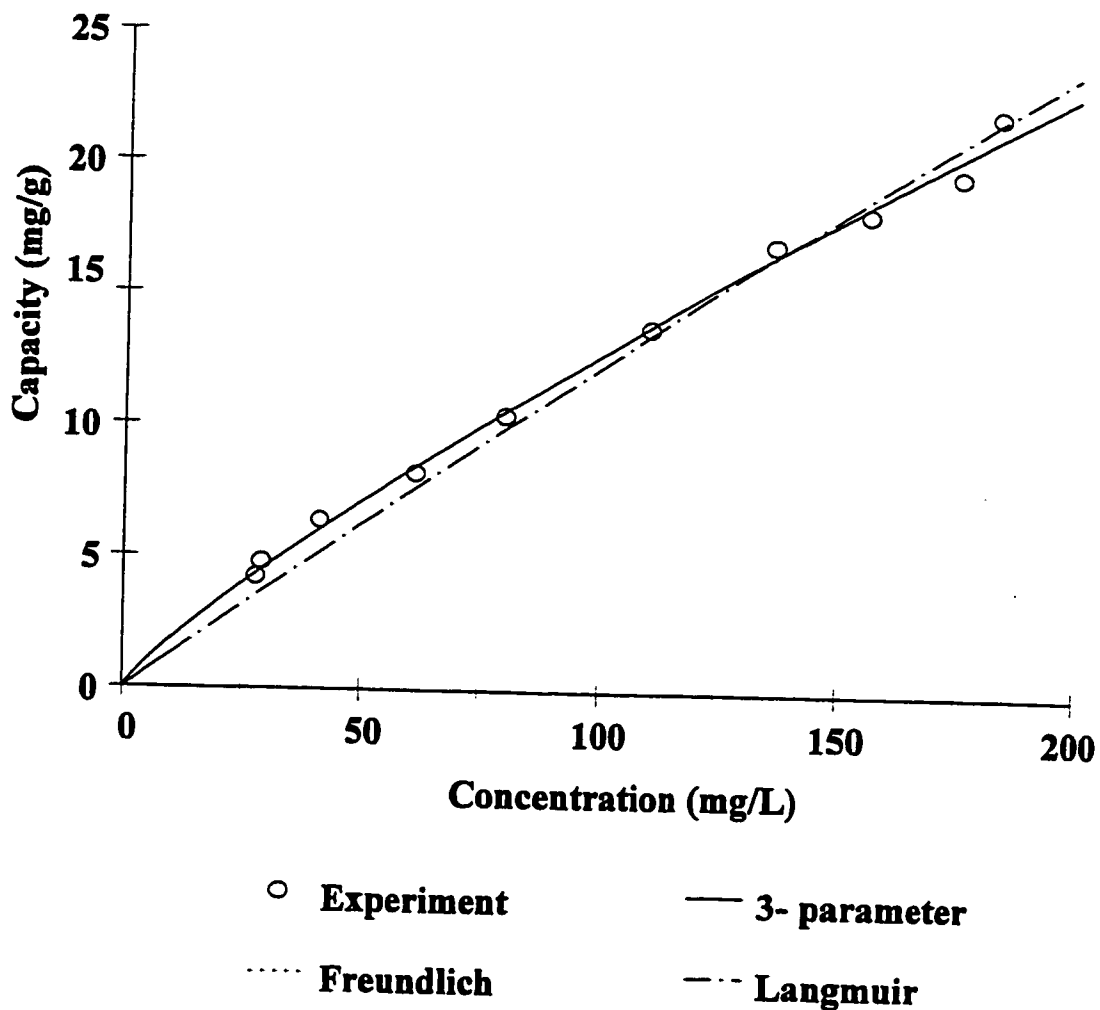


Figure 48: Equilibrium isotherm models applied to HiSiv 3000 (50×70) data at 40 °C. In this Figure Freundlich coincides with 3- parameter model.

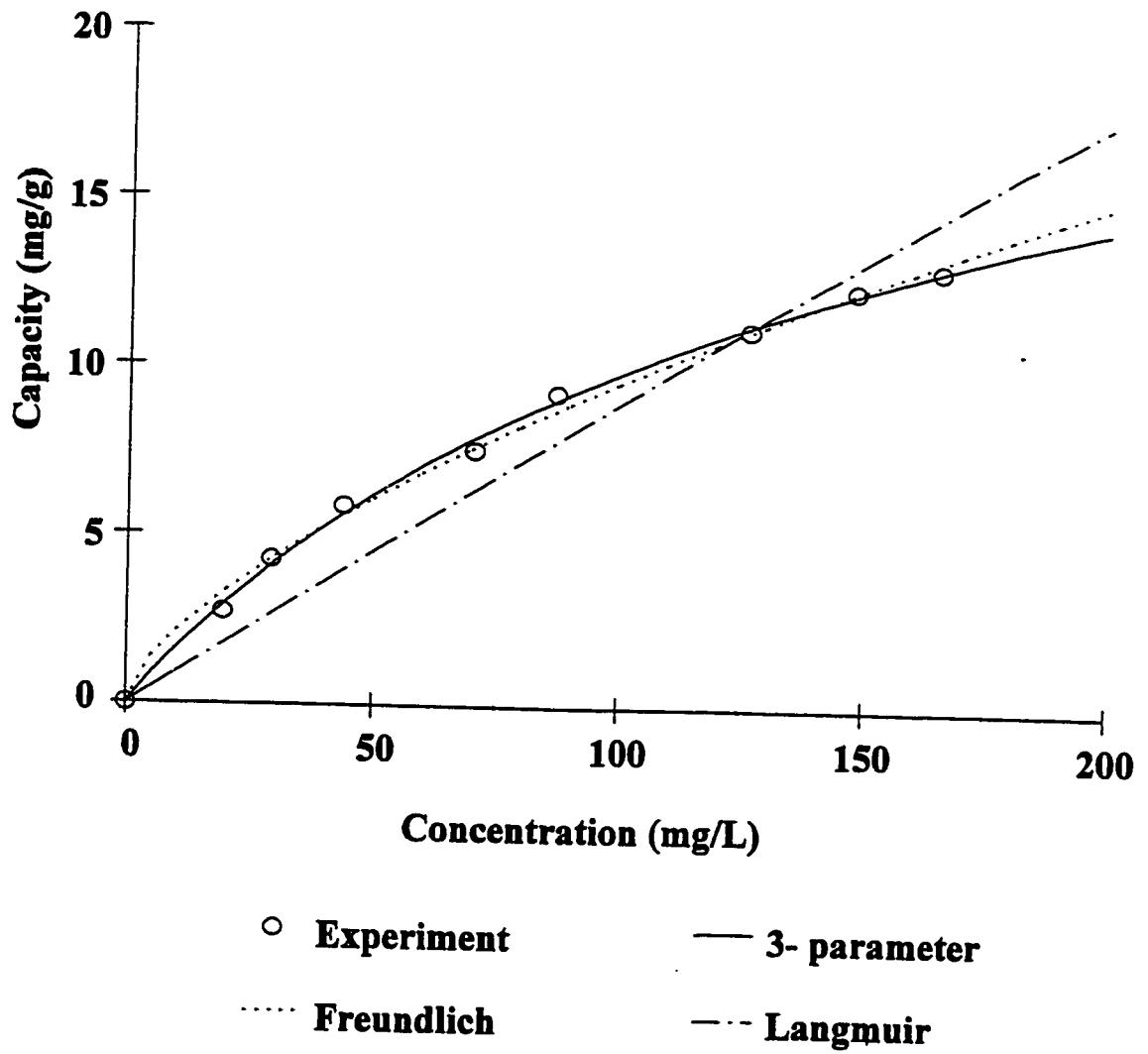


Figure 49: Isotherm models applied to HiSiv 3000 (50×70) adsorption data at 55 °C.

The results of applying equilibrium models to HiSiv 3000 with different particle sizes are shown in Figures 50 to 53.

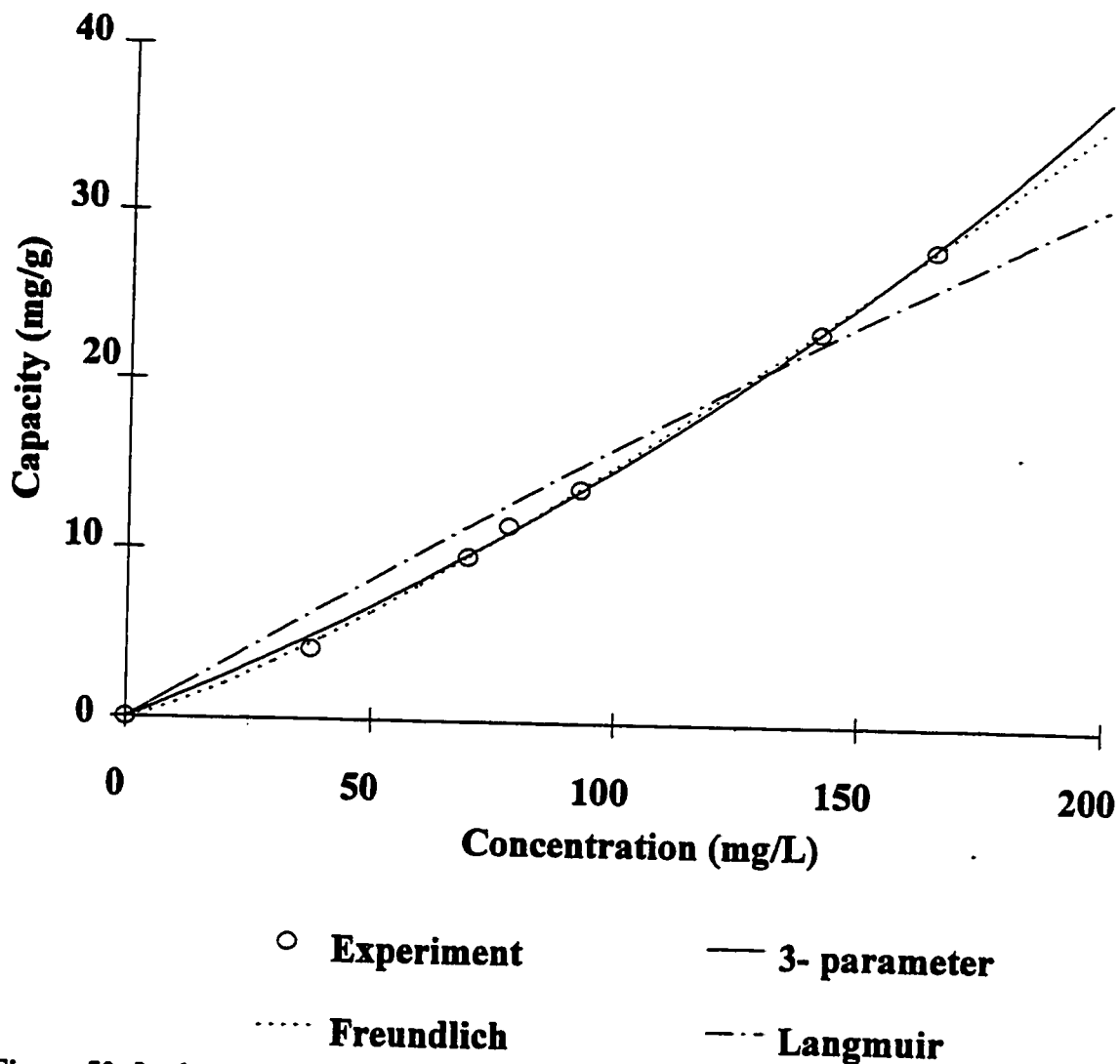
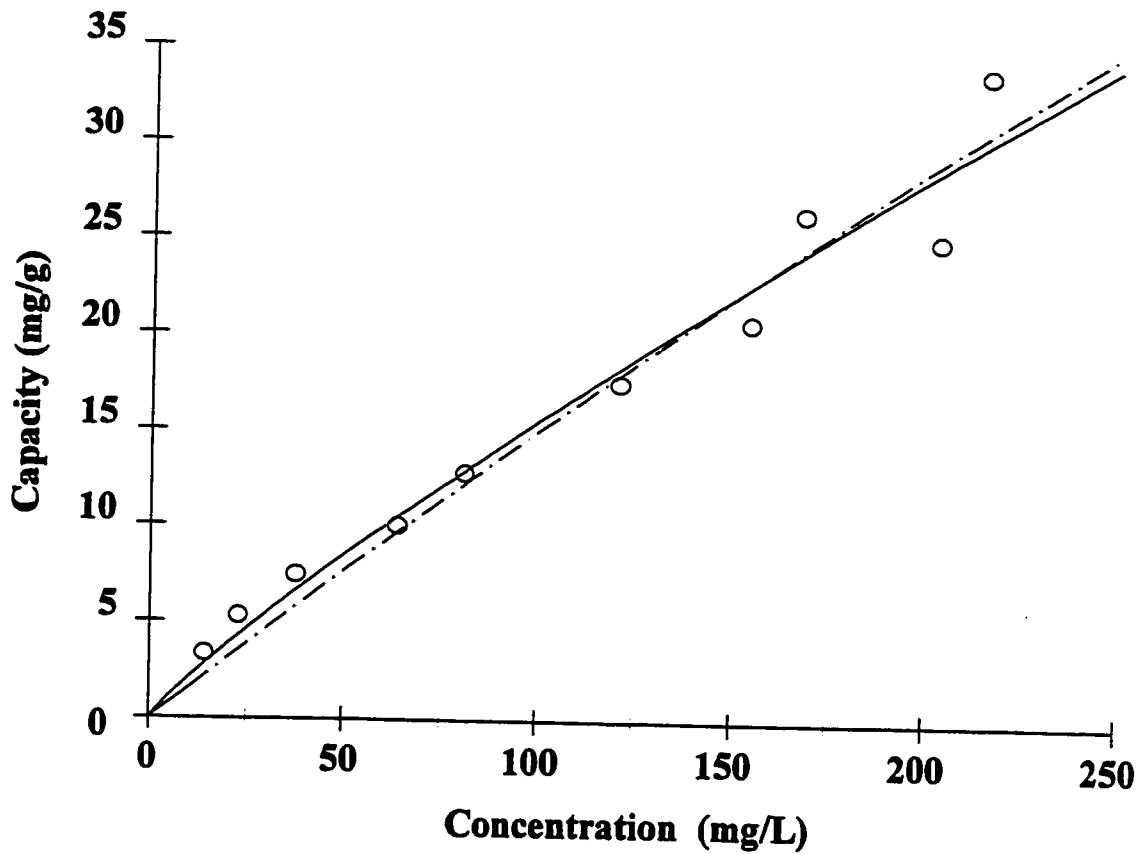
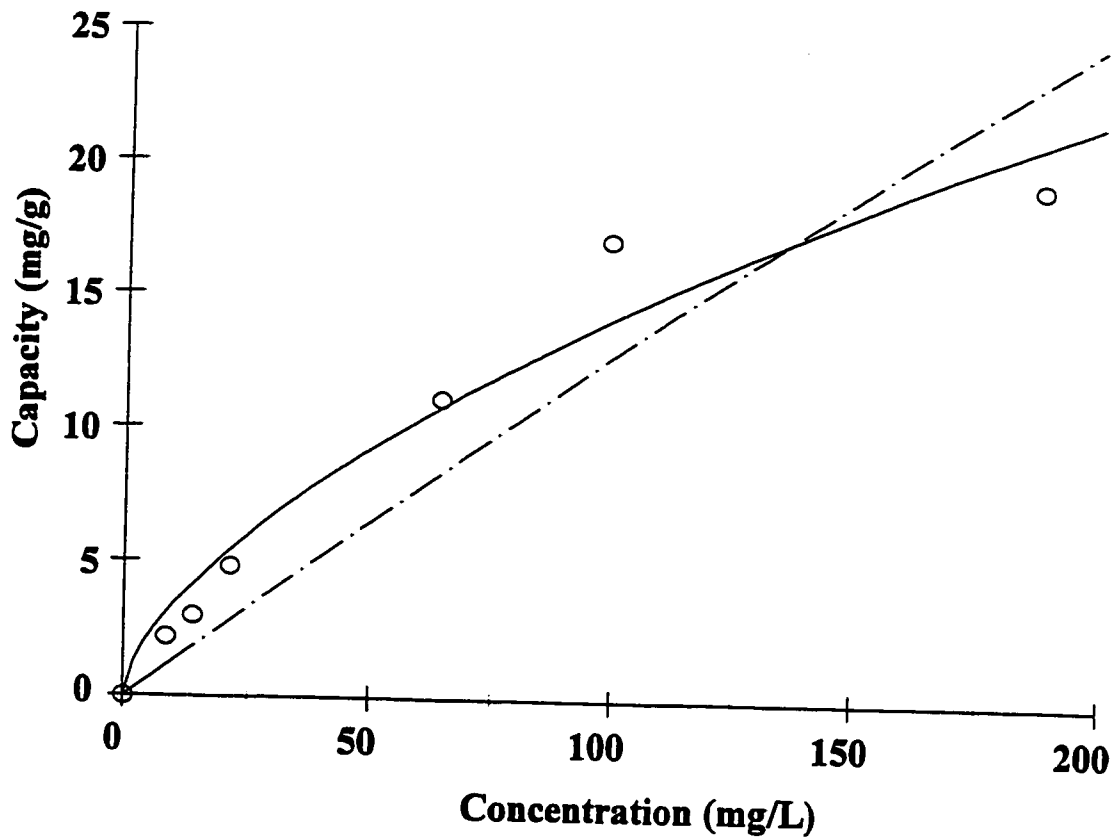


Figure 50: Isotherm models applied to HiSiv 3000 adsorption data at 25 °C, particle size = powder.



○ Experiment — 3- parameter Freundlich - - - Langmuir

Figure 51: Isotherm models applied to HiSiv 3000 adsorption data at 25 °C, particle size = 50×70 mesh. In this Figure Freundlich coincides with 3- parameter model.



○ Experiment — 3- parameter
 Freundlich - · - Langmuir

Figure 52: Isotherm models applied to HiSiv 3000 adsorption data at 25 °C, particle size = 20×50 mesh. In this Figure Freundlich coincides with 3- parameter model.

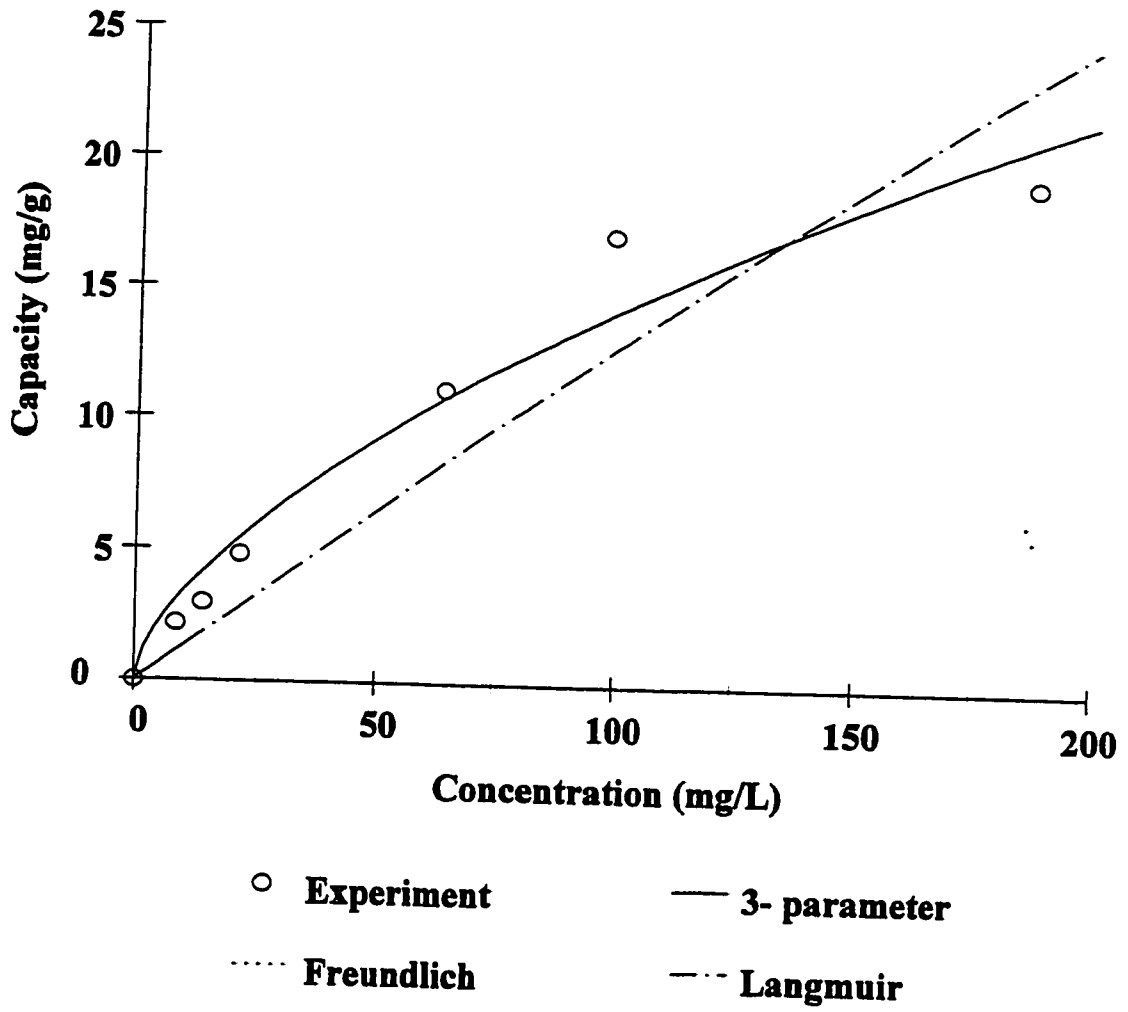


Figure 53: Isotherm models applied to HiSiv 3000 adsorption data at 25 °C, particle size = extrude (1.5 mm). In this Figure Freundlich coincides with 3- parameter model.